Putative HIV-1 Reverse Transcriptase Inhibitors: Design, Synthesis, *In vitro* Evaluation and *In Silico* Analysis

By

Preantha Poonan

A dissertation submitted in fulfilment of the academic requirements for the degree of Master of Science in the School of Life Sciences, University of KwaZulu-Natal, Durban

January 2018

ABSTRACT

One of the most significant treatments for HIV-1 infection has been the combination of drugs targeting the HIV life cycle with the aim of preventing further destruction of the host immune system. This study addresses the design, synthesis, *in vitro* evaluation, and *in silico* analysis of putative HIV-1 reverse transcriptase (RT) inhibitors. The inhibitors comprise two structurally diverse components which are intended to bind separately to the enzyme allosteric site and to a location at, or close to, the polymerase active site. Therefore, the hydrophobic N-tritylated p-halo-DL-phenylalanine derivatives (fluoro, chloro, bromo, iodo) have been coupled to 8-(6-aminohexyl) amino-adenosine-3',5'-cyclic monophosphate through N-hydroxysuccinimide-carbodiimide chemistry.

Compounds were characterized by thin layer chromatography, UV spectroscopy, MALDI-TOF mass spectrometry and proton NMR spectrometry. A reverse transcriptase colorimetric assay kit, which features a sandwich ELISA protocol, based on biotin-avidin and digoxygenin-anti DIG interactions, was used for quantitative determination of the inhibitory effect of synthesized compounds on recombinant HIV-1 reverse transcriptase activity *in vitro*. Molecular docking simulations of the chimeric inhibitors within the allosteric site of HIV-1 RT, were performed using AutoDock Vina. The predicted binding associations were compared with laboratory findings on HIV-1 RT inhibition. Two dimensional representations of protein-ligand interactions were generated using LigPlot.

The non-halogenated N-trityl-L-phenylalanine-8-(6-aminohexyl)amino-adenosine-3',5'-cyclic monophosphate derivative (4a) inhibited RT activity down to 57 % at 10^{-4} M, while the N-trityl-para-fluoro-DL-phenylalanine-8-(6-aminohexyl)aminoadenosine-3′,5′-cyclic monophosphate derivative (4b) was the strongest RT inhibitor reducing RT activity to 69 % at 10^{-7} M (IC_{50} = 29.2 μM). In the same assay, Nevirapine, a first-line anti-retroviral drug, showed a decline in RT activity down to 43% at 10^{-5} M (IC_{50} = 3.03 μM).

Ranking of inhibitors according to estimated docking energies obtained from *in silico* docking was in excellent agreement with potencies calculated from experimental studies. The docking

score of N-trityl-para-fluoro-DL-phenylalaline-8-(6-aminohexyl)amino-adenosine-3',5'-cyclic monophosphate was -8.8 kcal/mol, while that of Nevirapine was -9.9 kcal/mol. The benzene rings of the N-trityl-fluoro-DL-phenylalanine-8-(6-aminohexyl) amino-adenosine-3',5'-cyclic monophosphate derivative formed hydrophobic interactions with hydrophobic, non-aromatic amino acid residues Pro176 and Val179 in the allosteric site. Nevirapine, on the other hand showed strong van der Waals interactions with Val106 ,Val179 and Tyr188 due to the aromatic properties of the pyridine ring. Possible π-π stacking between phenyl rings of Nevirapine and Tyr 181/Tyr188 aromatic side chains may also be present. Other HIV-1 RT large subunit residues in the allosteric site common to the binding of Nevirapine and the active para-fluoro derivative include Lys101, Tyr318, Leu 100, Trp229 and Phe227. Apparent binding to the allosteric site suggests that compounds may be acting primarily as non-nucleoside reverse transcriptase inhibitors (NNRTIs).

PREFACE

The experimental work described in this thesis was carried out in the Discipline of Biochemistry, School of Life Sciences, University of KwaZulu-Natal, Durban from April 2016 to September 2017, under the supervision of Professor Abindra S. Gupthar and Professor Mario Ariatti.

These studies represent original work by the author and have not otherwise been submitted in any form for any degree or diploma to any tertiary institution. Where use has been made of the work of others it is duly acknowledged in the text.

Supervisors:

_____

Professor Abindra S. Gupthar

_____

Professor Mario Ariatti

DECLARATION

I, Preantha Poonan, declare that:

i.   The research reported in this dissertation, except where otherwise indicated or acknowledged, is my original work;

ii.   This dissertation has not been submitted in full or in part for any degree or examination to any other university;

iii.   This dissertation does not contain other persons' data, pictures, graphs or other information, unless specifically acknowledged as being sourced from other persons;

iv.   This dissertation does not contain other persons' writing, unless specifically acknowledged as being sourced from other researchers. Where other written sources have been quoted, then:

    a) their words have been re-written but the general information attributed to them has been referenced;

    b) where their exact words have been used, their writing has been placed inside quotation marks, and referenced;

v.   where I have used material for which publications followed, I have indicated in detail my role in the work;

vi.   this dissertation is primarily a collection of material, prepared by myself, for journal manuscripts or presented as a poster and oral presentations at conferences. In some cases, additional material has been included;

vii.   this dissertation does not contain text, graphics or tables copied and pasted from the Internet, unless specifically acknowledged, and the source being detailed in the dissertation and in the References sections;

viii. the turnitin plagiarism score (Appendix E) of the thesis compilation yielded 17 %.

Student signature   Date

_____   _____

TABLE OF CONTENTS

CHAPTER ONE
INTRODUCTION

CHAPTER TWO
MATERIALS AND METHODS

CHAPTER THREE
RESULTS AND DISCUSSION

CHAPTER FOUR
CONCLUSION

LIST OF FIGURES

LIST OF TABLES

LIST OF ABBREVIATIONS

ABC	Abacavir
AIDS	Acquired immune deficiency syndrome
Ala	Alanine
Asp	Asparagine
AZT	Azidothymidine
DDI	Didanosine
DLV	Delavirdine
D4T	Stavudine
EFV	Efavirenz
ETR	Etravirine
FDA	Food and drug administration
Gly	Glycine
Glu	Glutamic acid
HAART	Highly active antiretroviral therapy
His	Histidine
HIV	Human immunodeficiency virus
Ile	Isoleucine
IN	Integrase
Leu	Leucine
Lys	Lysine
M-MuLV RT	Moloney murine leukemia virus
MTCT	Mother to child transmission
NC	Nucleocapsid
Nef	Negative regulatory factor
NNRTI	Non-nucleoside reverse transcriptase inhibitor
NNRTI-BP	Non-nucleoside reverse transcriptase inhibitor binding pocket
NRTI	Nucleoside reverse transcriptase inhibitor
N(t) RTI	Nucleotide reverse transcriptase inhibitor

NVP	Nevirapine
PBS	Primer binding site
PBMC	Peripheral blood mononuclear cells
Phe	Phenylalanine
Ppt	Polypurine tract
PR	Protease
RPV	Rilpavirine
RSV	Rous sarcoma virus
RT	Reverse transcriptase
Ser	Serine
TFV	Tenofovir
Trp	Tryptophan
Tyr	Tyrosine
Val	Valine
Vif	Viral infectivity factor
Vpr	Viral protein R
WHO	World health organization

ACKNOWLEDGMENTS

CHAPTER ONE

INTRODUCTION AND LITERATURE SURVEY

1.1 Human immunodeficiency virus

A family of malignant human retroviruses, among them the human immunodeficiency virus, also known as HIV (Killian *et al*., 2011), is responsible for Aquired Immune Deficiency Syndrome (AIDS), a worldwide epidemic. HIV is a single stranded RNA, blood-borne virus that is most often transmitted via shared intravenous drug paraphernalia (Gostin, 1991; Gaskin *et al*., 2000) sexual intercourse with an infected partner, or mother-to-child transmission (MTCT), during birth process or breastfeeding. HIV retroviruses function by attaching themselves to a healthy host cell, fusing with the host cell membranes, integrating into the host cell nucleus and incorporating its viral DNA into a normal host cell genome (Perilla *et al*., 2016).

AIDS was first discovered in 1981 (Gottlieb *et al*., 1981) and two years later, HIV and human-lymphotropic virus type III were isolated as the causative agents of the disease (De Clercq, 2009). The ability of HIV to replicate rapidly in healthy cells and the errors made during the replication process, cause the virus to infect and evolve much faster in patients, making it a global health care crisis (UNIAIDS, 2013). At the end of 2014, approximately 36.9 million people were infected with HIV and 1.2 million people had died from HIV-related diseases worldwide (World Health Organization, 2015). However, according to recent statistics, approximately 36.7 million people were living with HIV in 2015 (UNAIDS, 2016).

HIV infections can't be cured (Ensoli *et al*., 2014) and drug administration is a lifelong commitment to those suffering with the virus (Sarafinos *et al*., 2010). Therefore, various anti-viral drug therapies have been studied and designed over the past years to provide HIV positive patients with a good quality of life (Figure 1.1). This, however, is an ongoing process since

HIV-1 has the tendency to show resistance to administered drugs, as the major enzyme in RNA replication, reverse transcriptase, lacks the ability to proof read (Asahchop *et al*., 2012). Other issues such as toxicity and harmful side effects such as nausea, diarrhoea and muscle disease are also common factors that contribute to HIV resistance. Therefore, new anti-viral drugs with low toxicity and possibly fewer side effects are continuously being sought and studied. Other approaches, such as bone marrow transplantation, have led to limited success.

With help from various funding organizations, HIV/AIDS victims have gained access to various anti-retroviral treatments as shown in Figure 1.1. According to World Health Organization (WHO), low income countries such as South Africa, Botswana and Guyana have gained access to drug therapy which have assisted 80% of HIV infected pregnant women (World Health Organization, 2012).
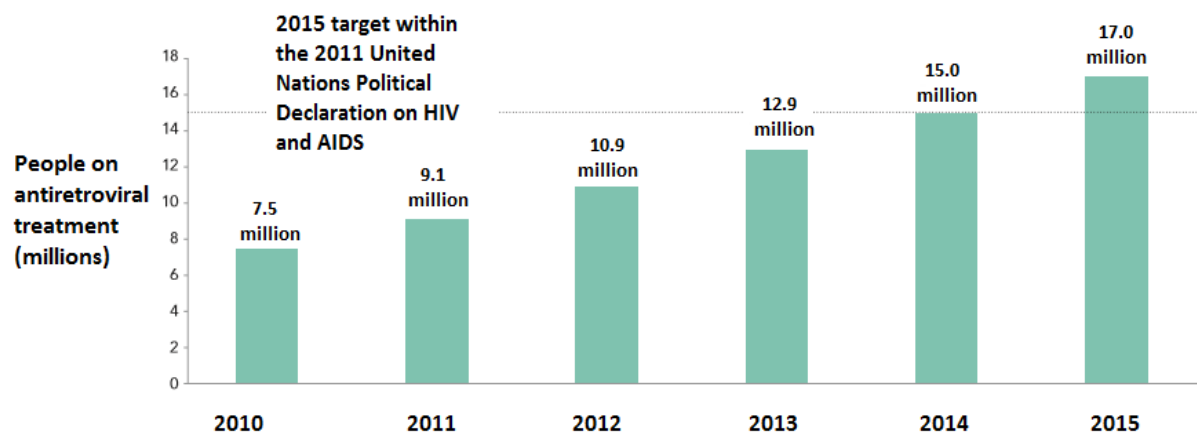
Figure 1.1 People on antiretroviral treatment from 2010-2016 (UNIAIDS, 2016).

According to statistics published in the UNICEF annual reports, (2013), mother to child transmission has decreased markedly in the period 2000 to 2013 in some African countries. Botswana was shown to have less than 5% mother to child transmission after breastfeeding, however more than 10 countries were shown to have more than 15% mother-to-child transmission (Figure 1.2). Highly Active Antiretroviral Therapy (HAART) has indeed caused a great decrease in HIV infections world-wide.
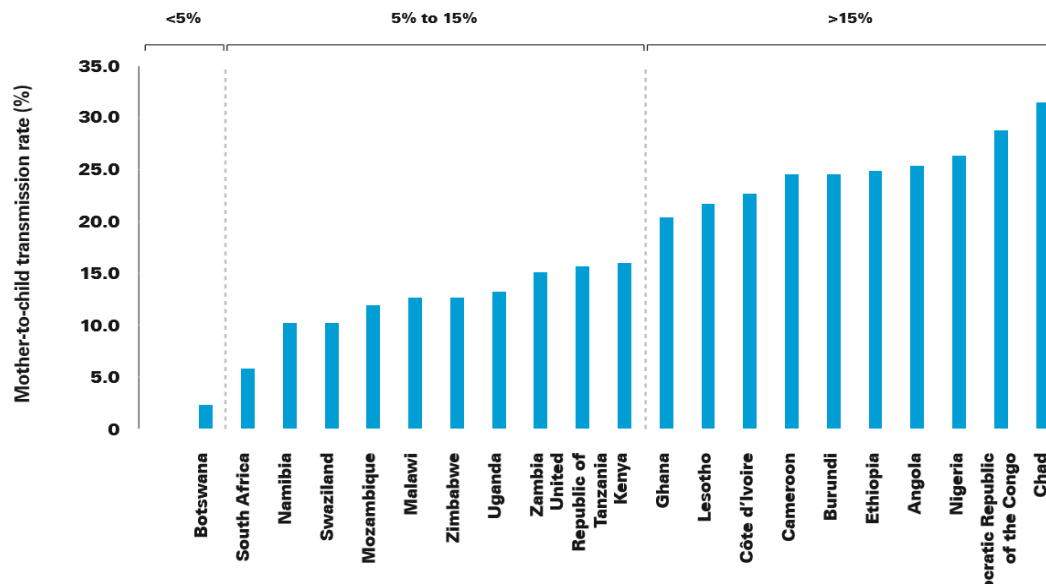
Figure 1.2 Mother to child transmission rate (%) from 2000-2013 (UNICEF annual report, 2013).

1.1.1 Structure of HIV

HIV-1 is a lentivirus belonging to a family of retroviruses. HIV is composed of an outer layer that contains the envelope glycoprotein gp160 (Figure 1.3). In its native form, the HIV trimeric envelope glycoprotein consists of gp120 and gp41 subunits (Lobritz *et al*., 2010). Both molecules work together through non-covalent interactions. The gp120 glycoproteins assist in viral replication by binding to the receptors on the target host cells while the gp41 proteins play a role in fusion of the host cell and viral membrane. Found below the outer shell of a mature virion, is a layer of matrix (p17) as well as a round-shaped core that is formed from the virus capsid (p24). This core serves as a protector as it shields the components found in the virion as well as the p6 protein that functions in late viral assembly. The components found within the virion are two copies of the positive sense genomic viral RNA and are shielded by the nucleocapsid (NC) from nuclease digestion. The core also contains three viral enzymes: integrase (IN), reverse transcriptase (RT) and protease (PR) (Sundquist and Kräusslich, 2012). PR, along with the viral proteins; negative regulatory factor (Nef), viral infectivity factor (Vif) and viral protein R (Vpr) are said to be located within the virion. Vpr plays a role in the replication and transcription of non-dividing cells (i) induces apoptosis of cells and (ii) causes death of cell cycle in proliferating cells (Bukrinsky and Adzhubei, 1999).

3

The HIV genome contains three genes namely, 5'gag-pol-env-3' that encode the viral enzymes as well as structural proteins. Gag precursor protein (p55) is 55 kD in length and is formed by the gag gene. After the budding process the enzyme, protease cleaves p55 into the p17 matrix, p6, p24 capsid and nucleocapsid. This causes conformational changes in the viral structure such that the p24 capsid encloses, surrounding the viral RNA while the p17 matrix remains intact (maturation).

Diagram of the HIV virion, illustrating protease, integrase and reverse transcriptase.
Source: U.S. National Institute of Health (U.S. Department of Health and Human Services)
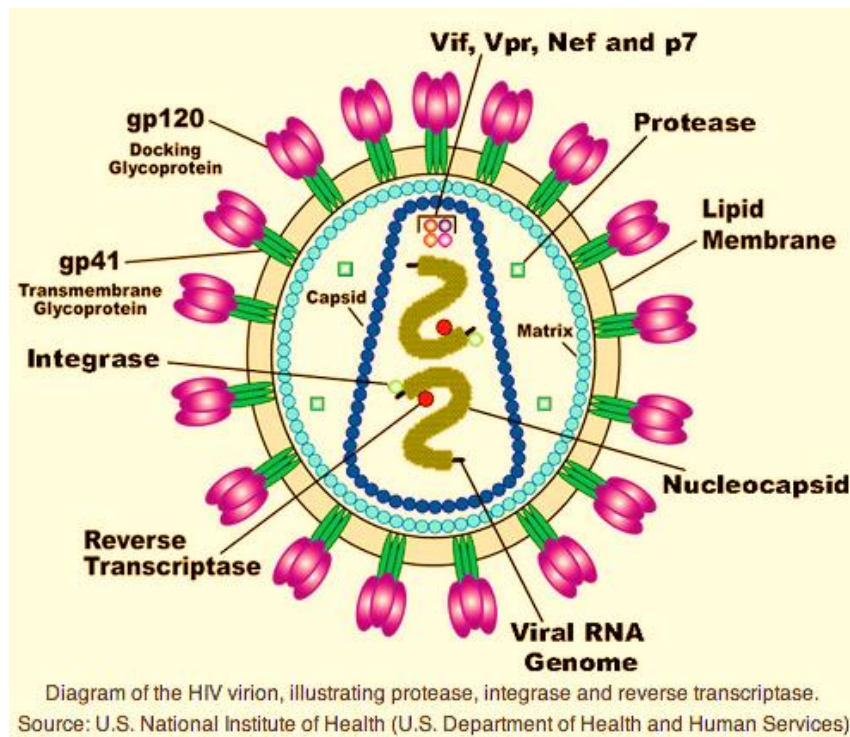
Figure 1.3   Diagram of HIV illustrating the viral RNA genome, nucleocapsid, lipid membrane, the gp120 docking glycoprotein, gp41 transmembrane glycoprotein, the viral enzymes (reverse transcriptase, integrase, protease) and viral proteins (Vif, Vpr, Nef, p7). https://www.google.co.za/search. Diagram of human immunodeficiency virus (HIV). Adapted from U.S. National Institute of Health (U.S. Department of health and human services).

1.1.2   Life cycle and viral replication

Most retroviruses, such as Rous sarcoma virus (RSV), tend to infect dividing cells during the process of mitosis. HIV, on the other hand, can infect non-dividing cells when certain endogenous or exogenous genotoxic agents damage DNA (Lyama and Wilson, 2013), leading to multiple human diseases. When a person is infected with HIV, the virus is said to remain latent for long periods of time. It then starts attacking specific $CD4^+$ T cells that serve in cell-mediated responses. Since HIV is a single-stranded ribonucleic acid (RNA) virus, it cannot replicate on its own and requires the formation of double-stranded DNA to replicate. The process and synthesis of viral DNA is shown in Figure 1.4.

1.1.2.1   Attachment, un-coating and fusion

T lymphocytes play a crucial role in protecting the body's immune system. They contain specialized antibody-like receptors on their surface that are used to recognize and detect harmful antigens on the surface of other infected cells. T cells have two important functions: (i) attacking infected, and (ii) regulating and directing immune system responses.

HIV is known to attack T helper cells, as they are essential in stimulating the activation of other important immune cells such as B cells. When HIV attacks these cells, the immune system cannot function properly and this causes the body to become prone to many other infections (Casiday and Frey, 2001). These cells are also called T helper cells because HIV uses the CD4 proteins found on the surface of the helper cells, to attach to and enter the cell. T helper cells also contribute to the activation of B cells and cytotoxic cells with chemical signals. Therefore, when HIV attacks T cells, it also prevents the activation of B cells and cytotoxic T cells, which leaves the immune system vulnerable to harmful foreign antigens.

The protein Nef (1.1.1), is expressed during the attachment step. Nef promotes the survival of infected cells by reducing the presence of essential complexes such as major histocompatibility complex (MHC I) and MHC II present on antigen-presenting cells (APCs) and target cells, and CD4 present on helper T cells (Das and Jameel, 2005, Das *et al.*, 2005).

The HIV-1 envelope (Env) contains spikes protruding from its binding site surface which comprise trimers of non-covalently-linked heterodimers consisting of glycoprotein gp120 and the transmembrane glycoprotein (Figure 1.3) (Engelman and Cherepanov, 2012). The process of replication occurs when glycoproteins (gp120) on the HIV-1 envelope bind to the $CD4^+$ receptors protruding from the surface of T helper cells (Engelman and Cherepanov, 2012). This interaction causes the formation of a bridging sheet and brings about a conformational change in the structure of both molecules, therefore exposing a site known as the chemokine co- receptor binding site. This enables co-receptors such as CCR5 or CXCR4 to facilitate viral entry into the cell by membrane fusion (Mehellou and De Clercq, 2010) after exposure of the gp41 peptide, which is inserted into the host cell membrane (Wilen *et al.*, 2012). This brings the host and viral membranes closer, permitting the fusion peptide of gp41 to fold at a hinge region, bringing a carboxy-terminal helical region (HR-C) and an amino-terminal helical region (HR-N) from the gp41 subunit together to form a six-helix bundle (6HB). Due to the proximity of HR-C to the viral membrane (caused by the glycoprotein, gp41) and the proximity of HR-N domain to the host membrane (caused by the gp41 peptide), the 6HB essentially links the two membranes causing a fused pore. The viral core is then released into the host cytoplasm (Wilen *et al.*, 2012). Once in the cytoplasm, host cell enzymes help in the removal of the viral capsid, resulting in structural change and the release of the viral RNA into the host cell. This process is known as un-coating.

1.1.2.2   Reverse transcription

Reverse transcription is the process of synthesizing a double-stranded DNA molecule from a single-stranded RNA template. It is called reverse transcription as it acts in the opposite direction to transcription. The process of reverse transcription was unaccepted at first as it contradicted the central dogma of molecular biology which states that DNA is the code which is transcribed into RNA which then carries the message to be translated into proteins. However,

due to the independent discovery of the enzyme reverse transcriptase in 1970, by Howard Temin and David Baltimore (Coffin and Fan, 2016) and its role in reverse transcription, the possibility that DNA could be copied from an RNA template in the reverse manner was accepted.

The formation of a complementary single-stranded DNA is carried out by the enzyme reverse transcriptase. The process of reverse transcription is essential as it involves the conversion of a single-stranded plus-sense RNA genome to a double-stranded cDNA which can be inserted or integrated into the host cell (Klickstein *et al*., 2001; Hu and Hughes, 2012). There are two enzymatic activities that are essential to carry out the process of reverse transcription. These include a DNA polymerase (reverse transcriptase) that can copy a DNA or RNA template, and an RNase H activity which helps degrade RNA during the synthesis of a provirus (Hu and Hughes, 2012). HIV-1 reverse transcriptase uses viral single-stranded RNA as a template, to catalyse the formation of a proviral DNA.

Viral genomic RNA is plus stranded and the synthesis of the first DNA strand, also known as (–) strand DNA, is synthesized by extending the 3′-end of a specific $tRNA_{lys3}$ using the viral RNA as a 3′-5′ template (Betancor *et al*., 2015). Reverse transcriptase, like many other polymerases also requires a primer and template to initiate strand polymerization. The 3′ end of the cellular $tRNA_{lys3}$ primer, is based paired to a complementary sequence of nucleotides at the 5′ end of the viral genome called the primer binding site (PBS). This site is approximately 180 nucleotides from the 5′ end of the viral genome.

1.1.2.2.1   First strand synthesis (Minus strand)

The enzyme reverse transcriptase attaches to the growing DNA strand and copies the 5′ end of the viral RNA genome to form a RNA-DNA hybrid duplex and with the help of RNases H, the viral RNA is degraded nucleolytically, exposing the newly synthesized single-stranded minus DNA. This creates direct repeats (long term terminal repeats) at the 5′ and 3′ ends of the viral RNA, which act as a bridge to allow the newly synthesized single-stranded minus DNA at the 5′ end to join with the complementary repeat sequence (R) at the 3′ of the viral RNA. Retroviruses contain two copies of their RNA genome; the minus strand (also called the first

jump) (Sarafianos *et al*., 2010) undergoes a transfer which involves the repeat sequence (R sequence) at the 3′ end of one of the two RNAs.

Once the minus strand DNA joins to the R sequence, the synthesis of the DNA strand continues along the viral genome in the 5′ direction. As synthesis of minus strand DNA continues, RNase H continues to degrade the RNA strand. However, at the 3′ end of the viral genome, there is a sequence that is rich in purines. This sequence is called the polypurine tract or ppt and is found to show resistance to RNase H activity. This purine sequence allows for a short stretch of RNA to remain attached to the newly synthesizing cDNA and serves to start the synthesis of the second strand DNA (plus strand), by serving as the primer sequence.

1.1.2.2.2   Second strand synthesis (Positive strand)

HIV- 1 has two polypurine tracts (ppts), one at the 3′ end and one at the middle of the RNA genome (Hu and Hughes, 2012). When RT creates the plus-strand DNA that is initiated from the 3′ ppt, it copies the minus-strand DNA, as well as the first 18 nucleotides of the tRNA$_{lys3}$ primer. This stops DNA synthesis. A study carried out by Swanstrom *et al*., (1981) with avian sarcoma-leukosis virus suggested that the ppt-primed plus strand DNA synthesis would stop when it comes across a modified Adenosine (A) that the enzyme reverse transcriptase cannot copy. The same applies to HIV. Once the 3′ terminal of the tRNA is copied into DNA, it becomes sensitive to RNase H. RT in HIV-1 is the only RT that cleaves the tRNA from the 3′ end, therefore leaving a ribo-A nucleotide at the 5′ end of the viral minus strand DNA.

1.1.2.3   Integration and re-infection

The newly synthesized double-stranded viral DNA in the core is in the host cell cytoplasm and migrates into the host cell nucleus, where it is integrated into the host cell genome as a provirus with the help of the enzyme, integrase (Craigie and Bushman, 2012). The provirus acts as a template to form messenger RNA (mRNA) and viral RNA during the process of transcription. The mRNA then travels to the host cell cytoplasm, where it undergoes translation to form Gag and Gagpol poly-proteins (Sarafianos *et al*., 2010). With the help of host enzymes, the viral

RNA and Gag and Gagpol poly proteins migrate to the cell surface to form new virus particles, each containing two copies of the RNA genome and the essential proteins needed for re-infection.
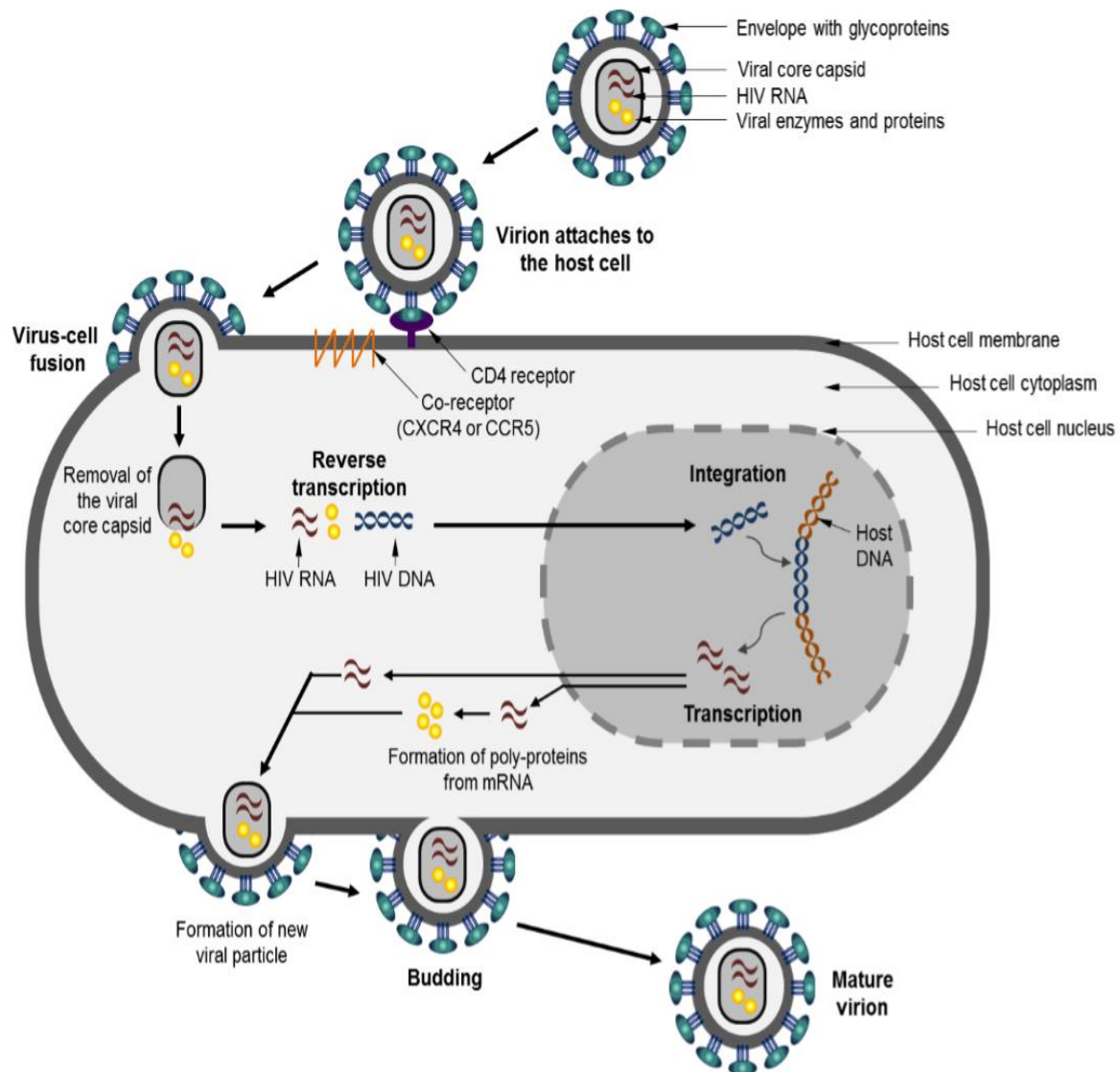
Figure 1.4   Illustrating the stages in the HIV life cycle. Virus adsorption, virus-cell fusion, uncoating, reverse transcription, integration, transcription, translation and budding (De Clercq, 2009).

1.2 The genesis, structure, and enzymatic functions of HIV-1 reverse transcriptase

A unique characteristic of the RT enzyme is that it can utilize both DNA and RNA templates. HIV-1 RT has three main functions: It can act as an RNA-dependant DNA polymerase to produce cDNA from an RNA template, it's Ribonuclease H activity degrades the RNA template during the formation of cDNA and it acts as a DNA-dependent DNA polymerase synthesizing double-stranded DNA using cDNA as the template (Sarafianos *et al*., 2010). Most of RT's functions are found in the same protein subunit although they are considered to be monomeric enzymes. However, HIV-1 RT is a heterodimer, consisting of two subunits, termed p66 and p51. The p66 subunit contains two domains: the DNA polymerase domain and the RNase H domain, which are located at different regions in the p66 subunit (Thammaporn *et al*., 2015).

The polymerase domain of the RT contains 4 subdomains: the connection, fingers, palm and thumb (Figure 1.5A). The connection domain connects the polymerase and RNase H domains as it acts as a bridge. These subdomains create a site for the binding of the primer, template, two divalent cations and dNTPs during the synthesis of DNA (Yokoyama *et al*., 2010). Hence it is called the polymerization active site. This site is composed of three key aspartic residues; Asp185, Asp110 and Asp186, which are in the palm domain. The Asp186 and Asp185 comprise part of the YMDD motif (Tyr-Met-Asp-Asp) corresponding to the more general YXDD motif (X = Met, Val, Leu or Ala) of HIV-1 RT. Tyr183 and Asp185 play a role in the formation of a hydrogen bond with the 3′-hydroxyl group at the primer end as well as act as a base to undergo a nucleophilic attack on the α-phosphate group of an incoming nucleoside-5′-triphosphate (Figure 1.5 B). The overall structure of the RT is often described as a right hand, where the polymerization active site is found in the "palm sub-domain'' between the ''fingers'' and the ''thumb'' and ''runs'' through the connection and RNase H domains (Das and Arnold, 2014).

The second subunit, p51 is similar to the p66 subunit, however it lacks the C-terminal RNase H domain and is formed by HIV-1 protease mediated cleavage of the C-terminal RNase H domain of the p66 subunit. The amino acid sequence that forms the polymerase active site of p66 domain is the same as the polymerase active site in the p51 domain, which is however not

functional (Xia *et al*., 2007). Therefore, the function of the p51 domain is to basically provide structural support to the RT enzyme.

The second site to which RT inhibitors bind is called the non-nucleoside binding pocket (Figure 1.5 C). A non-nucleoside binding pocket is found in the palm subdomain of the p66 subunit and is approximately 10Å away from the aspartic acid catalytic triad in the polymerization active site (Santos *et al*., 2015). The binding pocket is located between β6-β10-β9 and β12-β13-β14 sheets of the palm subdomain. The allosteric binding pocket is known to be hydrophobic in its natural form, consisting of aromatic residues (Tyr181, Tyr188, Phe227, Trp229, Tyr233), along with hydrophilic residues such as Ser105, Lys101, Lys103, Asp192, Glu22 and Glu138 of p51 subunit (Sarafianos *et al*., 2010). The hydrophobic binding pocket allows the template strand to bind to reverse transcriptase enzyme as it exposes the 3′-OH end of the primer to the catalytic site. The "thumb'' subdomain contributes to this exposure as it functions in the mobilization of the template and the primer to the polymerization active site when the reverse transcriptase enzyme forms a closed circle around the sub domains (Hu and Hughes, 2012). This brings the thumb and fingers to move closer to the palm subdomain and allows for binding of nucleic acids. It is also known to be more flexible than the 'palm and fingers' thus allowing for proper binding of strands (Kohlstaedt *et al*., 1992).

A

B

C
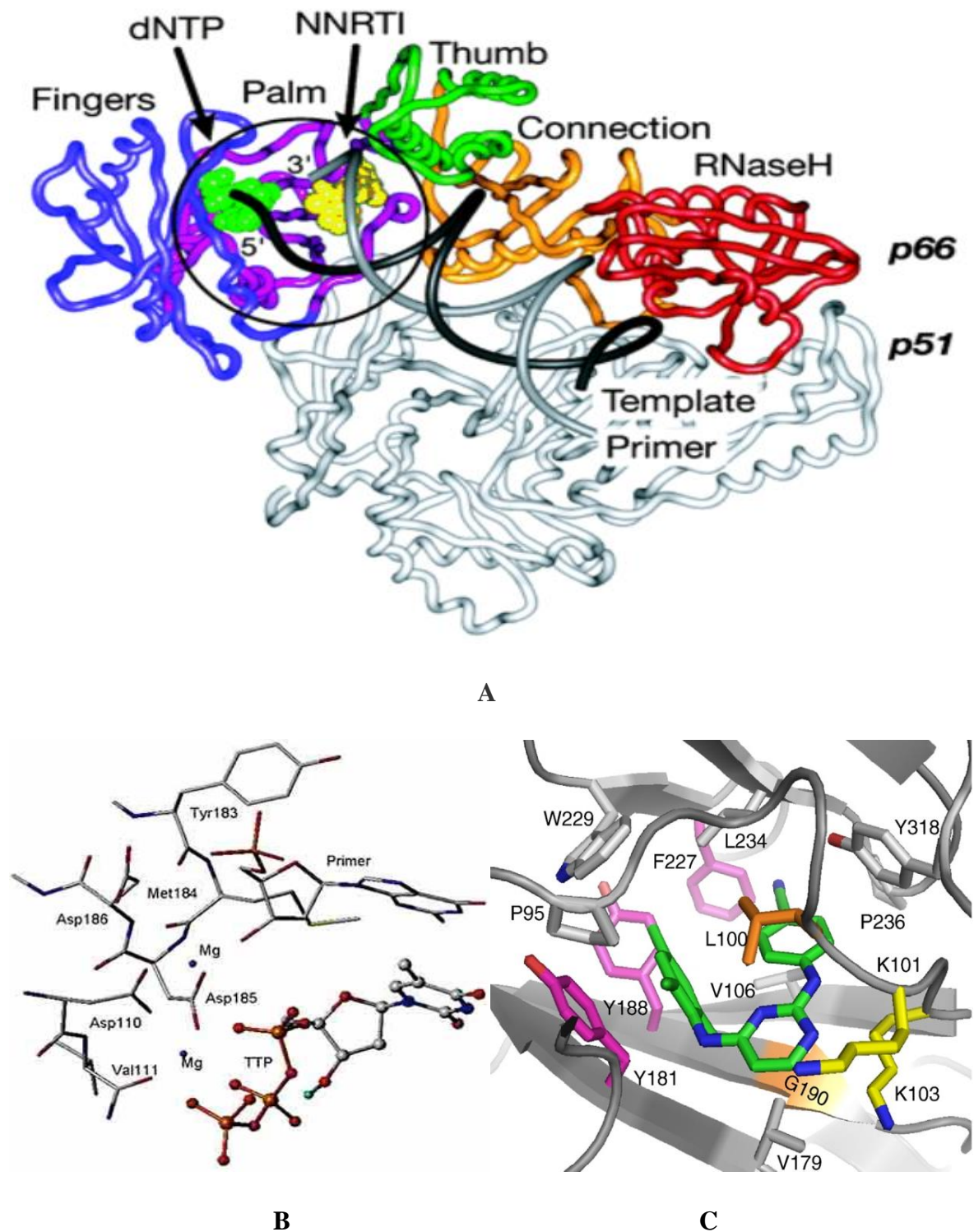
Figure 1.5 **(A)** Structure of HIV-1 RT and the different subdomains (Pata *et al*., 2004); **(B)** Polymerase active site with the YMDD motif and divalent ions. (Chong and Chu, 2004); **(C)** NNRTI-binding pocket, showing the residues at which NNRTI-resistance mutations occur (Sarafianos *et al*., 2010). Amino acid codes: F227=Phe, G190=Glu, K101, K103=Lys, L100, L234=Leu, P236, P95=Pro, V106, V106= Val, W229=Trp, Y181, Y188, Y318= Tyr.

1.3 Early history of therapeutic interventions

After the isolation of HIV-1 in 1983, extensive studies were carried out to control the spread of the chronic virus (Hoggs *et al*., 1999). The first anti-viral drug, Zidovudine (also known as AZT) was first synthesized in 1964 as an anti-cancer drug and thereafter became the first successful drug to be approved by the U.S. Food and Drug Administration (FDA) for extending the lives of those suffering with HIV infection up to 18 months in 1987 and later on became the preferred drug for the prevention of HIV infection (Corey *et al*., 2007). AZT at the triphosphate level was used to restore the immune system as it could enter the reverse transcriptase active site and block its activity in the HIV replication cycle (Furman, *et al*. 1986). The discovery of AZT's antiretroviral activity subsequently led to the development of other anti-retroviral drugs. However, one of the main limitations of AZT was that the HIV virus could easily show resistance to the drug within a short period of time as well as cause undesired side effects. For this reason, a second drug therapy, highly active antiretroviral therapy (HAART) was designed to overcome this problem (Asahchop *et al*., 2012). HAART was implemented after 1995 and has indeed improved the lives of HIV-infected patients, as this system brought about longer survival periods (Eswara Rao *et al*., 2015). The system of HAART consists of a mixture of 3 or more drugs usually from two different classes of anti-viral drugs, namely; nucleoside reverse transcriptase inhibitors (NRTI) and non-nucleoside reverse transcriptase inhibitors (NNRTI). Anti-retroviral treatment is very effective at preventing HIV from multiplying and spreading throughout the body. This prevention protects the immune system and thus allows the body to fight off other HIV-related opportunistic infections which eventually lead to AIDS.

1.3.1 Reverse transcriptase: The target for anti-retroviral drug therapy

Reverse transcriptase has long been a target for the development of anti-viral drug therapy, due to its major role in the replication process of HIV. HIV infections can't be cured easily and therefore, the administration of drugs is a lifelong commitment for those infected with the virus (Sarafianos *et al*., 2010). Therefore, compounds should be easily administered and non-toxic. There are different classes of drugs that intervene at different stages of the life cycle of HIV. However, drugs that specifically target the DNA polymerization activity of the reverse

transcriptase enzyme are said to be the backbone of current HIV-1 strategies (Betancor *et al*., 2015). These drugs can be split into two groups, namely, (i) nucleoside/nucleotide reverse transcriptase inhibitors (NRTIs) and (ii) non-nucleoside reverse transcriptase inhibitors (NNRTIs). NTRI and NNRTIs that target the DNA polymerization active site of the reverse transcriptase enzyme are said to be the backbone of current HIV-1 treatment strategies (Betancor *et al*., 2015). Several drugs have been successfully implemented to inhibit RT. These include Azidothymidine, Nevirapine, Tenofovir, Abacavir, Stavudine, Didanosine, Etravirine, Delavirdine, Efavirenz and Rilpivirine. However, due to their toxic side effects and the resistance caused by viral mutations, their therapeutic effects are sometimes limited (Padariya *et al*., 2016).

1.4 Nucleoside/ nucleotide reverse transcriptase inhibitors and their inhibitory mechanism

Nucleoside reverse transcriptase inhibitors (NRTIs) were the first successful retroviral agents used against HIV and are thus, the oldest group of antiretroviral agents. NRTIs are analogues of naturally occurring nucleosides and are therefore inactive in their normal forms. To display their anti-viral activity an NRTI requires host cell entry and must undergo phosphorylation twice by initial conversion to its 5′-monophosphate (NMP), followed by pyro-phosphorylation to its 5′-triphosphate (NTP) form by host cell kinases in order to compete with naturally occurring deoxynucleotide triphosphates (Michailidis *et al*., 2009). NRTIs lack a 3′-OH group on the deoxyribose sugar moiety thus preventing the formation of a 3′,5′-phosphodiester bond between the NRTI and a naturally occurring 5′-nucleoside triphosphates (Sarafianos *et al*., 2010). When reverse transcription occurs in the presence of a NRTI, RT may bind a NRTI triphosphate instead of a naturally occurring nucleotide building block and this, in turn, prevents reverse transcription. NRTIs may compete with and block the addition of naturally occurring substrates as well as become incorporated into the growing DNA molecule. When the NRTI triphosphates are incorporated into the nascent DNA, they act as chain terminators (Goody *et al*., 1991) by preventing the process of elongation; hence a double-stranded DNA is not fully formed and cannot be incorporated into a new host cell.

Along with the amino acid residues previously mentioned, there are two Mg^{2+} ions that are also present in the polymerase active site that are approximately 3.6 Å apart from each other (Figure

1.5 B) (Goldschmidt *et al.*, 2006). One of the ions, binds to the three phosphate groups of the incoming inhibitor as well as the Asp110 and Asp185 residues. This causes the Mg^{2+} to enter the catalytic site preventing exchange of free deoxynucleoside triphosphate. The second Mg^{2+} ion binds the three aspartate residues: Asp110, Asp185 and Asp186 as well as the α phosphate group of the incoming deoxynucleoside triphosphate (Goldschmidt *et al.*, 2006).
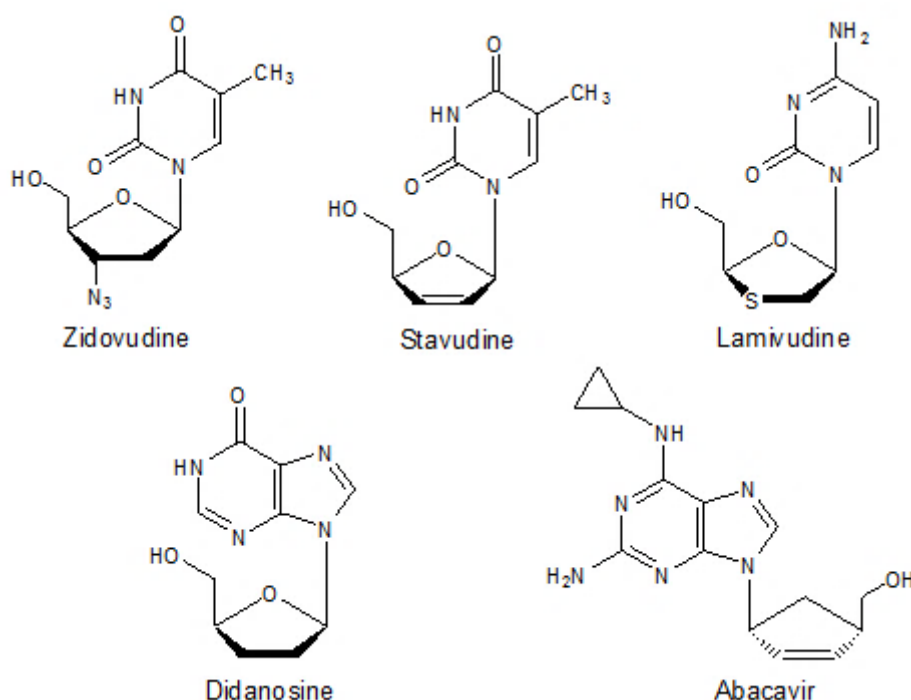
Figure 1.6   Clinically used NRTIs (Sarafianos *et al.*, 2010).

Nucleotide reverse transcriptase inhibitors (NtRTIs) generally display the same inhibitory mechanism. The only difference is that NtRTIs are nucleotide analogues and require further phosphorylation to be converted to their active triphosphate form as they already possess a phosphate group (De Clercq, 2009). NtRTIs are polar in nature as they contain a triphosphate group, a 5-carbon sugar and a nitrogenous base. Therefore, their polar property prevents their movement across the plasma membrane to enter the cell.

1.4.1 Clinically approved NRTIs

1.4.1.1 Azidothymidine (AZT)

AZT, also known as Zidovudine (Figure 1.6) is a potent inhibitor of reverse transcriptase, when it is converted to its 5′ triphosphate form. When reverse transcriptase utilizes AZT-5′-triphosphates to incorporate an AZT residue into a growing DNA strand, this serves as a chain terminator, therefore inhibiting reverse transcription (Corey *et al*., 2007). AZT possesses an azido group at the 3′-position on its 2′-deoxyribose sugar moiety, which prevents DNA chain extension using 2′-deoxynucleoside-5′-triphosphate building blocks. To display its anti-viral activity, AZT is first converted into its 5′- triphosphate form inside the cell. The triphosphate form of the drug cannot penetrate the cell membrane (Michailidis *et al*., 2009). Therefore, AZT in its monophosphate form also lowers the formation of 2′-deoxythymidine 5′-triphosphate (dTTP) by competitive inhibition. The mechanism and inhibitory effect of AZT was described in a study by Furman *et al*., (1987). In this study, the effect of AZT in its 5′- mono, di and triphosphate form on uninfected human fibroblasts and lymphocytes was investigated. It was shown that the inhibition of the growth of uninfected cells occurred at concentrations over 1mM and the conversion of AZT to its 5′-mono, di- and triphosphate forms was similar in HIV infected cells.

AZT is known to cause many harmful side effects including headaches and nausea (Santos *et al*., 2015). However, drug resistance allows for other opportunistic diseases to occur and to affect the patient. For this reason, AZT is mainly used in combination with other antiviral drugs. The combination of two or more anti-viral drugs in a patient's body not only reduces viral replication, but also minimizes the chances of the virus showing resistance to the drugs. Since AZT was the first successful anti-HIV drug, it was the most expensive medicine at the time, costing users $8,000-$10,000 per year. It was used exclusively until other anti-viral were developed. However, the quest for new more effective anti-viral with fewer side effects is an ongoing process.

1.4.1.2 Tenofovir (TFV)

Tenofovir, a NRTI was discovered in 1997 as a potent inhibitor of reverse transcriptase. In the same year, TFV was modified to Tenofovir disoproxil (TDF), making it the first oral prodrug of TFV (Wang *et al.*, 2016) and becoming one of the most commonly used drugs for the treatment of HIV-1 infection. TDF is used in many fixed-dose combinations such as with Efavirenz and Rilpivirine and one of its side effects is renal toxicity (Wang *et al.*, 2016). TFV is hydrophilic making it difficult to move across a hydrophobic membrane (Van Rompay *et al.*, 2012). After following a two-step phosphorylation process, TFV is converted into its active form, Tenofovir diphosphate (TFV-DP) which shows anti-HIV activity (Biswas *et al.*, 2014; Wang *et al.*, 2016).

1.4.1.3 Abacavir (ABC)

Abacavir (Figure 1.6) developed in 1998, is a carbocyclic 2′-deoxyguanosine nucleoside analogue (Adetokunboh *et al.*, 2014) mainly used for the treatment of HIV positive children. Analysis of the drug on peripheral blood mononuclear cells (PBMCs) revealed that it is considerably more potent than Didanosine (DDI) but as effective as AZT. Its low toxicity level and less harmful side effects such as; reduced hypersensitivity, fewer rashes and lower fever have allowed the drug to remain well tolerated long-term (Volberding *et al.*, 2008). The drug is metabolically converted to its triphosphate form, carbovir triphosphate and competes with the natural substrates dGTP for incorporation in the growing DNA strand.

1.4.1.4 Stavudine (D4T)

Stavudine (Figure 1.6) was first approved by the FDA in 1994 and is effective when used in combination with other anti-viral drugs. In a study carried out by Kline *et al.*, (1996), combination treatment of D4T and Didanosine (DDI) showed strong inhibition against HIV-1 infection in a small group of children. Three children with CD4 counts higher than 50 cells/mL showed a 20% increase in CD4 counts after being treated with the combination therapy for 12

weeks. One of the main side effects of D4T is peripheral neuropathy. This symptom can be tolerated for a short while, however, cannot be tolerated in the long term. Therefore, alternative antiviral drugs or combination of other antiviral drugs continues to expand (Volberding *et al*., 2008).

1.4.1.5   Didanosine (DDI)

Didanosine (Figure 1.6), a purine nucleoside became the second approved NRTI in 1991 (Brittain, 1993). This inhibitor acts against both HIV-1 and HIV-2. It requires intracellular phosphorylation by cellular kinases to initiate its inhibitory mechanism. Earlier studies have shown DDI to be an effective antiviral drug. However, when used in drug combination with AZT, it has been shown to be more effective. Side effects of Didanosine include diarrhoea, abdominal pain, dose-related peripheral neuropathy, vomiting and nausea.

1.5   Non-nucleoside reverse transcriptase inhibitors and their inhibitory mechanism

Non-nucleoside RT inhibitors (NNRTIs) are an important component of antiretroviral therapy. NNRTIs and protease inhibitors are more potent inhibitors of viral replication than nucleoside RT inhibitors (NRTIs) and integrase inhibitors (Seckler *et al*., 2011). NNRTIs are structurally diverse antiviral drugs that are shown to be less effective to HIV-2. HIV-2 is less readily transmitted and is generally less pathogenic than HIV-1. Given the slow development of immunodeficiency and limited clinical experience with HIV-2, it is unclear whether antiretroviral therapy significantly slows progression. NNRTIs do not inhibit HIV-2 due to the residues at codon 181 and 188 (Tyr181 and Tyr188 in HIV-1; Ile181 and Leu188 in HIV-2) which prevent the drugs from binding to HIV-2 RT (Sluis-Crèmer and Tachedjian, 2008). For this reason, NNRTIs are described as selective inhibitors of HIV-1 reverse transcriptase (Famiglini and Silvestri, 2016). NNRTIs are a group of compounds that are known to act as allosteric inhibitors of RT, thus preventing DNA polymerization. There are 5 compounds that are commonly used against HIV-1 infection. These include: Nevirapine, Efavirenz, Delavirdine, Etravirine and Rilpivirine. NNRTIs differ from NRTIs as they do not mimic or

compete with naturally occurring substrates, instead they bind directly to the hydrophobic binding site/pocket in the palm subdomain of the p66 domain of the RT enzyme. This site is termed the non-nucleoside reverse transcriptase inhibitor binding pocket (NNRTI-BP) and is approximately 10Å from the polymerase active site (Arts and Hazuda, 2012).

NNRTIs block the process of reverse transcription by binding to the NNRTI-BP and altering the mobility of the DNA polymerase allosteric site, more specifically, the thumb subdomain of the RT. NNRTIs are also known to deform a region in the RT, known as the 'primer grip region'. This region functions in correctly positioning the DNA primer in the polymerase active site located in the p66 subunit. Therefore, an alteration in the primer grip region tends to cause a change in template/primer conformation and position, thus blocking formation of a ternary complex. It is also known that the NNRTI binding pocket functions as a bridge between the thumb and palm subdomains. Therefore, any alteration to the binding pocket will affect the functions of the thumb and palm subdomains.

During favourable conditions of DNA synthesis, the RT fits a "closed" conformation bringing the fingers and thumb subdomains closer to the palm subdomain and thus allow for the binding of nucleic acids. However, in the presence of an NNRTI, an open conformation is created that restricts the thumb to a hyperextension position, which prevents the polymerization of DNA (Das *et al*., 2012). It restricts the movement of the thumb subdomain, which prevents the template or primer strands from binding to the polymerization active site. Thus, preventing strand elongation and termination of reverse transcriptase.

It was shown that in the absence of an inhibitor, the aromatic side chains of Tyr181 and Tyr188 in the non-nucleoside RT binding pocket are positioned towards the hydrophobic core. However, in the presence of an inhibitor the two aromatic residues move away from the hydrophobic core thus accommodating space for the incoming inhibitor (Sluis-Cremer *et al*., 2005).

In a study by Das *et al*., (2012) the mechanism of binding interactions of the NNRTI, Nevirapine on RT-DNA was compared with binding interactions of AZTTP on RT-DNA. Upon binding of Nevirapine to the non-nucleoside binding pocket, the two amino acid residues Tyr181 and Tyr188 rotamer conformations are switched off, while β12-β13-β14 part ways from the β6-β10-β9 sheet. The β6-β10-β19 sheet contains the polymerase "catalytic triad" (Asp110, Asp185, and Asp186), while the β12-β13-β14 sheet contains the "primer grip" that keeps the primer strand in position for the incorporation of a nucleotide. With the aid of crystal

structures, the binding interaction of Nevirapine was shown to cause a shift in the primer gap of about 4Å. This caused the shifted primer grip to lift the primer away from the P-site leading to lost interactions with the Tyr183MDD motif (at the polymerase active site).

In a recent study by Lu *et al*., (2011) an analogue of the RT inhibitor Calanolide A, 10-chloromethyl-11-demethyl-12-oxo-calanolide A, also known as (F18) and the NNRTI, Nevirapine were bound by the HIV-1 wild type, Leu100 mutant and Tyr181 mutant RTs separately. Results indicated that Nevirapine showed better binding interactions with wild type RT compared to F18. This was probably due to the rigid structure of F18. The structure of Nevirapine, on the other hand, has aromatic rings that contribute to its hydrophobicity and this property is favourable in the NNRTI-BP and thus formed aromatic interactions with the aromatic side chains of Tyr188 and promoted RT inhibition. The structure of Leu100 mutant RT was altered when bound to F18. The NNRTI-BP is hydrophobic in nature and many hydrophobic compounds will be accommodated. However, in this study, the NNRTI-BP was shifted, indicating that the hydrophobic and aromatic side chains in this site must have shifted causing fewer interaction with the ligand and thus contributing to resistance. The Tyr181 mutant structure showed better spatial flexibility with F18 and resulted in excellent antiviral activity. The change from Tyr181 to a cysteine amino acid residue was shown to contribute to this result.

1.5.1 Commonly used NNRTIs
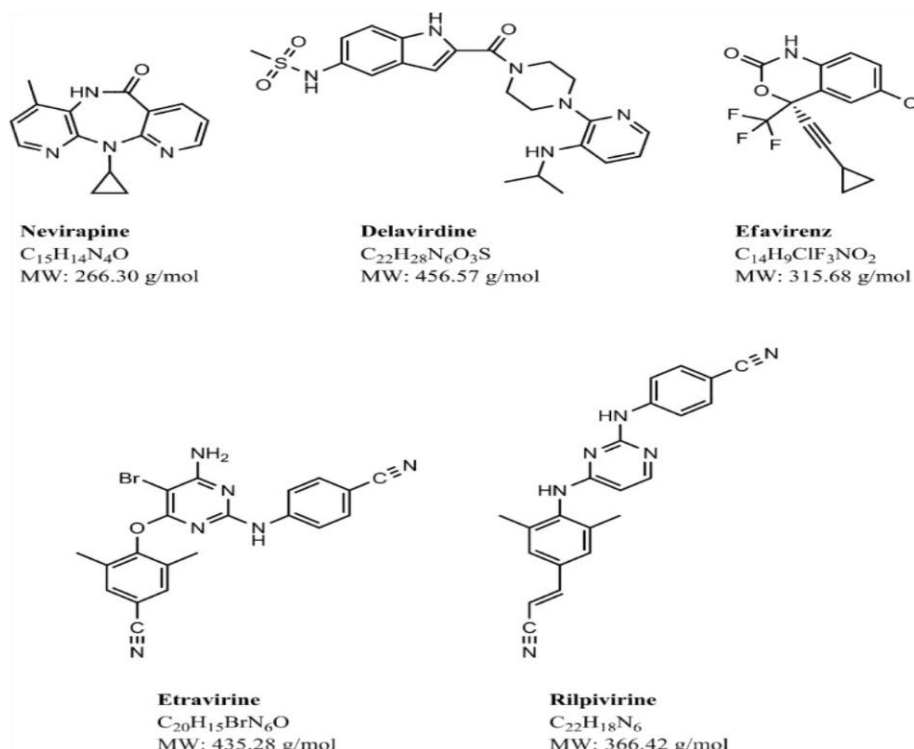
Figure 1.7 Structures of common NNRTIs (Usach *et al*., 2013).

1.5.1.1 Nevirapine (NVP)

Nevirapine (Figure 1.7) was approved by the FDA to be the 9th successful anti-viral drug against the enzyme reverse transcriptase in the year 1996. In a study done by Sluis-Cremer *et al*., (2004), a single dose of Nevirapine was shown to have prevented HIV-1 transmission from mother to child. However, the virus was shown to develop resistance to the drug when administered as an immunotherapy. However, Nevirapine when given in combination with one or more other drugs was shown to be more efficient. This was first validated by Montaner *et al*., (1998) where the combinations of Nevirapine and Zidovudine and Didanosine with Zidovudine were compared with the combinations of Nevirapine, Zidovudine and Didanosine. The triple combination treatment brought about a 51% drop in HIV-1 RNA levels at week 52 in patients, while the duel combinations: Zidovudine and Didanosine, Nevirapine and

Zidovudine showed a drop of 12% and 0% in HIV-1 levels respectively (Montaner *et al.*, 1998). This showed that the outcome of combining three types of drugs was much more effective and superior to that of combing two types of drugs. Although Nevirapine is widely used in the treatment of HIV-1 RT, it is also noted that 5% of individuals treated with Nevirapine develop allergic reactions with symptoms of drug reactions that occur rarely (idiosyncratic drug toxicity) (Isogai and Hirayama, 2016).

1.5.1.2   Etravirine (ETR)

Etravirine (Figure 1.7) previously known as TMC125, is a diarylpyrimidine-based NNRTI that exhibits effective antiviral activity against wild type HIV-1 as well as some viruses that show resistance to some NNRTIs (Wainberg, 2012).

1.5.1.3   Delavirdine (DLV)

Delavirdine (Figure 1.7) belongs to the bis(heteroaryl) pyridinyl group of non-nucleoside reverse transcriptase inhibitors. This compound was first described in 1993, but due to its high toxicity levels and its inability to inhibit human DNA polymerases, it is rarely used in clinical treatment. The structure of delavirdine is extremely bulky and projects from the hydrophobic binding pocket in the reverse transcriptase enzyme (Esnouf *et al.*,1997).

1.5.1.4   Efavirenz (EFV)

Efavirenz (Figure 1.7) is an NNRTI and is a generally safe and highly effective antiretroviral drug. This drug is one of the most commonly prescribed antiviral drugs in the world (Kryst *et al.*, 2015). However, it is also known to cause side effects such as anxiety, insomnia, dizziness and abnormal dreams (Highleyman, 2014). Efavirenz is known to possess a half-life of 40-55 hours (Gaida *et al.*, 2015) and is primarily metabolised in the liver by the CYP450 enzyme

system. The specific isoform within the system most important for the metabolism of Efavirenz is CYP2B6. According to a recent study, 50% of all patients administered with Efavirenz experience at least some of the above-mentioned side effects. This, however only occurs during the first few days of intake and subsides after a few weeks.

In a study by Highleyman, (2014) (http://www.hivandhepatitis.com, Accessed 17/11/2017) the effect of Efavirenz given at different doses was investigated. In this study, two separate groups of participants were orally given 400 mg of Efavirenz and 600 mg of Efavirenz respectively (once daily), on a 48 week analysis. Results, showed equivalent effects between the two groups. After 96 weeks, 90% of participants on each treatment had a reduced HIV RNA <200 copies/mL in an intent-to-treat analysis (ITT). Fewer side effects were also witnessed in participants administered with 400 mg Efavirenz.

ITT involves all the randomized patients in each group that undergo treatment irrespective of the treatment they had initially received, irrespective of withdrawal and irrespective of protocol deviations (Gupta, 2011).

1.5.1.5 Rilpivirine (RPV)

Rilpivirine (also known as TMC278) is a diaryl pyrimidine NNRTI (Figure 1.7). It is one of the few NNRTIs that show strong inhibitory action against wild type and mutant HIV-1 RT at doses of 25-75 mg/day (Das *et al*., 2007).

1.5.1.6 Azvudine

Azvudine, is a cystidine analogue which has shown good inhibition on HIV-1 RT, hepatitis B virus as well as hepatitis C virus. In a study by Wang *et al*., (2014), Azvudine exercised effective inhibition on HIV-1 with EC_{50} (concentration of a drug that gives a half-maximal response) values ranging from 0.03 to 6.92 nM.

1.6 Combination of NNRTIs

In a recent study by Getell, 2015 (https://www.aidsmap.com, Accessed 12/11/2017), Doravirine, belonging to the group NNRTIs, was shown to be as effective as the antiviral drug, Efavirenz, while displaying fewer side effects. In this study, two separate groups of participants were orally given Doravirine and Efavirenz respectively, once daily. Thereafter, 100 mg of Doravirine was administered along with Tenofovir to participants in group one and 600 mg of Efavirenz was given to participants in group two on a 24-week analysis daily. However, after 24 weeks, the overall treatment response showed that 88.9% of patients treated with Doravirine and 87.0% of those who were administered Efavirenz were shown to have a viral load count below 200 copies/ml while the CD4 cell counts were 154 and 146 cells/mm^3, respectively. The similarity of viral load and CD4 counts in the two groups indicated that the two regimens were equally effective. However, Doravirine was shown to cause fewer side effects than Efavirenz.

In a study by Borges *et al*., (2016) NNRTIs were compared with protease inhibitors such as Ritonavir. In this study, clinical investigation using both inhibitors were conducted and showed equal outcomes. This was substantiated by calculating risk ratios or mean differences. In previous studies, NNRTIs exhibited much faster suppression effect on the virus while protease inhibitor, Ritonavir was shown to recover damaged CD4 cells (Ridder *et al*., 2008). In another study by Pozniak, (2000) patients were switched from Indinavir, a protease inhibitor to Efavirenz, a NNRTI because of its short-term toxicity and virologic failure on viral loads.

Other derivatives such as oxochromenyl xanthenone and indolyl xantheone were recently studied as anti-HIV reverse transcriptase inhibitors by Kasralikar *et al*., (2015). Chromene derivatives have been useful inhibitors as they possess anti-HIV pharmacological properties and have shown potent activity against wild type HIV-1 replication. Two DCP (3′ R,4′ R-di-O-(-)-camphanoyl-2-ethyl-2′-2′-dimethyldihydro-pyranol[2,3-f] chromone) analogs, 2,5-dimethyl DCP and 2-ethyl DCP have shown remarkable inhibitory effects on wild type HIV replication as well as on the drug-resistant strains, making chromene derivatives highly potent inhibitors. In this study, structure activity relationship (SAR) plays a major role in revealing the inhibitory mechanism (Kasralikar *et al*., 2015). A planar ring system on these inhibitory structures was shown to be a requirement for the anti-HIV activity against the wild type HIV strains as well as resistant HIV strains. Therefore, with the addition of an indole and coumarin ring onto the xanthenone core, a more planar structure was created. The use of xanthene

derivatives has been extensive due to their diverse properties which include anti-bacterial, anti-viral as well as anti-inflammatory activities. In this study, a one-pot three component reaction of salicylaldehyde, 1,3-cyclohexadione component and a 4 hydroxy chromene (as nucleophile) were used to prepare 4H-chromenes in the presence of 1-hexyl-3-methylimidazolium hydrogen sulfate ([Hmim]HSO$_4$) as a catalyst, which was required in relatively small amounts (Kasralikar *et al*., 2015). Molecular docking studies were also performed to rationalize the structural activity relationship of the compounds as well as to determine the possible binding conformation between the designed compounds and how well they interact with the HIV enzyme. According to the study the most active compounds were the indolyl xanthenone compounds with docking scores of -12.487, -12.457 and -12.256 (kcal/mol) while the native compound was found to be -13.413 (kcal/mol). It was observed that the xanthenone ring structures interacted better with the hydrophobic binding pocket in the presence of hydrogen bonds. The indolyl xanthenone derivatives not only formed hydrogen bond interactions with the Lys101, they also formed π-π interactions in the hydrophobic binding pocket with the aromatic side chain of Trp229. Some compounds showed reduced binding activities due to the lack of hydrogen bond interaction with Lys101. It was also observed that compounds with hydrogen bonding with the side chain backbone of Lys101 as well as π-π interactions with the aromatic side chain of Trp229 displayed improved inhibitory effects.

In a similar study reported by Wang *et al*., (2014), novel substituted nitropyridine derivatives were synthesized and designed via a structure-based core method to evaluate their effects as anti- HIV agents. Results showed that most of the compounds were effective against wild-type HIV-1 with EC$_{50}$ values ranging from 0.056 µM to 0.16 µM. Compounds showed better inhibitory activity than Nevirapine (EC$_{50}$= 0.23).

1.7 Mutations that cause HIV resistance

The discovery of HAART, the combination of two or three drugs from different classes has indeed brought about a drastic decrease in HIV infection over the past few years. This has been a major discovery in the development of anti-HIV protocols. However, these antiretroviral agents tend to leave thousands even millions of dormant or latent T lymphocytes cells that are infected with HIV, which can become active at any time and re-infect healthy CD4 cells (Shan and Siliciano, 2013). For this reason, patients are advised to stay on long term treatment.

However, this serves as a major problem as drug-resistant mutants cause the virus to become less susceptible to the various inhibitors (Hsiou *et al*., 2001). An amino acid substitution in the reverse transcriptase enzyme can often cause resistance to the reverse transcriptase inhibitors. HIV RT lacks the ability to proof read and it is error prone. It has been estimated that a single mutation occurs in every 1000-10000 incorporated nucleotides (Arts *et al*., 2012). When these substitutions occur at different stages of the life cycle, they are carried along during replication and allow the virus to evade the immune system and develop resistance to the various antiviral drugs (O'Brien, 2016).

1.7.1   NRTI Mutations

There are several mechanisms that HIV uses to evade inhibitory effects of NRTIs and NNRTIs. These are: (i) discrimination (ii) primer unblocking (iii) interference between the hydrophobic amino acids that assist in the binding between inhibitor and the hydrophobic binding pocket and (iv) alteration in the size of the NNRTI-BP thus making it less specific for each inhibitor (Asahchop *et al*., 2012).

The first mechanism involves mutations that would prevent the incorporation of NRTIs while allowing for binding of the naturally occurring nucleotide substrates (dNTPs). Thus, the virus continues to multiply and spread throughout the body. The second mechanism involves the excision of NRTIs from the 3′ end of the viral DNA that elongates from the primer; this process is known as primer unblocking (Iyidogan *et al*., 2014). In this process, RT uses ATP or inorganic pyrophosphate (PP_i) as a co-substrate to remove the incorporated NRTI that inhibits the process of DNA elongation. (Iyidogan *et al*., 2014). Similarly, primer unblocking may block the binding of the inhibitor drug into the NNRTI-BP.

In a study done by Yokoyama *et al*., (2010) NRTI-resistant RT was shown to catalyze the synthesis of dinucleoside polyphosphate in the presence of NTP. Thus, the ATP molecule served as a pyrophosphate donor to remove the nucleoside RT inhibitors, thereby allowing for DNA synthesis to resume.

Nevirapine, being a NNRTI, has two major disadvantages as an inhibitor. Firstly, it causes side effects such as rashes, liver problems, nausea, loss of appetite, upper stomach pain, tiredness, fever, unexplained muscle pain or weakness, dark urine, clay-coloured stools, or jaundice

(yellowing of the skin or eyes) and secondly, Nevirapine is known to have a low genetic barrier (Wang *et al*., 2014), which means that a single substitution/mutation can lead to HIV resistance. Some of the major mutations associated with the resistance to Nevirapine have been Tyr181Cys, Lys103Asn and Gly180Ala. In a study reported by Wang *et al*., (2014) a population survey was conducted on patients with HIV infection. Patients were administered with Nevirapine and observed after specific periods. After 6-18 months of treatment 84.8% of patients had their CD4 cell counts over 200 cells/ml while after 72 months of treatment 78.7 % of patients registered CD4 cell counts >200 cells/ml. Viral load on the other hand did not increase for most patients after initial treatment. Single genome amplification sequencing was used to measure the decrease or increase of viral mutations. The first-line ART was proven to be an effective long-term treatment even in the presence of mutations. However, of the three mutations, Lys103Asn is one of the clinically imperative NNRTI mutations, as it causes a 20-50-fold resistance to NNRTI. At the end of this study, it was shown that first-line ART provided effective treatment to patients over 72 months, however, over a long-term period, patients showed resistance towards the treatment due to Tyr181Cys and Gly190Ala mutations.

Resistance to NNRTIs mainly occurs in the allosteric binding pocket situated 10Å away from the polymerization active site. In the case of 8-10 mutations at the binding pocket, reverse transcriptase will show resistance to NNRTIs by preventing the hyperextension of the thumb subunit and thus reducing the binding affinity of nucleic acids to the active site. However, past studies have shown Rilpivirine (TMC278) to adapt to the Lys103 mutation (Nizami *et al.*, 2016). It displayed an ability to act against both the wild type HIV-1 RT and mutant HIV-1 RT. Its flexibility and the hydrogen bond formed by the linker N atoms make Rilpivirine a powerful inhibitor.

Studies by Das *et al*., (2007) have shown crystalized images of TMC278/ HIV-1 RT (ligand-receptor interaction), which revealed that the cyanovinyl group of TMC278 is in a hydrophobic tunnel connecting the NNRTI-binding pocket to the nucleic acid-binding cleft. TMC278 belongs to a family of diarylpyrimidine (DAPY) NNRTIs and is quite effective against mutant and wild type RTs administered at low dosage (25-75 mg/day). In this study, the chemical structure of TMC278 and its inhibitory action against wild type and mutant HIV-1 RTs was compared to other non-nucleoside RT inhibitors and their action against wild type and mutant HIV-1 RT (Table1.1). TMC278 showed a remarkably strong inhibitory effect against the wild type RT (EC_{50} = 0.0004 µM), and the Tyr181Cys (EC_{50} = 0.0001 µM), Lys103Asn (EC_{50} = 0.0003 µM), Leu100Ile (EC_{50} = 0.0005 µM) mutant RTs as well as the double mutant RT,
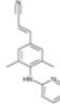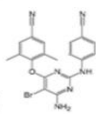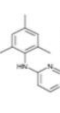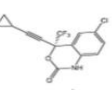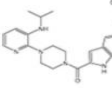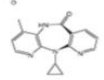
Lys103Asn/Tyr181Cys ($EC_{50} = 0.0008$ µM) (Table 1.1). The TMC125 and TMC120 NNRTIs produced higher EC_{50} values (Table 1.1) and were less effective than TMC 278. The EC_{50} of TMC 278 against the double mutant Leu100Ile/Lys103Asn RT was however an order of magnitude higher (0.008 µM), indicating a marked negative effect on the potency of TMC 278 against this mutant RT.

Entry of TMC 278 into the Leu100Ile/Lys103Asn mutant RT NNRTI-BP is rendered possible by ''conformational wiggling" (torsional flexibility) and ''positional jiggling" (ability to reposition). In this study, the Tyr181Cys mutation causes a loss of aromatic interactions between the Lys103Asn/Tyr181Cys RT and TMC278. However, this is partially compensated by the cyanovinyal group on the TMC278 which forms strong hydrophobic interactions with aromatic side chain of Tyr183.
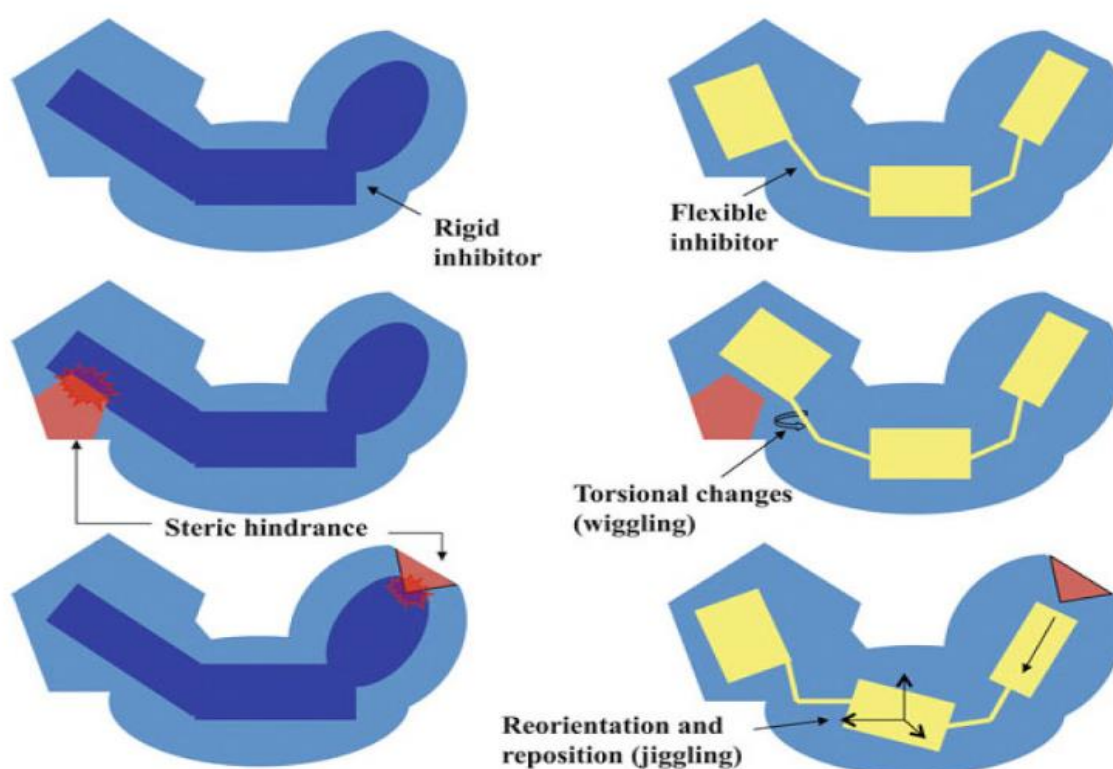
Figure 1.8   Illustrating the strategic flexibility of NNRTIs to handle resistance mutations by conformational wiggling and positional jiggling (Adapted from Das *et al*., 2004).

Table 1.1 Commonly used non-nucleoside reverse transcriptase inhibitors, chemical structures and their EC_{50} values (µM) against wild type and mutant HIV-1 RT. (Das *et al.,* 2007). Amino acid codes: K= Lys, Y=Tyr, L=Leu, N=Asn, C=Cys.

Compound	Chemical structure	Wild-type	K103N	Y181C	K103N/ Y181C	L100I	L100I/ K103N
TMC278		0.0004	0.0003	0.0001	0.0008	0.0005	0.008
TMC125		0.002	0.001	0.006	0.005	0.003	0.01
TMC120		0.001	0.004	0.008	0.044	0.016	>10
Efavirenz		0.001	0.039	0.002	0.04	0.038	> 10
Delavirdine		0.016	>1	>1	>10	>1	N/A
Nevirapine		0.085	>1	>1	>100	0.6	N/A

A unique characteristic of NNRTIs is that they can adopt many conformational modes in the binding pocket, such as 'butterfly' or 'horseshoe' (Nizami *et al*., 2016)(Figure 1.9). In a study by Nizami *et al*., (2016), TMC278 was shown to flexibly change its shape once inside the binding pocket. For this reason, conformational changes in HIV-1 RT resulting from mutations may not necessarily lead to resistance to TMC 278 as this molecule may adopt a shape which is accommodated by the mutant NNRTI-BP. During DNA synthesis, reverse transcriptase forms a closed conformation bringing the fingers and thumb subdomains closer to the active site (Section 1.2), however, in the presence of a NNRTI, the thumb domain is restricted to a hyperextension position, thus preventing the connection of nucleic acid and template DNA into the catalytic site. Therefore, the distance between the amino acids on the fingers and thumb sub domain were measured in the presence of TMC278. It was shown that the distance between the fingers and thumb sub domains of HIV-1 RT and mutated HIV-1 RT in the absence of TMC278 were low (43.9 Å and 37.5Å, respectively), while, HIV-1 RT and mutated HIV-1 RT in the presence of TMC278 were higher (52.2 Å and 44.6 Å, respectively) (Figure 1.8).

Tivirapine

RT- bound

Extended linker

Lipophilic site

Benzene ring

Extended π- system

108°–115°

'Butterfly-like' model

'U' or 'horseshoe' model

A   **B**
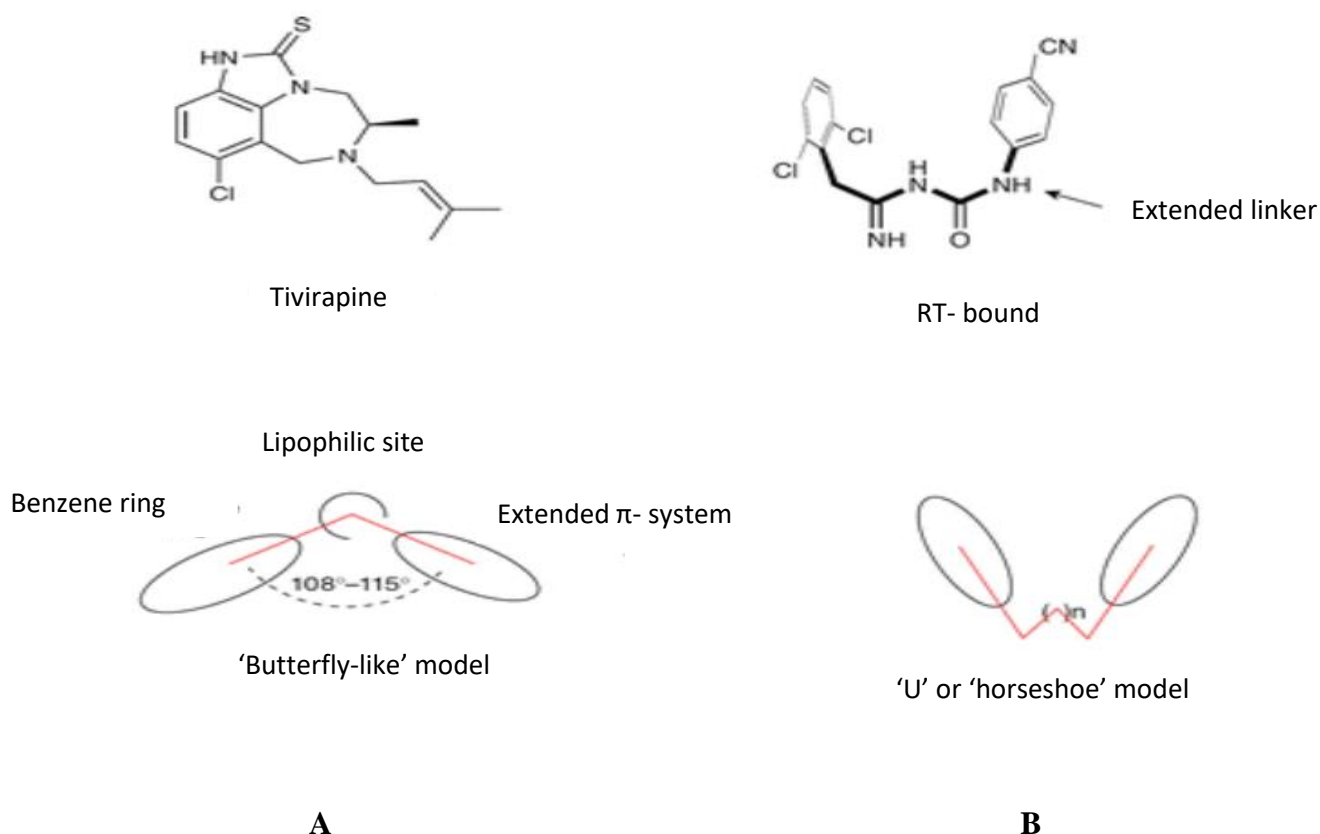
Figure 1.9   Illustrating different conformational modes in the binding pocket **(A)** butterfly-like model **(B)** Horseshoe model. (Adapted from Regina *et al*.,2010).
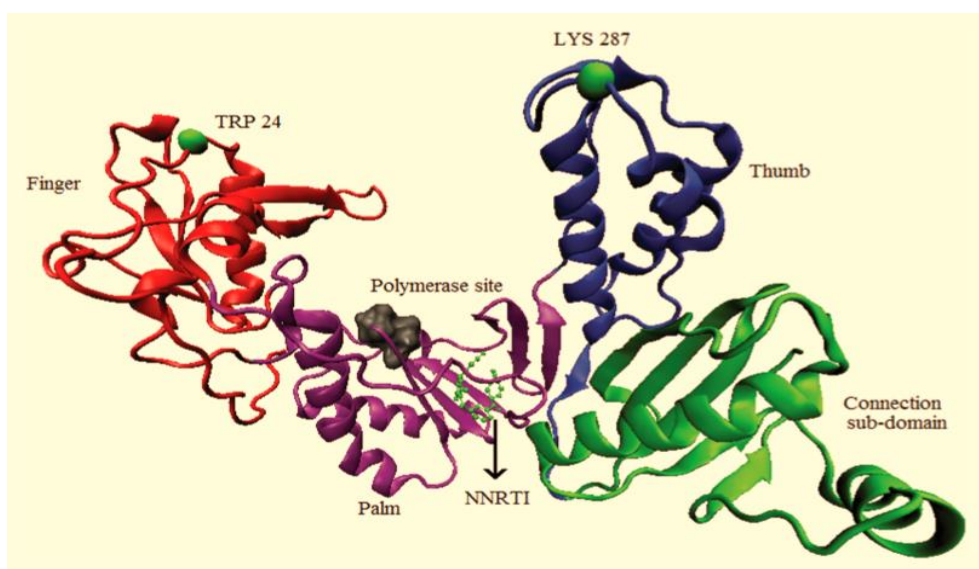
Figure 1.10   Conformation of the subdomains of the HIV-1 RT subunit with NNRTI Riplivirine accommodated in the hydrophobic binding pocket. Trp24 on the finger subdomain and Lys287 on the subdomain are represented by green circles. Adapted from (Nizami *et al.,* 2016).

In another study undertaken by Zhang *et al*., (2016), two mutations, Leu228Ile and Tyr232His were found to have caused resistance to the drug Etravirine. However, Leu228Ile in combination with mutation Tyr188Cys revealed a high level of cross-resistance to both Efavirenz and Nevirapine. Moreover, other combinations, such as Tyr232His and Ala139Val also showed moderate resistance to Efavirenz and Nevirapine (Zhang *et al*., 2016). It was concluded that the combination of mutations caused higher levels of resistance compared to those observed with a single mutation. Therefore, combination (two or three drug) treatment is most reliable.

1.8 Chiral Inhibitors

One of the major causes of treatment failure in HIV infection is drug resistance, and the combination of selected drugs has emerged as a powerful means of combatting this problem (Bock and Lengauer, 2012). In a second approach, new drugs are being designed to bind to both the active site and NNRTI-BP simultaneously (Iyidogan, 2013). This class of 'chiral' drugs may therefore be less likely to lead to drug resistance. The approach of joining two types of HIV inhibitors targeting two different sites in the HIV-1 RT has received attention over the past 20 years (Muhanji *et al*., 2007). In a previous study by van Zyl *et al*., (2010) chimeric compounds comprising a nucleotide component separated from a hydrophobic amino acid derivative by a hydrophobic spacer element have shown promising activity against Moloney murine leukaemia reverse transcriptase (M-MuLV RT). The synthesis of various N-tritylated para substituted phenylalanine derivatives (fluoro, nitro and iodo) coupled to the 8-(6-aminohexyl) amino-adenosine 3′,5′-cyclic monophosphate was designed to form a chiral compound, where the 8-(6-aminohexyl) amino-adenosine 3′,5′-cyclic monophosphate would bind to the polymerization active site, while the tritylated para substituted phenylalanine would serve as the non-nucleoside and bind to non-nucleoside hydrophobic binding pocket, simultaneously. It was reported that all three compounds displayed inhibitory effects on the reverse transcriptase with IC_{50} values ranging between 1 µM and 65 µM. The strongest inhibitor was the para-iodo compound ($IC_{50} = 1$ µM), while the weakest were the para-fluoro and para-nitro compound with IC_{50} values of 65 µM and 45 µM respectively. It was also noticed that as the atomic radius of each atom increased, so did its inhibitory activity. Thus,

iodine with an atomic radius of 1.33 Å had the strongest inhibitory effect on reverse transcriptase. It is interesting to note that the polymerase site of the monomeric M-MuLV RT has remarkable similarities to the polymerase site of the heterodimer HIV-1 RT (Cote and Roth, 2008).

However, it was reported by van Zyl *et al*., (2010) that the chimeric compounds N-tritylated meta-fluoro-DL-phenylalanine-8-(6-aminohexyl)amino-adenosine3′,5′-cyclic monophosphate acted as a non-competitive inhibitor. Thus, it was concluded that other sites on the M-MuLV RT may not be involved in the binding of this N-tritylated compound. It was therefore of interest to examine the efficacy of related compounds in an HIV-1 RT system following the encouraging results obtained in the M-MuLV RT assay. In this study attention has been focused on the effect of para halo substituted phenylalanines (fluoro, chloro, bromo, iodo) linked to 8-(6-aminohexyl)amino-adenosine 3′,5′-cyclic monophosphate on the DNA polymerase activity of the HIV-1 RT *in vitro*.

The structures of RT on the p66 subunit of HIV-1 and the Moloney murine leukemia virus reverse transcriptase (M-MuLV RT) are similar (Cote and Roth, 2008). Therefore, to study inhibitory effects of certain compounds on HIV-1 RT, many studies have been carried out on the M-MuLV counterpart. In a study undertaken by Hawtrey *et al*., (2008), three N-acyl derivatives of 8-(aminohexyl) amino-5′-AMP were prepared: (i) palmitoyl derivative, (ii) nicotinyl derivative, (iii) bis-nucleotide with glutaryl spacer. These non-nucleotide compounds were attached to the nucleotide component via a spacer, thus affording chimeras (Hawtrey *et al*., 2008). In a poly A template-oligo dT primer extension assay using [^{3}H] dTTP and M-MuLV RT, all three putative chimeras were inhibitory at 10^{-4} M, with 8-(6-aminohexyl) amino-5′-AMP-nicotinamide displaying the highest activity 60 % inhibition at 10^{-4} M while dropping to 35% inhibition at 10^{-5} M.

It was concluded that attachment of certain groups to the aminohexyl side chain of the nucleotide component led to inhibitory effects on DNA polymerase activity of the M-MuLV. Other larger, hydrophobic groups were also attached to a nucleotidyl component and their effects on reverse transcriptase enzyme of M-MuLV were examined. The attachment of N-trityl amino acids; phenylalanine, glycine to the 8-(6-aminohexyl) amino-5′-AMP nucleotide was therefore carried out. Inhibition concentrations (IC_{50} values) were calculated for each compound to determine their effects on the incorporation of [^{3}H dTTP] in a poly (rA) - d(pT)$_{16}$ template primer using M-MuLV RT. This study showed that attachment of a bulky

hydrophobic N-trityl aminoacyl moiety to the 8-(6-aminohexyl) amino-5′-AMP via a spacer, resulted in higher inhibitory activity than the starting N-trityl amino-acid alone. Possible reasons that contributed to this effect include (i) phenylalaline may bind to the hydrophobic binding pocket of the RT enzyme, (ii) the spacer between the purine ring and trityl group is approximately 10 Å, which is the same distance between the polymerase active site and the hydrophobic binding pocket. This study concluded that the more hydrophobic aromatic structures bound to the non-nucleoside binding pocket and were more effective in their inhibitory activity on the M-MuLV RT.

1.9   Characterization methods

1.9.1   Nuclear magnetic resonance spectrometry (NMR)

 Nuclear magnetic resonance (NMR) has become a common method for studying HIV-1 RT and its ability to bind to specific anti-viral drugs (Thammaporn *et al*., 2015). The use of NMR spectroscopy in drug screening was first described by Shuker *et al*., (1996) and is currently one of the main techniques used in the development of anti-viral drugs. One of the main advantages of NMR, apart from providing information on structure, is its ability to provide information on the molecular interactions at the atomic level (Pellecchia *et al*., 2008). This is very advantageous, especially in the design of drugs to determine the binding abilities of a protein or ligand. NMR spectrometry affords detailed information for compound atoms of structures in the form of signature chemical shifts. The chemical shift is highly sensitive to the environment around the atom and this produces information on how well certain compounds bind and interact with other molecules. The use of NMR in the analysis of large proteins has been and is still a challenge. However, this method is increasingly popular in the identification of small molecules as well as the validation of molecule binding (Dias *et al*., 2014).

1.9.2   Ultra violet (UV) spectroscopy

UV spectroscopy is one of the easiest, fastest and most accurate tools used in pharmaceutical analysis and drug discovery. (Behera *et al.*, 2012). The absorbance of a solution depends on the concentration of the compound (c), Molar absorptivity (ε), and the path length of the sample (l). The above parameters form the Beer's law, which states that the extinction co-efficient/molar absorptivity is constant and the absorbance is directly proportional to the concentration of compound dissolved in a solution and measured at a given wavelength. As light passes through a solution, the amount absorbed at various wavelengths is measured. UV spectra in the range 210-320 nm are of particular importance in the characterization of aromatic compounds.

1.9.3   Mass Spectrometry (MS)

Mass spectrometry (MS) was developed in 1913 by J. Thompson, but only became commercially available in 1918 after A.J Dempster's development of the modern mass spectrometer (Griffiths, 2008). Over the past decade, MS has become an essential analytical and quantitative tool in drug design used to detect, identify and quantitate simple as well as complex chemical compounds as they are ionized into charged molecules based on their mass to charge (m/z) ratio (Singhal *et al.*, 2015). MS may also determine a compounds molecular weight with a very high degree of accuracy. Laser desorption in combination with time of flight (TOF) was commonly used for molecule analysis. However, its limitation is that it can only measure the masses of small molecules (<1000 Da). Thereafter, the development of matrix-assisted laser desorption ionization (MALDI) in association with TOF, commonly known as MALDI-TOF MS method and electron spay ionization (ESI) increased the applicability of MS to large biological molecules such as proteins (Singhal *et al.*, 2015) and allowed better analysis of compounds over a broad size range. MALDI-TOF has many qualities that contribute to its wide use. For example, further purification of samples is not required as it has a high sensitivity rate. Furthermore, only an extremely small volume of sample solution (1µl) is needed and the process is not time consuming, requiring approximately 20 minutes (Smolira and Szponder,2015).
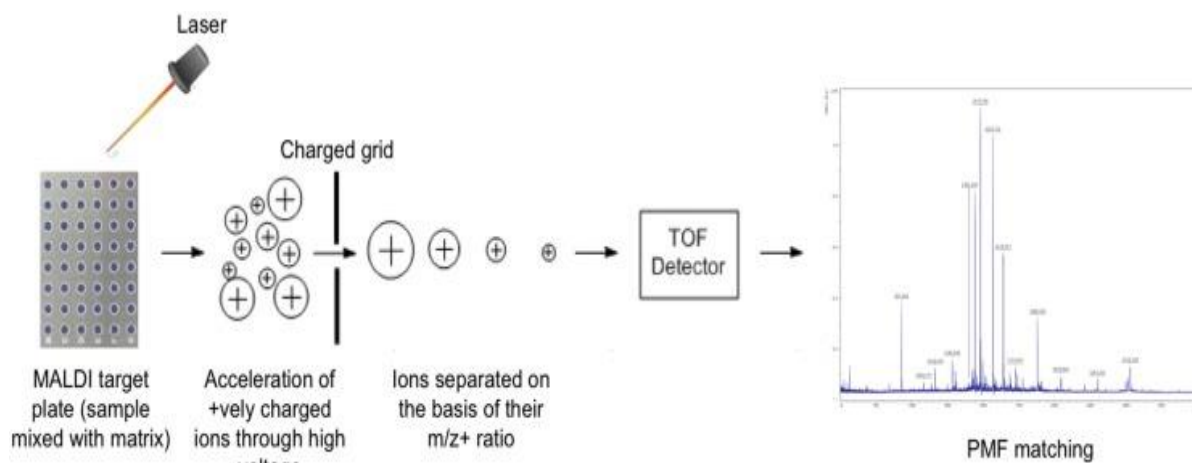
Figure 1.11   Mechanism of work-flow in a MALDI-TOF MS (Singhal *et al.*, 2015).

1.9.4   Computational Molecular Modelling

Currently, computational methods are an important part of drug design and this kind of modeling is often referred to as computer-aided drug design (CADD). Computational methods can offer detailed information about the interaction between compounds and targets, increasing the efficiency and lowering the cost of research in several stages of drug discovery. Knowledge of the relationship between structural characteristics of compounds as well as their biological properties is extremely important as this determines the activity of future drugs against specific viruses and diseases. This specific process is called Quantitative Structure-Activity Relationship (QSAR), and is defined as the mathematical modeling of chemical structures of compounds and their relationship with biological properties (Nizami *et al.*, 2015). Docking allows us to accurately predict the best interactions and conformations of a ligand within an enzyme binding site by using a score function to estimate the binding strength between the two (Ramírez, 2016). Programmes commonly used in such studies are listed in Figure 1.10.
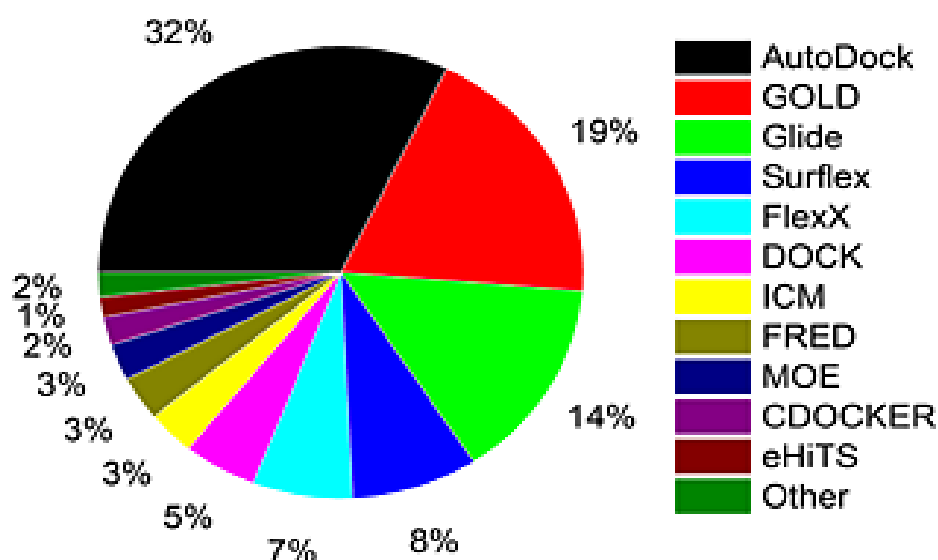
Figure 1.12 Various docking programmes (%) commonly used (Yuriev *et al*., 2013).

In a study carried by Santos *et al*., (2015), it was shown that the development of resistance of HIV-1 to NRTIs and NNRTIs can be rapid. Thus, rendering some of these antiviral drugs ineffective. In recent studies, computational methods are being adopted as they yield detailed information about the compounds and their target sites, as well as, the interactions between them. Despite their inhibitory effects on HIV-1, all antiviral drug activities are limited by factors such as mutational changes in the respective target sites (the polymerase active site and hydrophobic binding pocket) and toxicity to the patients leading to long term difficulties. Therefore, when combining *in vitro* work with computational programming and crystal structures of compounds, their complexity provides clear molecular understanding on the interactions between the target sites and the drug compounds. One of the commonly used computational methods in science research is molecular docking. In a study by Kasralikar *et al*., (2015), computational studies helped in the discovery of binding interaction between oxochromenyl xanthenone and indolyl xantheone derivatives to a common RT enzyme. In the design and synthesis of drug compounds, *in vitro* work alone is not sufficient for the identification of probable *in vitro* activity. For this reason, molecular docking in silico studies are being used increasingly to explain and complement experimental data and to provide virtual screening in drug design.

In a study by Miceli *et al*., (2013) marine diterpenes were investigated as inhibitors of wild-type and mutant HIV-1 reverse transcriptase using docking studies. Three isolates from

36

Dictyota species: diterpenes dolabelladienotriol (THD), (6R)-6-hydroxydichotoma-3,14-diene-1,17-dial (HDD) and (6R)-6-acetoxydichotoma-3,14-diene-1,17-dial (ADD) were docked into wild type and mutant RT. Docking studies showed that there existed van der Waals interactions between ligand and specific amino acid residues such as Lys101, Lys103, Leu100, Gly190, Phe227, Val106, Val179, Tyr181, Val189, Leu234, His235, Pro236 and Tyr318. Moreover, compounds formed hydrogen bond interactions with the aromatic side chain of Tyr188 and the Glu138 residue. As previously reported by Nizami *et al.*, (2016) most NNRTIs can adopt a ''butterfly'' or ''horseshoe'' shape to facilitate accommodation in the allosteric BP. However, in this study HDD showed a weak interaction with HIV-1 RT as it showed no signs of the butterfly-like characteristics, such as interaction with hydrogen bond donors and acceptor groups in the area surrounding K101 and hydrophobic residues Tyr188, Tyr181 and Trp229. ADD on the other hand showed van der Waals bonds with Tyr181, Tyr188, Leu100, Val106, Val179, Val189 and Gly190 as well as a hydrogen bond with Lys101. This is probably due to the acetoxy group in its structure. The last ligand, THD showed two hydrogen bonds with Tyr188, one hydrogen bond with Lys101 as well as van der Waals interactions with Leu100, Lys103, Val106, Val179, Ile180, Tyr181, Trp229, Leu234, His235, Pro236 and Tyr318 residues. The general orientation of an NNRTI is stabilized by hydrogen bonding with Lys101 as well as π-π stacking with the aromatic side chain residues such as those of Tyr181 and Tyr188. (Miceli *et al.*, 2013). The structure of THD is unrelated to those of ADD and HDD and ππ interactions with the aromatic ring of Tyr181 were absent (Figure 1.13). This is a unique conformation that allows the molecule to form van der Waals interactions with a larger number of residues including Trp229, a highly-conserved residue of the binding site.
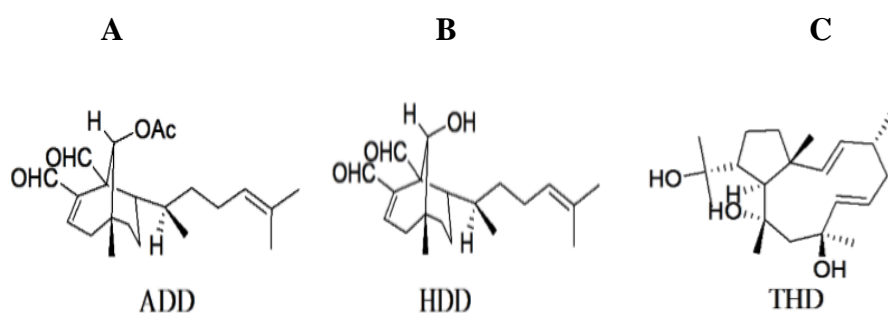
Figure 1.13 Chemical structures of **(A)** (6R)-6-acetoxydichotoma-3,14-diene-1,17-dial (ADD), **(B)** (6R)-6-hydroxydichotoma-3,14-diene-1,17-dial(HDD) and **(C)** diterpenes dolabelladienotriol (THD). Adapted from Miceli *et al.*, (2013).
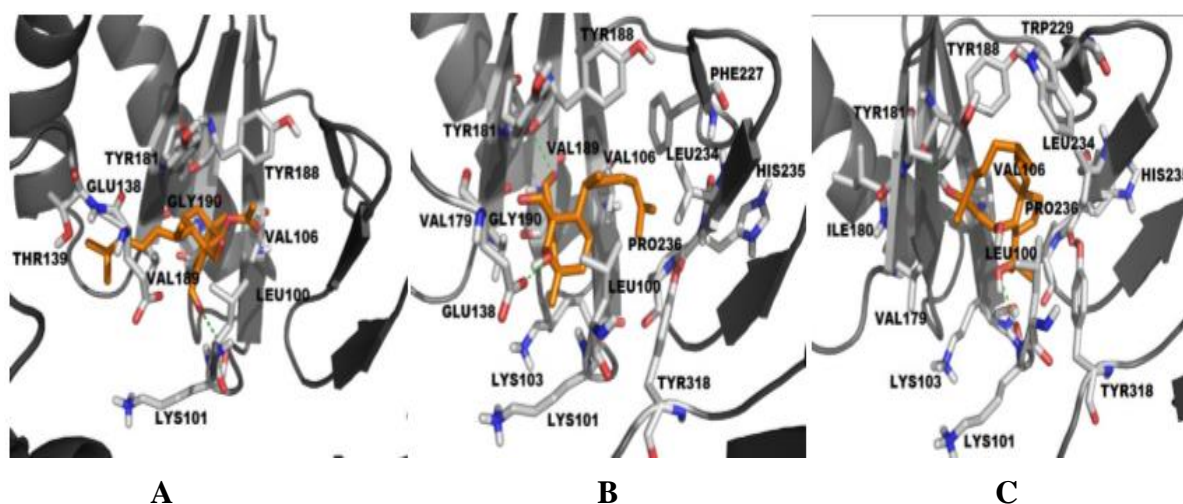
Figure 1.14 Docking complexes of **(A)** ADD, **(B)** THD and **(C)** HDD (orange) bound to HIV-1 RT enzyme (grey) showing hydrogen bonding (blue) and van der Waals interactions (red) with specific NNRTI-BP residues. Adapted from Miceli *et al*., (2013).

In a study reported by Das *et al*., (2004), the NNRTIs Tivirapine, Loviride, and Nevirapine were separately docked with the HIV-1 RT enzyme. With the help of structure activity relationship/ molecular docking studies, key design features of bonding interactions and modes of bonding were observed. Despite their structural diversity, all three inhibitors were bound to the NNRTI-BP through interactions between their aromatic rings and the aromatic side chain of Tyr181.

In a recent study, Seniya *et al*., (2015) described the inhibitory effects of herbal compounds of 4-thiazolidinone against HIV-1 reverse transcriptase activity. As seen below (Figure 1.15) the NNRTI 4-thiazolidinone was shown to locate and interact with the three key apartate residues (Asp110, Asp185, Asp186) of the polymerase active site.
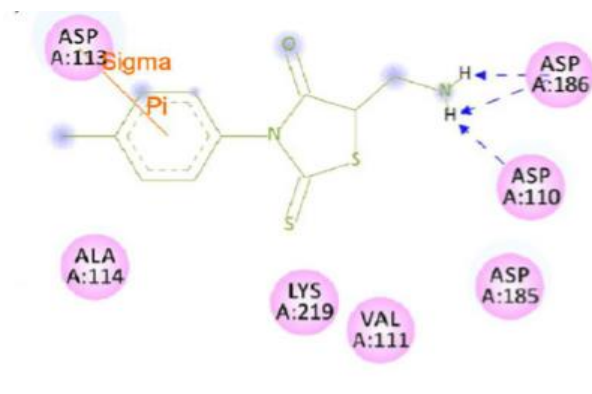
Figure 1.15   A 4-thiazolidinone derivative (1656714) forms interactions with aspartate residues (Seniya *et al*., 2015).

In another study by Esposito *et al*., (2011) Alizarin derivatives and their effect on HIV-1 reverse transcriptase-associated DNA polymerases were analysed using docking studies. Anthraquinones (AQs) are secondary metabolites occurring in bacteria, fungi, and lichens and Alizarin, a member of this class of natural products has shown an inhibitory effect against reverse transcriptase RNA-dependent DNA polymerase (RDDP) activity. Interactions between the derivative K-49 with wild-type RT is shown in (Figure 1.16). More particularly three of the four benzene rings, highlighted below, were shown to enter the binding pocket resulting in favourable interactions with the hydrophobic residues Tyr188, Leu100, Phe227, Val106, Tyr318 and Leu234. In addition, the central aromatic planer ring was shown to form π-π interactions with the aromatic side chain of Trp229.
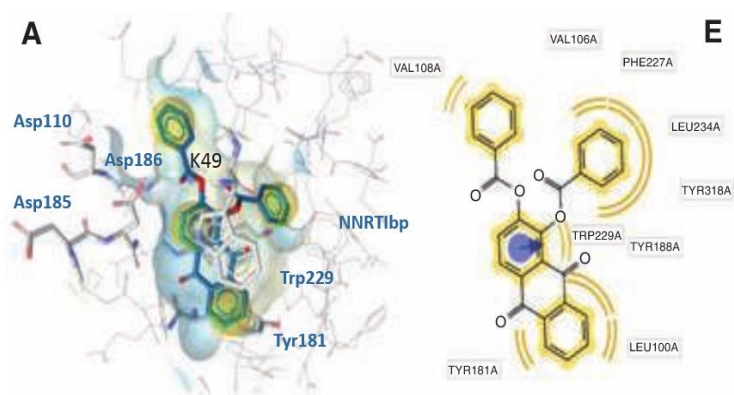
Figure 1.16   2D Structure of **(A)** Alizarine derivative K-49 docked into wild type RT **(E)** Alizarine derivative K-49 showing possible binding interactions with Tyr188, Leu100, Val106, Phe227, Tyr318, Leu234. (Esposito *et al*., 2011).

In a study by Yang *et al*., (2008) 4-ethynyl Stavudine triphosphate (4′-Ed4T), a Stavudine analogue, showed better inhibitory action against HIV-1 RT than Stavudine (d4T). 4′-Ed4T showed five-fold higher potency against HIV-1 replication and lower cytotoxicity than d4T in the cell culture studies that were performed. Docking studies revealed that the analogue engaged in a better binding interaction with HIV-1 RT than the 'parent' inhibitor. This was attributed to the two hydrogen bond interactions formed between the 3′-OH group of (4'-Ed4TTP) with the amide residue Tyr115 and the side chain of residue Gln115. It was also suggested that nucleotide analogues that lack a 3′-OH group have poor binding interactions at the catalytic active site through loss of hydrogen bonding.

1.9.5   Principle of HIV-1 Reverse Transcriptase Assay

Commercially available kits such as a colorimetric HIV-1 Reverse Transcriptase Assay kit are commonly used for quantitative determination of reverse transcriptase activity *in vitro*. In the past radiochemical assays were commonly used to assay for RT activity. However, since these probes contained radioactive isotopes (typically [^{32}P]), this was deemed to be a disadvantage since labels were characterized as unstable, had a short shelf-life and were extremely costly to dispose of (Mansfield *et al*., 1995). For these reasons, alternative protocols, such as colorimetric assays were developed, as detection techniques.

The assay adopted in this study used a poly (A)-oligo (dT)$_{15}$ template-primer system. The detection and quantification of the synthesized DNA as a parameter for RT activity was followed, using a sandwich ELISA protocol: (i) Biotin/digoxygenin labelled DNA bound to a microtitre plate already pre-coated with biotin-binding streptavidin; (ii) This was followed by incubation with an anti-digoxigenin antibody, conjugated to the enzyme peroxidase; (iii) In the final step, the peroxidase substrate, ABTS, was added to reaction mixtures and the green coloured oxidation product was measured using an ELISA plate reader to indicate the extent HIV-1 RT activity.
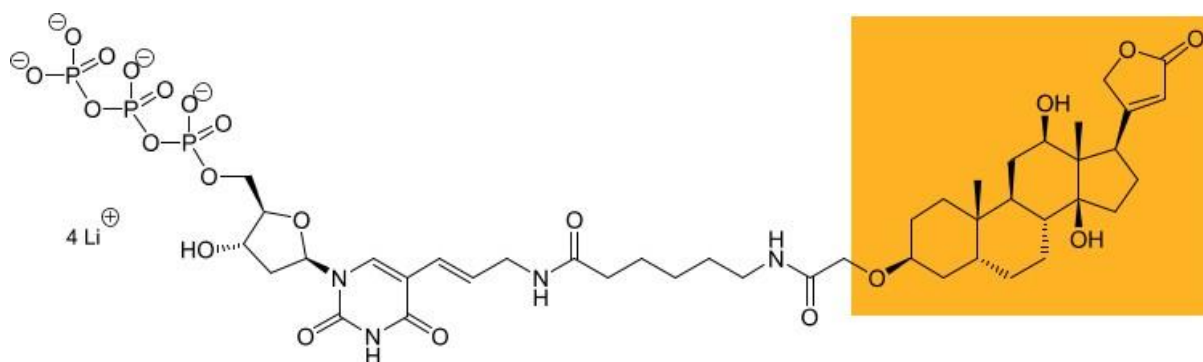
A
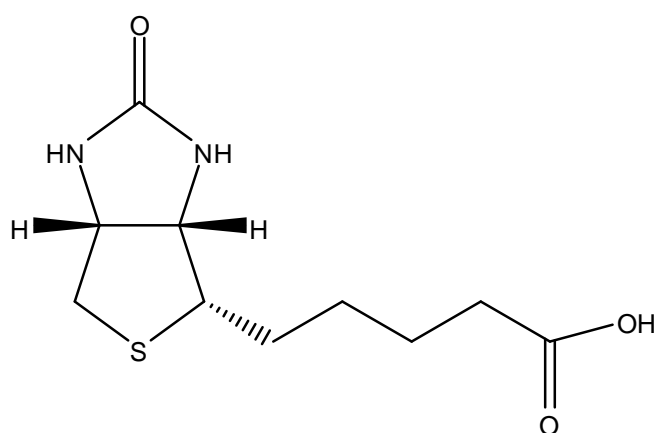
B

Figure 1.17   Structures of: **(A)** digoxigenin-dUTP (DIG-dUTP) indicated in the orange box and **(B)** D-(+)-biotin (only biologically active isomer of 8 possible isomers).

Nucleotide tags such as biotin (300 Da) and digoxigenin (391Da), which is found in certain members of the Digitalis germs (foxgloves) (Chevalier *et al*., 1997), have increasingly replaced radioactive nucleotides in recent years. Many are the advantages of biotin and digoxigenin as labels for nucleic acids. These include their size (they are relatively small) and their stability and safety. Due to the rapid rate of reverse transcription by the RT enzyme and the small size of these tags, they may be easily incorporated into the growing DNA template strand in a DNA/RNA heterodimer. Thus, instead of utilizing thymidine triphosphate alone as a building block, 5'-biotinylayted deoxyuridine-5'-triphosphate and 5'-digoxigeninylated uridine-5'-triphosphate are also used as substrates.

Biotin labelled RNA/ DNA duplexes are anchored to microtitre plates using streptavidin. Streptavidin forms one of the strongest non-covalent interactions with biotin. It can bind up to

four biotin molecules at a time. There is a high shape complementarity between the binding pocket of streptavidin and biotin. Secondly, there is an extensive network of hydrogen bonds formed with biotin when in the binding site. On the other hand, digoxigenin labeled RNA/DNA is visualized by the attachment of anti-digoxigenin antibody conjugated to a horse radish peroxidase enzyme (HRP).
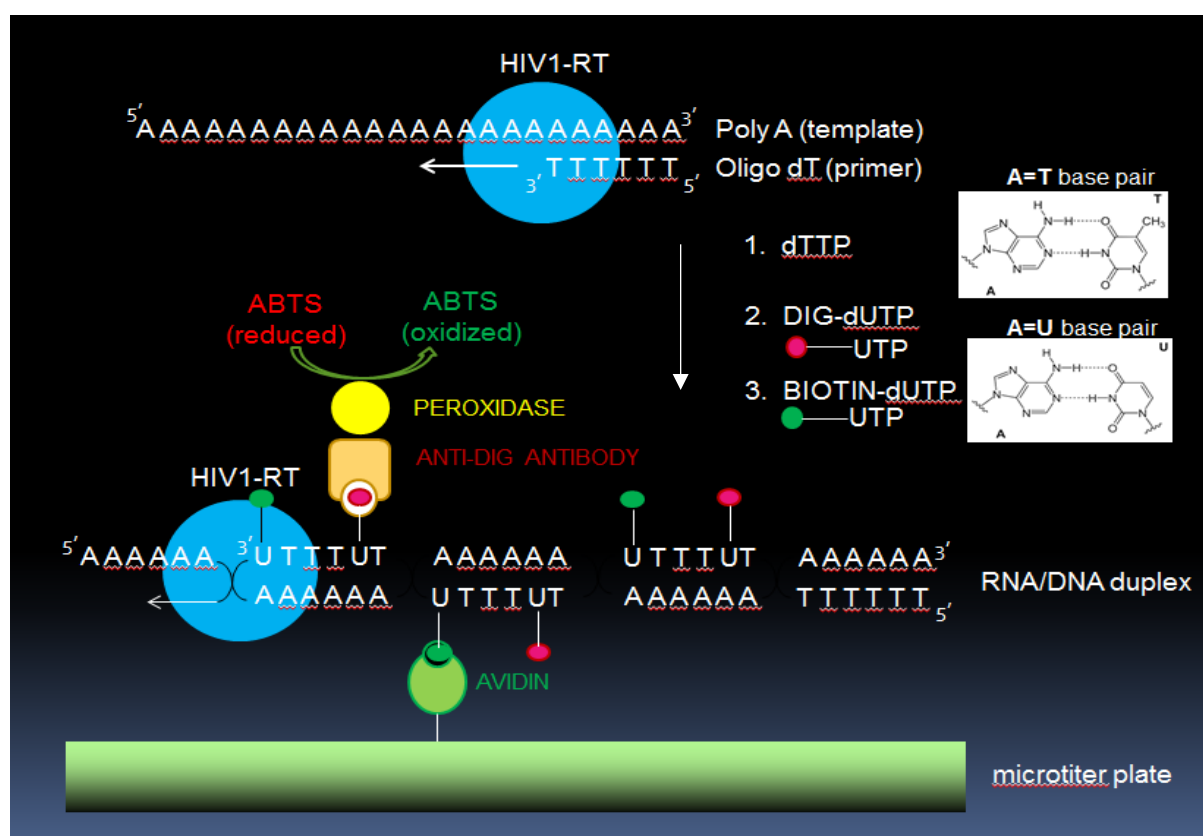
Figure 1.18   Colorimetric HIV-1 reverse transcriptase assay

Apart from reverse transcriptase colorimetric and radiochemical assays, other methods have been used for the detection of reverse transcriptase activity. Sharma *et al*., (2015) developed a continuous, real-time reverse transcriptase assay in which RT-catalysed polymerization was monitored using Förster Resonance Energy Transfer (FRET). Although RT is a major target for anti-viral drug therapy, certain proteins in the HIV-1 transcription complex, which promote RT activity may also be considered in this regard. For instance, HIV-1 nucleocapsid protein NCp7, a 55-amino acid protein (Sharma *et al*., 2016) is known to stimulate reverse transcription in the reverse transcription complex (RTC). For this reason, NCp7 can be targeted to decrease RT polymerization activity. The assay that was used in this study was shown to distinguish

between NRTIs and NNRTIs by monitoring changes in FRET signals. However, this does not permit the assay of wild-type and mutant HIV-1 RTs as a mutant with a single accessible Cys fluorophore is required in the assay. For this reason, a commercially available template/ primer in a novel one-pot, one-step assay was used. This assay was used to determine the potency of the NRTI, AZT and Nevirapine. IC_{50} values for AZTTP were found to be 7 ($\pm$1) μM and 6 ($\pm$1) μM for k_{obs1} and k_{obs2}, respectively, while IC_{50} values for Nevirapine calculated from k_{obs1} and k_{obs2} (Observed kinetic rate constants) were found to be 71 ($\pm$8) nM and 74 ($\pm$9) nM respectively and in good agreement with published values (Sharma et al., 2016). This versatile assay has the design capacity to measure and distinguish the inhibitory effects of NRTIs and NNRTIs, and of those agents acting against the RNA- dependent DNA polymerization activator protein NCp7.

1.10   Rationale framing the entire study

One of the most significant treatments in HIV-1 infection has been the combination of drugs targeting the HIV life cycle with the aim of preventing further destruction of the host immune system (Gungarth *et al*., 2014). In a study by van Zyl *et al*., (2010), chimeric compounds comprising a nucleotide component separated from a hydrophobic amino acid derivative by a hydrophobic spacer element have shown promising activity against M-MuLV RT. One of the major causes of treatment failure of HIV infection is drug resistance, and the combination of selected drugs from different classes has emerged as a powerful means of combatting this problem (Bock and Lengauer, 2012).

This research addresses the design, synthesis, *in vitro* evaluation and *in silico* analysis of putative HIV-1 reverse transcriptase (RT) inhibitors. Inhibitors included in this study comprise two structurally diverse elements viz: a nucleotide component and a hydrophobic tritylaminoacyl component. This class of bidentate drugs may therefore be less likely to lead to drug resistance.

1.11   Aims and objectives

The purpose of this study is to design, synthesize and investigate the efficacy of certain novel chimeric inhibitors of HIV-1 reverse transcriptase.

Objectives:

i.   To synthesize and characterize a series of putative HIV-1 reverse transcriptase inhibitors embodying structural elements directed to the enzyme polymerase active site and the NNRTI-binding pocket.

ii.   To assess the inhibitory capabilities of the novel compounds against recombinant HIV-1 RT in a non-radioactive microtiter plate colorimetric assay, and to compare their *in vitro* inhibitory effects with those of Nevirapine, a front-line NNRTI in current use.

iii.   To carry out computer simulations regarding the association of the chimeric inhibitors with HIV-1 RT and to compare predicted associations with laboratory findings.

iv.   To assess findings and to recommend further structural development for potentiation of activity

CHAPTER TWO

MATERIALS AND METHODS

2.1 Materials

2.1.1 Chemicals and reagents

N-hydroxysuccinimide (NHS, $C_4H_5NO_3$), diethylamine ($C_4H_5NO_3$), methanol (MeOH, CH_3OH), absolute ethanol (EtOH, C_2H_6O), trityl chloride (TrCl, $C_{19}H_{15}Cl$), N, N′-dicyclohexylcarbodimide (DCCI, $C_{13}H_{22}N_2$), deuterodimethylsulfoxide (deuterated DMSO, C_2D_6OS) (99.9%) containing 1% tetra methylsilane and Methanol-d_4 (CD_3OD) (99%) were obtained from Aldrich Chemical Company (Milwaukee, Wis, USA). Silica gel $60F_{254}$ chromatography glass plates, dimethylsulfoxide (DMSO, C_2H_6OS), diethyl ether ($C_4H_{10}O$), pyridine (PY, C_5H_5N), sodium sulphate (Na_2SO_4), chloroform ($CHCl_3$), petroleum ether (60-80° C) and isopropanol (C_3H_8O) were supplied by Merck (Darmstadt, Germany). HIV-1 Reverse transcriptase assay, colorimetric kit (Cat. No. 11468120910) was purchased from Roche (Basel, Switzerland). All glassware used was cleaned in chromic acid and rinsed thoroughly and excessively with distilled H_2O and deionised 18 Mohm water (Milli-Q500) prior to use.

All other reagents were of AnalaRgrade from BDH Chemicals Ltd (Poole, England).

N-trityl-para-halo-DL-phenylalanines had been previously prepared in our laboratory by a method adapted from that of Zervas and Theodoropoulos (1965).

2.2   Methods

2.2.1   Drug design and synthesis

In designing the proposed HIV-1 RT inhibitors (Figure 2.1) two structurally diverse regions of widely diverging polarity and which are separated by a spacer element were envisioned. Thus, (4a-e) comprise of the strongly hydrophobic and bulky triphenyl methyl (trityl) group attached to the amino function of the hydrophobic para-halo-substituted-DL-phenylalanines (1b-e) and L-phenylalanine (1a). These components were intended for accommodation in the allosteric hydrophobic pocket of HIV-1 RT. In turn, the trityl amino acid derivatives are attached via their carboxyl groups to the terminal amino group on the spacer, 1,6 diaminohexane through an amide link. The second terminal amino group on the spacer is attached to the adenyl 8 position of adenosine 3′,5′-cylic-monophosphate to afford a family of N-trityl-phenylalanyl 8-(6-aminohexyl) 3′,5′-cylic-monophosphate (4a-e). The nucleotidyl component was included for possible additional anchorage to a hydrophilic region at or near the HIV-1 RT polymerization site.

2.2.2   Synthesis of N-trityl-L-phenylalanine (Figure 2.1, 2a)

Synthesis of N-trityl-L-phenylalanine derivative was adopted from the method described by Zervas and Theodoropoulos (1956) and performed in the laboratory in the biochemistry department, UKZN. Briefly, L-phenylalanine (495.6 mg, 3 mmol) was dissolved in 1.8 ml diethylamine (18 mmol), water (1.8 ml) and isopropanol (6 ml). To this solution trityl chloride (1.1783 g, 4 mmol), was added in 10 equal portions with stirring and the reaction mixture was left overnight at room temperature on a magnetic stirrer. To the turbid reaction mixture was added chloroform ($CHCl_3$) until two clear layers were observed. With the use of a separating funnel the $CHCl_3$ layer was separated from the aqueous layer and to it was added sodium sulphate to remove residual water leaving a clear yellow solution. Solvent was removed by rotatory evaporation (Büchi Rotavapor R, bath temperature 37 °C) and remaining traces of $CHCl_3$ were removed by co evaporation with ethanol. Crude product was dissolved in 15 ml diethyl ether, followed by the addition of 5 drops of a moderately strong organic base diethylamine ($pK_b = 3.07$) and the solution was kept at 4 °C overnight to afford the crystalline

diethylammonium salt of N-trityl-L-phenylalanine. During N-tritylation, HCl was generated and reacted with diethylamine to yield dimethylammonium chloride. The product was dissolved in an aqueous potassium hydroxide solution (34 ml, 0.05 M) and the solution was placed *in vacuo* at room temperature with swirling to remove the liberated diethylamine. The desired N-trityl-L-phenylalanine free acid was obtained after acidification with acetic acid at pH < 4 and isolated by filtration. The amorphous white product was rinsed in distilled water (3 x 5 ml) and dried in a drying pistol (Büchi TO-50) *in vacuo* (2 mbar) at 37 °C.

2.2.3   Synthesis of the N- hydroxysuccinimide ester of N-trityl-L-phenylalanine (Figure 2.1, 3a).

To a solution of N, N'-dicyclohexylcarbodiimide (DCCI) (20.63 mg, 0.1 mmol) in 0.2 ml of dimethylformamide (DMF) was added a mixture of N-hydroxysuccinimide (NHS) (11.51 mg, 0.1 mmol) respective and N-trityl-L-phenylalanine (0.1 mmol) in DMF (0.3 ml) (3b). Electron withdrawal by the succinimide carbonyl functions renders the N-trityl amino acid carboxyl carbon susceptible to nucleophilic attack by unprotonated amino group to generate an acid amide link with racemization (Izumiya and Muraoka, 1969). These 'active esters' are generally crystalline and stable (Anderson *et al*., 1967). The reaction mixture was incubated for 3 hours at room temperature and the insoluble dicyclohexylurea (DCU) byproduct was removed by filtration and the filtrate was subjected to evaporation *in vacuo* (37 °C) to remove DMF. Residual DCU was removed from the concentrated reaction mixture by microcentrifugation. Remaining traces of the solvent DMF were removed by repeated co-evaporation with ethanol *in vacuo*. The crude product was extracted with petroleum ether (60-80 °C) to remove traces of unreacted DCCI and crystallization of product was brought about from isopropanol by gentle heating followed by cooling. Weighed product was stored overnight at 4 °C.

2.2.4 Synthesis of N-trityl-phenylalanyl 8-(6-aminohexyl) aminoadenosine 3′,5′-cylic monophosphates.

Synthesis of N-trityl-phenylalanyl 8-(6-aminohexyl) aminoadenosine 3′,5′-cyclic monophosphate were carried out on a 0.01 mmol scale with respect to the 3′,5′-cyclic-nucleotide component. In all cases reaction mixtures were incubated overnight at room temperature in the dark before isolation of desired products.

2.2.4.1 Synthesis of N-trityl-L-phenylalanyl 8-(6-aminohexyl) aminoadenosine 3′,5′-cylic monophosphate (4a).

To a solution of 8-(6- aminohexyl) aminoadenosine-3′,5′-cyclic monophosphate (4.7 mg, 0.01 mmol) in DMF: H_2O: pyridine (300 µl, 2:1:3 v/v/v) was added the N- hydroxy-succinimide ester of N- trityl-L-phenylalanine (8.1 mg, 0.016 mmol) in DMF (100 µl).

2.2.4.2 Synthesis of N-trityl-F-DL-phenylalanyl 8-(6-aminohexyl) aminoadenosine 3′,5′-cylic monophosphate (4b).

To a solution of 8-(6-aminohexyl) aminoadenosine-3′,5′-cyclic monophosphate (4.7 mg, 0.01 mmol) in 200 µl pyridine: water (7:3 v/v) was added the N-hydroxy-succinimide ester of N-trityl-para-fluoro-DL-phenylalanine (5.3 mg, 0.01 mmol) in 200 µl pyridine: H_2O (7:3 v/v).

2.2.4.3 Synthesis of N-trityl-Cl-DL-phenylalanyl 8-(6-aminohexyl) aminoadenosine 3′,5′cylic monophosphate (4c).

To a solution of 8-(6- aminohexyl) aminoadenosine-3′,5′-cyclic monophosphate (4.7 mg, 0.01 mmol) in pyridine: H_2O: DMF (300 µl, 3:1:2 v/v/v) was added the N-hydroxy-succinimide ester of N-trityl-para-Cl-DL-phenylalanine (5.3 mg, 0.01 mmol) in pyridine: H_2O: DMF (150 µl, 1:1:1 v/v).

2.2.4.4 Synthesis of N-trityl-Br-DL-phenylalanyl 8-(6-aminohexyl) aminoadenosine 3′,5′-cylic monophosphate (4d).

To a solution of 8-(6-aminohexyl) aminoadenosine-3′,5′-cyclic monophosphate (4.7 mg, 0.01 mmol) in pyridine: H_2O (300 µl, 2:1 v/v) was added N-hydroxy-succinimide ester of N-trityl-para- Br-DL-phenylalanine (8.75 mg, 0.15 mmol) in pyridine: H_2O: DMF (350 µl, 3:1:3 v/v/v).

2.2.4.5 Synthesis of N-trityl-I-DL-phenylalanyl 8-(6-aminohexyl) aminoadenosine 3′,5′-cylic monophosphate (4e).

To a solution of 8-(6- aminohexyl) aminoadenosine-3′,5′-cyclic monophosphate (4.7 mg, 0.01 mmol) in pyridine: H_2O: DMF (300 µl, 3:1:2 v/v/v) was added the N-hydroxy-succinimide ester of N-trityl-I-DL-phenylalanine (9.45 mg, 0.15 mmol) in pyridine: H_2O: DMF (300 µl, 3:1:2 v/v/v).
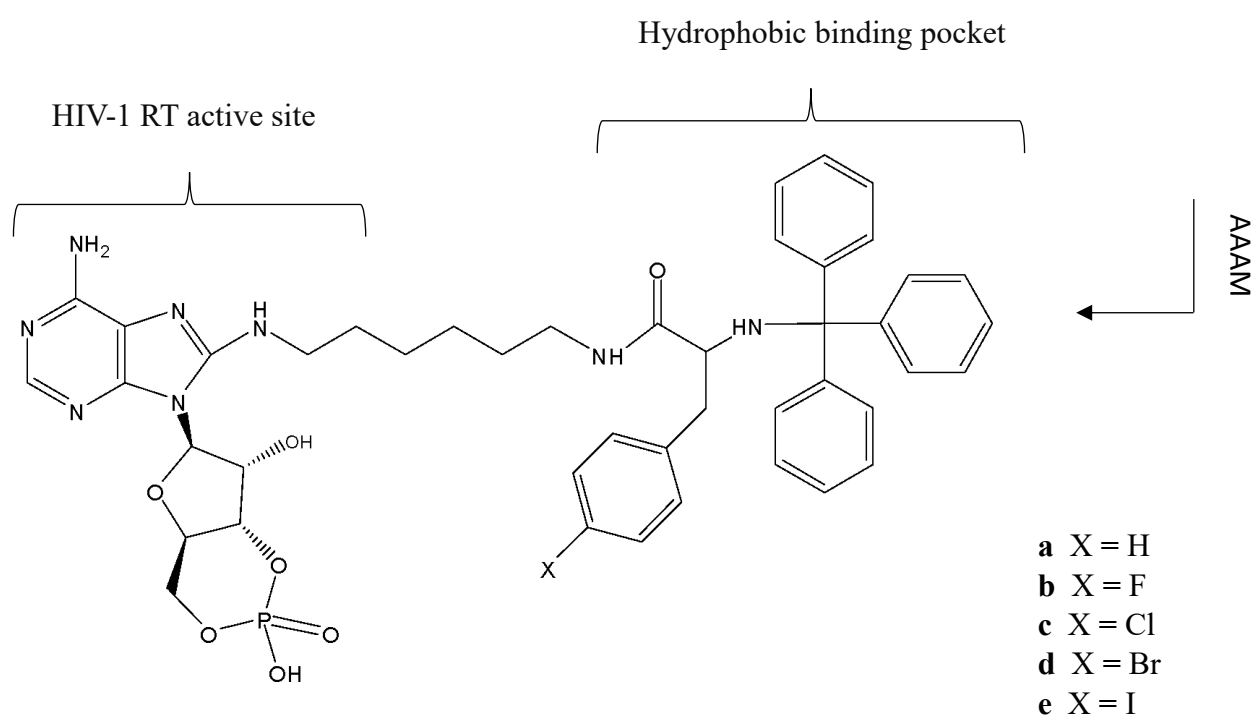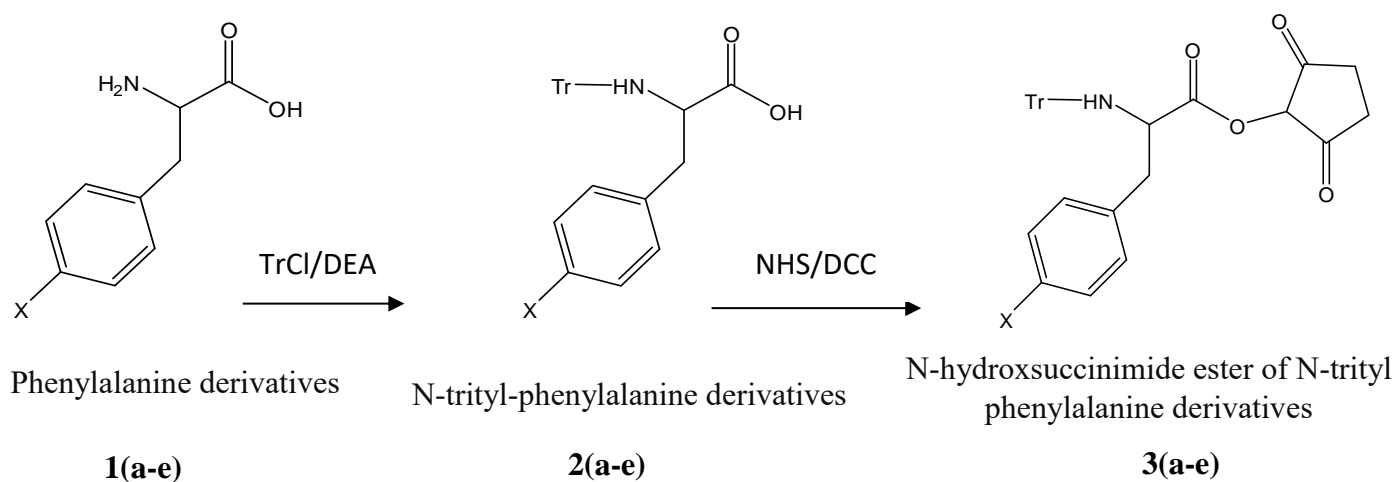
Figure 2.1 Reaction scheme for the synthesis of N-trityl-phenylalanyl -8-(6-aminohexyl) amino adenosine-3′,5′-cyclic monophosphates. TrCl = Trityl chloride, DEA = Diethylamine, Tr = Triphenylmethyl, NHS = N-hydroxysuccinimide, DCC = Dicyclohexylcarbodiimide, AAAM = 8-(6- aminohexyl) amino adenosine-3′,5′-cyclic monophosphate.

2.3 Thin layer chromatography (TLC)-Detection of the desired product using aluminium backed sheets of silica gel 60 F$_{254}$.

Components:

1. Reaction mixture

2. N-hydroxysuccimide esters of N-trityl-phenylalanines

3. 8-(6- aminohexyl) aminoadenosine-3′,5′-cyclic monophosphate

4. N-Hydroxysuccinimide (NHS)

One to two milligrams of components 2 and 4 listed above were dissolved in chloroform (100 µl). The stock 8-(6-aminohexyl) aminoadenosine-3′,5′-cyclic monophosphate (3) was dissolved in H$_2$O (2 mg in 100 µl) Each component including the reaction mixture was spotted on the 2 cm origin of TLC silica gel 60 F$_{254}$ aluminium sheets (2 cm x 7 cm). Traces of pyridine in reaction mixtures were removed from TLC plates *in vacuo* (Büchi TO-50 drying pistol) at 37 °C for 5 minutes. A solvent system of CHCl$_3$: CH$_3$OH, (4:1 v/v, 4 ml) was prepared and used for analytical TLC in spice jars. Plates were left to develop for approximately 15 minutes, followed by visualization of aromatic compounds under ultraviolet (UV) light at 254 nm. Trityl group-containing compounds were visualized as yellow spots (trityl cation) upon spraying plates with 5% aqueous H$_2$SO$_4$ (v/v) and heating at 100 °C in the fume hood.

2.4 Isolation of N-trityl-phenylalanyl-8-(6-aminohexyl) aminoadenosine-3′,5′-cyclic monophosphates by preparative TLC.

Reaction mixtures were evaporated by rotary evaporation (40 °C, 2 mbar). The dried product was dissolved in ethanol: DMF: H$_2$O (320 µl, 1:1:1, v/v/v). This was applied as a 19 cm streak to one glass-backed silica gel 60 F$_{254}$ plate (20 x 20 cm). After air drying, the plate was developed in CHCl$_3$: CH$_3$OH (4:1, v/v). The glass plate was air dried in the fume hood and the product band marked under UV$_{254}$ illumination. This was scraped off the glass (scalpel) and the product extracted into absolute ethanol (99.5%). The silica gel was removed by filtration in a Hirsch funnel. Filtrate was concentrated under rotary evaporation. Traces of ethanol were

removed by extraction with diethylether, followed by rotary evaporation (37 °C). Product was stored at -20 °C.

Table 2.1 Summary of synthesis of N-trityl subsituited-phenylalanyl-8-(6-aminoadenosine-3′,5′-cyclic monophosphates.

Compound	Molecular Weight (Da) [a]	Reaction scale with respect to N-trityl aminoacyl component [b]	Reaction solvent	Product Yield (mg)	% Yield
4 a	878.33	0.016	DMF:H$_2$O:Pyridine (400 μl, 4:1:3, v/v/v)	3.18	36
4 b	886.41	0.01	Pyridine : H$_2$O (200 μl, 7:3, v/v)	4.61	52
4 c	913.30	0.01	DMF:H$_2$O:Pyridine (450 μl, 2:1:2, v/v/v)	4.35	48
4 d	956.24, 958.23	0.015	DMF:H$_2$O:Pyridine (650 μl, 3:1:1, v/v/v)	4.63	48
4 e	959.38	0.015	DMF:H$_2$O:Pyridine (600 μl, 4:1:1v/v/v)	5.24	55

[a] Confirmed by MALDI-TOF mass spectrometry

[b] 3′,5′-cyclic nucleotide was 0.01 mmol in all syntheses

2.5   Characterization method:

2.5.1 ^{1}HNMR spectrometry

Samples (3-5 mg) of the five N-trityl-phenylalanyl-8-(6-aminoadenosine)-3′,5′-cyclic monophosphates were dissolved in tetra deuteromethanol (CD_3OD, 0.6 ml, 99 atom % D). Spectra were obtained on a Bruker Avance-III 400 MHz NMR spectrometer fitted with an ultrashield magnet and operating at 400.2200 MHz. Chemical shift values are relative to the methyl proton signal of undeuterated methanol in the solvent (3.32 ppm). The ^{1}HNMR spectrum of 8-(6-aminoademosine)-3′,5′-cyclic monophosphates (*circa* 4 mg) was obtained in deuterodimethylsulphoxide [$(CD_3)_2$ SO, 0.6 ml, 99.9 % containing 1 % tetramethylsilane]. Chemical shift values are relative to tetramethylsilane (0.00 ppm).

2.5.2   Ultraviolet (UV) absorbance spectra of N-trityl-phenylalanyl-8-(6-aminohexyl) aminoadenosine-3′,5′-cyclic monophosphates.

Samples of compounds (approximately 130 μg) in (20 μl CD_3OD) were added to absolute ethanol (3 ml). A Shimadzu double beam spectrophotometer (Model UV-1800, Shimadzu, Japan) was used to measure the absorbances of compounds in the range 210-320nm. Matched quartz cuvettes were used in the study.

2.5.3   MALDI-TOF mass spectrometry

Matrix Assisted Laser Desorption Ionization Mass Spectrometry (MALDI MS) analysis was conducted on Bruker Autoflex III Smartbeam system. Sample solutions were analysed using MALDI-TOF MS reflectron, linear and LIFT modes with the help of the Autoflex III MALDI TOF/TOF 1 KHz smartbeam laser (Bruker Daltonics, Germany). Data was produced in positive ion mode using FlexControl (version 3.4, build 119) software. In the LIFT mode, the re-acceleration of ions occurs in such a way that all fragment ions infiltrate distant enough into the reflector to provide a spectrum of fragment ions with enhanced spectral resolution. The

instrument was calibrated using standard peptides and standard concentrations of the sample spotted with HCCA matrix on a ground steel target (Bruker Daltonics, Bremen, Germany) for m/z 450-1200. Each spectrum was attained from 200 laser shots with a laser frequency of 200 Hz. The spots were analysed in linear and reflectron mode by collecting 200 shots per spot. The MS/MS experiments were completed using the LIFT method optimized for the sample by exact tuning of the timing of the LIFT cell and of the precursor ion selector. The LIFT method has a major advantage of acquiring data for both parent and fragments of the analyte consecutively, providing adequate information on the analyte. For the analysis of the deposited spots, spectra consisting of 1000 laser shots were in the range between m/z 450-1200 with a laser frequency of 200 Hz, and the digitalization rate was 2 GS/s with a laser power of 70%. An increase in the laser power led to production of other product ions but with lower sensitivity.

2.6   Colorimetric HIV-1 reverse transcriptase assay

The underlying principle of the commercial assay used in this study has been described in section 1.9.5

2.6.1   Preparation of solutions required for the assay

2.6.1.1   Reaction mixture containing poly (A). oligo (dT)$_{15}$ and nucleotides

Incubation buffer (50 mM Tris-HCl, 319 mM KCl, 33 mM MgCl$_2$ and 11 mM DTT, pH 7.8 ,1 ml) was added to a nucleotide mixture (100 µl) containing DIG-dUTP, biotin-dUTP and dTTP in 50 mM Tris-HCl, pH 7.8 (concentration of individual component not given). Separately, 430 µl autoclaved, deionized 18 Mohm water (Milli-Q50) was added to lyophilized poly (A). oligo (dT)$_{15}$ template/primer (3.8 A$_{260}$ units). Final nucleotides and template/primer solutions were stored at -20 °C. The above solutions were thawed on the day of the assay and reconstituted template/primer solutions (100 µl) was added to the nucleotide working solution (1.1 ml). The reaction mixture without enzymes and inhibitors was prepared by adding 100 µl of the final template/primer solution to the nucleotide mixture (1.1 ml) and contained 266 mM KCl, 27.5 mM MgCl$_2$ 9.2 mM DTT and 46 mM Tris-HCl at pH 7.8.

2.6.1.2 Washing buffer (solution 6)

Ultrapure water (225 ml) was added to 10 × concentrated incubation buffer obtained from the assay kit. The solution was mixed by inversion and stored at +2 to +8 °C.

2.6.1.3 Anti-DIG-peroxidase stock solution (Solution 5)

Ultrapure water (500 µl) was added to the lyophilized anti-DIG-POD (vial 6) and the resulting solution was stored at +2 to +8 °C until use.

2.6.1.4 Working solution of anti-DIG-peroxidase (Solution 5a)

An aliquot (30 µl) of the above reconstituted anti-DIG-POD (solution 5) was added to 2.59 ml conjugation dilution buffer containing sodium phosphate (undisclosed concentration, pH 7.4) (solution 8). This afforded a final concentration of 200 mU/ ml. Solution 5a was prepared immediately before use (Section 2.6.3, step 5). Unused solution 5a was discarded.

2.6.1.5 2,2'-Azino-bis (3-ethylbenzothiazoline-6-sulphonic acid) (ABTS) substrate solution (Solution 7)

A solution of (substrate buffer) containing sodium perborate was left to thaw at room temperature. Thereafter, two tablets of ABTS substrate solution (vial 10) was added to 10 ml of substrate buffer. Solution was kept in the fridge at +2 to+8 °C.

2.6.1.6 Stock recombinant HIV-1 reverse transcriptase solution (Solution 1)

To a lyophilizate of 500 ng recombinant HIV-1 RT obtained from a potassium phosphate buffered solution containing 0.2 % bovine serum albumin (molecular biology grade) was added 250 µl ultrapure water. The contents, in a 1.5 ml microcentrifuge tube, were gently mixed by inversion. Thereafter the tube was centrifuged for 2 minutes at 12500 rpm in a bench top microcentrifuge (Eppendorf model, 5810R, Hamburg, Germany). This solution was divided into five equal aliquots (50 µl each) which were stored at -70 °C in a biofreezer. On the day of use one aliquot (50 µl) was thawed and added to lysis buffer (460 µl, 80 mM potassium chloride, 2.5 mM, DTT, 0.75 mM EDTA, 0.5 % Triton X-100 in 50 mM Tris-HCl, pH 7.8, (solution 4).

2.6.1.7 Ready to use solutions (as per Assay kit)

- Lysis buffer (solution 4)
- Conjugate dilution buffer (solution 8)
- Incubation buffer (solution 2)

2.6.2 Stock nucleotide solution and Nevirapine

Stock solution of (10^{-3} M) of the five synthesized N-trityl-phenylalanyl nucleotide conjugates in DMSO (99%) were prepared from solutions in CD_3OD. Briefly the appropriate volumes of the deuteromethanolic solutions were dispended into 500 µl microcentrifuge tubes. Solvent was removed *in vacuo* at room temperature in a savant speed vac concentrator (Thermo scientific at 37 °C and the residues dissolved in DMSO. Nevirapine (1.39 mg) was dissolved in DMSO (523 µl) to afford a stock 10^{-2} M solution while a 10^{-2} M stock solution of N-trityl-phenylalanyl-8-(6-aminohexyl) aminoadenosine-3',5'-cyclic monophosphate was obtained by dissolving 1.12 mg in 523 µl DMSO.

Stock solutions in DMSO (100 µl each) at lower concentrations of inhibition (10^{-4}, 10^{-5}, 10^{-6} M) were prepared by serial dilution of initial 10^{-3} M N-trityl-phenylalanyl nucleotide and

10^{-2} M Nevirapine stock solutions. Solutions were briefly vortexed at each dilution step (vortex -1 Genie, Scientific Industries).

2.6.3 HIV-1 reverse transcriptase colorimetric ELISA protocol

Reaction mixtures (60 μl) contained lysis buffer (24 μl), incubation buffer (10 μl), recombinant HIV-1 RT solution (10 μl, 2 ng enzyme), solution 3a containing primer/template and deoxynucleotide triphosphates (10μl) and inhibitor solutions at various concentrations in DMSO (6 μl). Reactions were conducted in 500 μl microcentrifuge tubes at 37 C° for 1.5 hours. Positive control mixtures contained no inhibitors, while negative controls contained no enzyme. Experiments were conducted in triplicates.

Thereafter, the following steps were followed:

Step 1: Reaction mixtures (60 μl) were transferred directly into the wells of the microplate streptavidin precoated modules (MP), which had also been postcoated with a blocking agent by the manufacturers.

Step 2: Modules were then covered with a cover foil and incubated for 1.5 hours at 37 °C.

Step 3: Solutions were removed completely from microtitre plate wells and each well was again washed with washing buffer for 30 seconds (240 μl, 5 repeats).

Step 4: Anti-DIG-POD working solution (200 μl) was added to each well. Modules were once again covered with foil and incubated for 1.5 hours at 37 °C.

Step 5: Anti-DIG-POD solutions were removed completely and module wells were washed with washing buffer as described in step 3.

Step 6: ABST substrate solution (200 μl) was added to each well and modules were incubated at 22° C until their colour (green) had developed to a point that was sufficient for clear colorimetric detection (15 minutes. Roche recommends 10-30 minutes). Modules were tapped gently to ensure even distribution of the green reaction product before reading absorbances.

Step 7: Absorbances were measured at 405 nm (reference wavelength, 492 nm) in a Mindray -MR-96 A microplate reader. The activity of HIV-1 RT in the absence of inhibitor was set at 100 %. Enzyme activates in the presence of Nevirapine and putative inhibitors at the concentrations selected for the assays were recorded relative to this value. Test results from experiments in triplicate are shown as means +/- standard deviations (SD).

Table 2.2   Components for colorimetric HIV-1 reverse transcriptase ELISA.

Reagents (μl)	Controls						Inhibitors [a]					
	Negative			Positive								
Enzyme solution	-	-	-	10	10	10	-	-	-			
Lysis buffer	34	34	34	24	24	24	-	-	-			
Incubation buffer	10	10	10	10	10	10	10	10	10			
DMSO (99 %)	6	6	6	6	6	6	-	-	-			
Nevirapine	-	-	-	-	-	-	6	6	6			
Compounds 4 (a-e)	-	-	-	-	-	-	-	-	-	6	6	6

[a] final concentration in assays ranged from 10^{-4} M to 10^{-7} M (4a-e)

2.7   Computational Methods

Computational studies were performed at the Discipline of Pharmaceutical Chemistry, UKZN. Docking studies were performed using the AutoDock Vina programme. The crystal structure of the 3D HIV-1 RT was obtained and downloaded from Protein Data Bank (Code 1RT1, 2.55 Å resolution). Structures of all the synthesized anti-HIV compounds were modelled with ChemDraw Ultra 8.0. Three dimensional structures of all the drugs were optimized with B3LYP level of theory using Gaussian 09 software. All structures were docked inside the NNRT-BP of the HIV-1 RT enzyme. AutoDock tools and AutoDock were used to predict the modes of binding of all the drug structures. Two dimensional representation of ligand-protein interactions were presented using LigPlot. This computer based programme provided detailed information of the hydrophobic and hydrogen bond interactions involved.

CHAPTER THREE

RESULTS AND DISCUSSION

3.1   Thin Layer Chromatography (TLC)

In the work reported here, products 4a-e were synthesised (by Preantha Poonan) only at the 0.01 μmole level, with respect to 8 (6-aminohexyl) adenosine due to the high cost of this nucleotide component. Isolation of purified products was achieved by preparative thin later chromatography (TLC).

In this study analytical TLC was used extensively to monitor reaction mixtures and to confirm purity of products. This inexpensive technique, which is one of the most commonly used analytical methods (and is characterized by low cost), requires small quantities of analyte (usually < 0.5 mg) and results may be obtained within 10-30 minutes (Pyka, 2014). Moreover several samples maybe analysed simultaneously on one TLC plate. The TLC silica solid phase is polar and the solvent (liquid phase) polarity may be varied for each application. Thus $CHCl_3$: MeOH mixed in varying ratios may be used to generate solvents with dielectric constants from 4.8 (100% $CHCl_3$, relatively non-polar) to 32.6 (100% MeOH, relatively polar) (Weast, 1956).
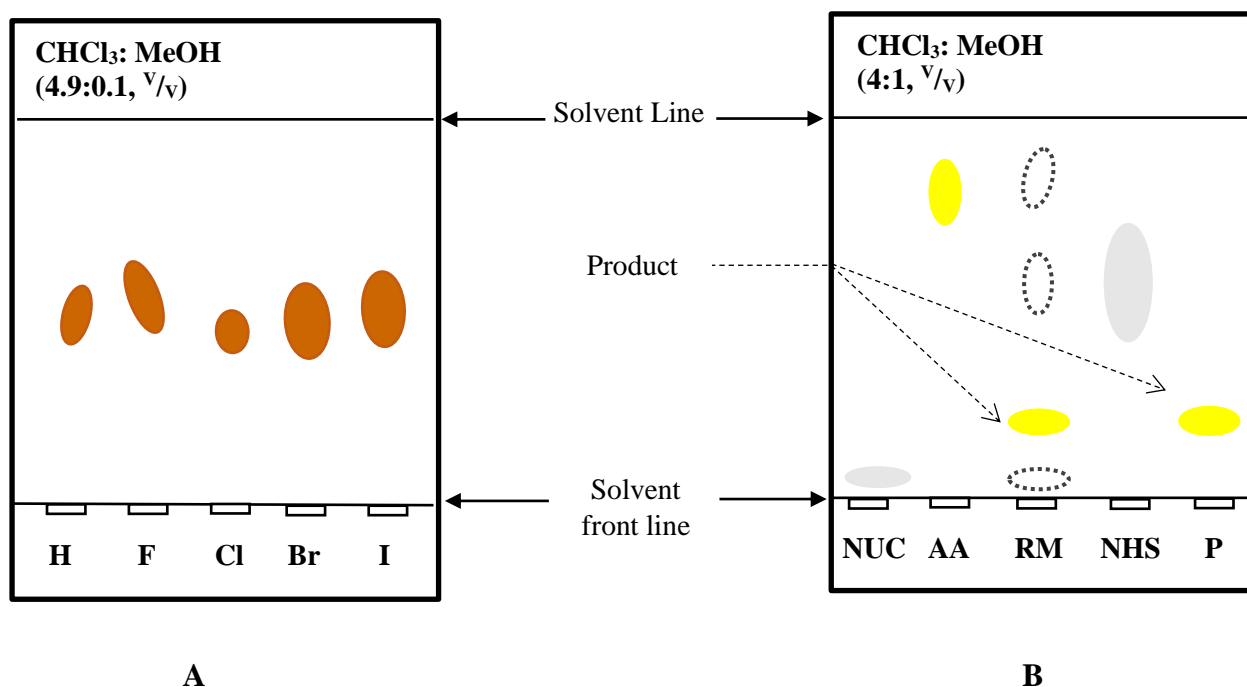
Figure 3.1 Thin layer chromatograms (**A**) N-hydroxysuccinimide esters of N-trityl phenylalanine derivatives, H, F, Cl, Br, I (3a-e respectively). (**B**) Synthesis of p-fluoro conjugate 4b; 8-(6-aminohexyl) adenosine-3',5'-cyclic monophosphate (NUC), NHS ester of N-trityl-p-F-DL-phenylalanine (AA), reaction mixture (RM), N-hydroxysuccinimide (NHS) as well as the purified product.

Silica gel $60F_{254}$ TLC plates display a bright yellow-green fluorescence at 254 nm. This is quenched by compounds that absorb UV light at this wavelength thus appearing as dark spots on chromatograms. Moreover, analytical TLC plates may be sprayed with a range of reagents to reveal the presence of particular structural features. Thus, the N-trityl NHS esters (3a-e) which were examined for purity on silica gel $60F_{254}$ TLC plates developed in $CHCl_3$: MeOH (4.9:1 v/v) were weakly visible under UV_{254} illumination. Plates were sprayed with H_2SO_4 (10 mole %) and heated to 100 °C in the fume hood whereupon yellow spots, coincident with UV absorbing spots, confirmed the presence of the trityl cation. NHS esters were also visualized by spraying chromatograms with a mixture of aqueous 14% (w/v) hydroxylamine hydrochloride and 3.5 M NaOH (20:8.5, v/v). After drying on a hotplate TLC plates were sprayed with $FeCl_3$ (5% w/v) in 1.2 M HCl. 'Active esters' appeared as brown-purple spots on a yellow background (Feigl ,1943).

Reaction mixtures containing NHS esters (3a-e) and 8-(6-aminohexyl)3',5'-cylic-monophophate were monitored by TLC on silica gel $60F_{254}$ plates deveoped in $CHCl_3$:MeOH

(4:1, v/v). Adenine-containing compounds were strongly visible under UV_{254} illumination as was NHS, a byproduct of the coupling reaction. Products (4a-e) were well separated from the more polar 8-(6-aminohexyl)3,5-cylic-monophophate and the less polar NHS and N-trityl aminoacid NHS esters (Figure 3.1 B). Confirmation of product assignment on analytical plates was obtained by acid treatment (H_2SO_4, 10 µmole %) to reveal trityl group-containing compounds. Desired products were isolated from reaction mixtures by preparative TLC (Section 2.4) and shown to migrate as single spots by TLC in the polar solvent ethanol: H_2O (2:1v/v) (Table 3.1) with relatively high R_f values.

Table 3.1 R_f values of N-trityl-phenylalanyl derivatives in ethanol: H_2O (2:1, v/v) solvent.

Compounds	R_f
4a	0.81
4b	0.88
4c	0.94
4d	0.83
4e	0.93

Table 3.2 Melting points of starting materials.

N-hydroxysuccinimide esters of N-trityl-phenylalanyl derivatives	Melting Points °C [a]
4a	85-89
4b	173
4c	167
4d	165
4e	159

[a] melting points are uncorrected

3.2 Melting points of N-trityl-phenylalanyl NHS esters

Melting points of pure organic compounds are usually sharp and occur at the given temperature or over a narrow range. Compounds 3(a-e) were shown to co-chromatograph with authentic samples and displayed sharp melting points (Table 3.1). Of particular interest is the observed decrease in melting point of para-halo compounds 4(a-e) as the atomic radius increases (F⟶I, 173 ⟶ 159 °C). However, the melting point of the unsubstituted N-trityl-L-phenylalanine NHS ester was considerably lower (85-89 °C) and is very likely indicative of the presence of a contaminant.
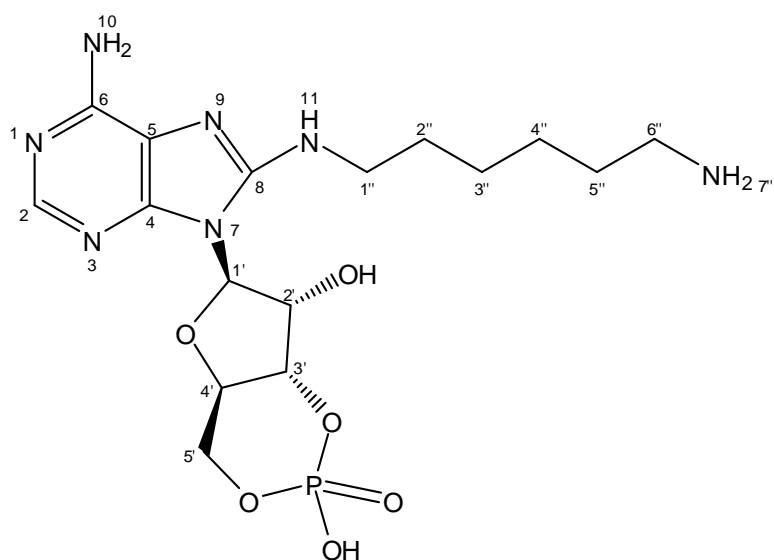
A
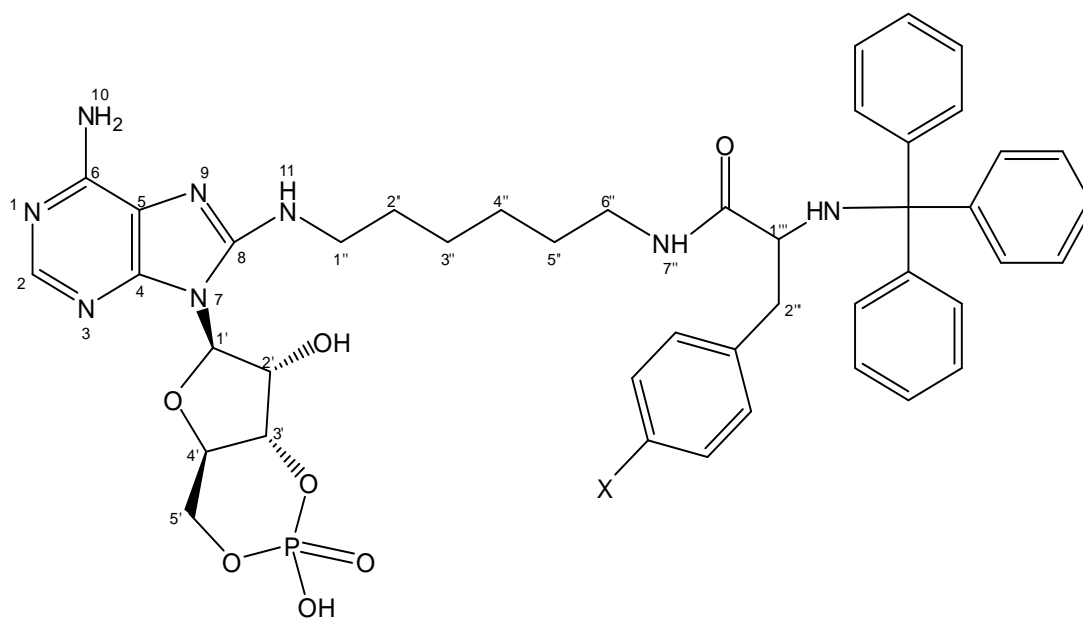
B

Figure 3.2   **(A)** Numbering of 8-AHA-cAMP and **(B)** conjugate with hydrophobic
trityl components via a 6-carbon spacer to form the N-trityl-
phenylalanyl derivatives (4a-e).

Table 3.3 ^{1}HNMR spectral analysis of N-trityl-phenylalanyl -8(-6-aminoadenosine) 3',5'-cyclic monophosphate and of 8-AHA-cAMP.

Compounds	NMR
4a	^{1}HNMR (400MHz, CD$_3$OD) δ : 7.99 (1H, s, H-2), 7.37 (6H, d, J = 7.5 Hz, ortho in trityl), 7.27-7.07 (14H, m, H-Bz), 5.77 (1H, s, H-1'), 5.23-5.19 (1H, m, H-2'), 5.12-5.10 (1H, m, H-3'), 4.32-4.10 (3H, q, m, H-4', H-5'a, H-5'b), 1.69-1.60 (2H, m, spacer H-5"), 1.42-1.32 (2H, m, spacer H-2"), 1.23-1.13 (4H, m, spacer, spacer H-3", H-4").
4b	^{1}HNMR (400MHz, CD$_3$OD) δ : 8.00 (1H, s, H-2), 7.40 (6H, d, J = 7.4 Hz, ortho in trityl), 7.24-7.07 (11H, m, H-Bz), 6.98 (2H, d, J = 8.7 Hz, ortho in p-F-phenyl), 5.79 (1H, s, H-1'), 5.25-5.21 (1H, m, H-2'), 5.13 (1H, d, J = 5.4 Hz, H-3'), 4.33-4.31 (1H, q, J = 4.3 Hz, H-4'), 4.29-4.11 (2H, m, H-5'a, H-5'b), 3.40 (2H, t, J = 7.0 Hz, spacer H-1"), 2.82-2.76 (2H, m, spacer H-6"), 1.69-1.63 (2H, dd, J = 15.0, 7.2 Hz, spacer H-5"), 1.37-1.33 (2H, m, spacer H-2"), 1.15-1.11 (4H, m, spacer H-3", H-4").
4c	^{1}HNMR (400MHz, CD$_3$OD) δ : 8.00 (1H, s, H-2), 7.40 (6H, d, J = 7.4 Hz, ortho in trityl), 7.30-7.14 (11H, m, H-Bz), 7.04 (2H, d, J = 8.4 Hz, ortho in p-Cl-phenyl), 5.79 (1H, s, H-1'), 5.25-5.21 (1H, m, H-2'), 5.13 (1H, d, J = 5.4 Hz, H-3'), 4.33-4.30 (1H, t, J = 4.7 Hz, H-4'), 4.24-4.17 (2H, m, H-5'a, H-5'b), 3.40 (2H, t, J = 7.1 Hz, spacer H-1"), 2.79 (2H, dd, J = 13.3, 6.3 Hz, spacer H-6"), 1.70-1.63 (2H, m, spacer H-5"), 1.39-1.37 (2H, m, spacer H-2"), 1.21-1.12 (4H, m, spacer H-3", H-4").
4d	^{1}HNMR (400MHz, CD$_3$OD) δ : 8.00 (1H, s, H-2), 7.40 (2H, d, J = 8.2 Hz, meta in p-Br-phenyl), 7.24-7.07 (11H, m, H-Bz), 7.02 (2H, d, J = 8.3 Hz, ortho in p-Br-phenyl), 5.78 (1H, s, H-1'), 5.25-5.21 (1H, m, H-2'), 5.13 (1H, d, J = 5.3 Hz, H-3'), 4.33-4.31 (1H, t, J = 4.3 Hz, H-4'), 4.28-4.11 (2H, m, H-5'a, H-5'b), 3.40 (2H, t, J = 7.1 Hz, spacer H-1"), 2.80-2.73 (2H, td, J = 13.1, 6.3 Hz, spacer H-6"), 1.69-1.63 (2H, dd, J = 14.7, 7.3 Hz, spacer H-5"), 1.39-1.32 (2H, m, spacer H-2"), 1.15-1.13 (4H, m, spacer H-3", H-4").

4e	^{1}HNMR (400MHz, CD$_3$OD) δ : 8.00 (1H, s, H-2), 7.57 (2H, d, *J* = 8.1 Hz, meta in p-I phenyl), 7.41-7.39 (6H, m, meta in trityl), 7.24-7.12 (9H, m, ortho and para in trityl), 6.88 (2H, d, *J* = 8.2 Hz, ortho in p-I-phenyl), 5.78 (1H, s, H-1'), 5.25-5.21 (1H, m, H-2'), 5.13 (1H, d, *J* = 5.3 Hz, H-3'), 4.33-4.31 (1H, t, *J* = 4.8 Hz, H-4'), 4.19-4.11 (2H, m, H-5'a, H-5'b), 3.41 (2H, t, *J* = 7.0 Hz, spacer H-1"), 2.79 (2H, dd, *J* = 13.2, 6.8 Hz, spacer H-6"), 1.66 (2H, dd, *J* = 7.6, 7.4 Hz, spacer H-5"), 1.34 (2H, d, *J* = 7.5 Hz, spacer H-2"), 1.14 (4H, bs, spacer H-3", H-4").
8-AHA-cAMP	^{1}HNMR (400MHz, (CD$_3$)$_2$ SO) δ : 7.95 (1H, s, H-2), 5.76 (1H, s, H-1'), 4.82-4.65 (2H, m, H-2', H-3'), 4.11-4.03 (1H, ddd, *J* = 4.2, 9.0, 13.3 Hz, H-4'), 3.98-3.81 (2H, m, H-5'a, H-5'b), 3.31-3.38 (2H, m, spacer H-1"), 2.76 (2H, t, *J* = 13.2, 6.8 Hz, spacer H-6"), 1.57 (bs, 4H, spacer H-2", H-5"), 1.34 (4H, bs, spacer H-3", H-4").

3.3 Spectral analysis of N-trityl phenylalanyl amino adenosine- 3′,5′-cyclic monophosphate

3.3.1 ^{1}HNMR spectrometry

Nuclear magnetic resonance (NMR) spectrometry is an indispensable tool used in the structure elucidation of organic molecules. The nuclei of atoms having spin values of (½) behave as small magnets and therefore respond to the application of an external magnetic field. Nuclei exhibiting this property (^{1}H, ^{19}F, ^{13}C, ^{31}P) when placed in a magnetic field (H$_o$) therefore adopt either a low energy state in which the nuclei are aligned with magnetic field (+ ½) or a high energy orientation in which the nuclei are antiparallel (-½) to the field. Upon application of electromagnetic radiation in the radio frequency range to the sample being analysed in the field H$_o$, nuclei may be induced to flip to the high energy state by absorption of a quantum of electromagnetic radiation. However, the field experienced by the nuclei of each atom (typically ^{1}H and ^{13}C) varies according to its unique electronic environment, which may shield or deshield

the nuclei. Therefore, the true field (H) at each atom in a molecule under analysis may be expressed

 as:

$$H = H_o (1-\sigma)$$

where σ is a shielding parameter. This, in turn, will affect the frequency required to bring individual nuclei into 'resonance'. The NMR signals or chemical shifts are recorded against a standard. Typically, in ^{1}HNMR spectrometry carried out in a deuterated solvent (eg. $CDCl_3$, CD_3OD) tetramethylsilane (TMS) is introduced in trace amounts as a reference and the resonance of its very shielded equivalent protons is set at 0.00 ppm. ^{1}HNMR signals of carbon-linked protons in organic molecules occur downfield from the reference in the range 0.00-10.00 ppm. In the absence of TMS, spectrometry may be tuned to lock on the signal from the small quantity of undeuterated solvent ($< 0.1\%$) in the deuterated solvent being used for calibration (CH_3OH: 3.34 ppm; $CHCl_3$: 7.26 ppm) (Gottlieb *et al*., 1997).

In the study reported here ^{1}HNMR was of particular importance in the assignment of structures to tritylated conjugate 4a-e. Thus, the aromatic protons are extensively deshielded and resonate downfield in the region 6.8-7.6 ppm, whereas the protons on the spacer methylene (C-2" – C-5") are well shielded and give signals in the range 1.1-1.7 ppm. However, the H-1" and H-6" protons in the spacer element form part of the spacer methylenes directly coupled to the electron-withdrawing heteroatom N and resonate at higher frequencies (downfield) due to its inductive effect. In particular, protons on the methylene group in secondary amine (R-NH-CH_2) linked with the amino group at C-8 of the adenine ring (H-1") resonate as triplets at around 3.4 ppm, while signals for protons on C-6", in amide link with the N-trityl phenylalanyl components (CO-NH-CH_2---) present as a doublet of doublets (4c, 4e), a multiplet (4b) and a triplet of doublets (4d), centred at about 2.8 ppm.

Protons associated with the sugar moiety ribose resonate as multiplets in the 3.8-5.2 ppm range due to extensive spin-spin coupling with neighbouring protons. The anomeric proton (H-1'), however, resonates further downfield (5.77-5.79 ppm) as the anomeric carbon to which it is attached is linked to the ribose ring oxygen resulting in strong deshielding. The H-2 proton of the 8- substituted adenosine moiety presents as a sharp singlet at 8.00 ppm in the ^{1}HNMR spectra of 4b-e and at 7.99 ppm in that of 4a. Quantification of protons assigned to shifts was

achieved by integration of peak areas. Values were calculated relative to the area under the H-2 signal, which was set at 1.0. Each tritylated derivative contained 15 trityl protons and 4 phenylalanyl protons in the aromatic region. Therefore, the theoretical H-2/aromatic/ anomeric proton ratio in each case is 1:19:1. This also serves to confirm that compounds comprise of an adenine base, a carbohydrate moiety (ribose) and the N-trityl phenylalanyl component.

Structures of conjugates 4a-e were drawn using ChemDraw Ultra 8.0 and assignment of peaks in experimental ^{1}HNMR spectra of compounds in CD$_3$OD was guided by the programme's predictive software and the proton magnetic resonance spectrum of 8-(6-aminohexyl) aminoadenosine-3',5'-cyclic monophosphate (Evans et al., 1978).

Anomeric protons, which usually present as a doublet in ribosyl nucleoside and the nucleotide however appeared as singlets indicating little or no spin-spin coupling with the neighbouring H-2' proton takes place (Appendix C, Figure 4.2, 4a-e). The ribose pucker of 8-AHA-cAMP has been reported to be C2' $endo$ as space filling models show that this form more easily accommodates the adenine C8 substituents (Evan et al., 1978). Moreover, the preferred conformation about the glycosidic bond was shown to be $anti$. The N-trityl phenylalanyl derivative was isolated in 80% purity as determined by the integration of the anomeric proton region (Appendix C, Figure 4.3). The small amount of product recovered precluded further purification.

The ^{1}HNMR spectrum of the first preparation of the chloro derivative (4c) revealed two anomeric proton peaks of roughly equal abundance (Appendix C, Figure 4.4) corresponding to the desired product (5.80 ppm) and 8-AHA-cAMP (5.84 ppm). The pure product was obtained by further preparative TLC as described (Section 2.4), although the sample submitted for proton magnetic resonance revealed the presence of small amounts of water (4.86 ppm singlet), methanol (3.34 ppm singlet) and ethanol (3.65 ppm quartet, 1.19 ppm triplet). These solvents were also evident in small amounts in the ^{1}HNMR spectra of fluoro (4b), chloro (4c), bromo (4d) and iodo (4e) derivative, which were submitted for analysis, while the presence of ethanol in the phenylalanine derivative 4a was barely discernible (Appendix C, Figure 4.2 B). The presence of water and methanol in spectra may be directly attributed to the CD$_3$OD solvent used in this study, which was only 99% deuterated and had hydrated after prolonged storage (pierced vial), while ethanol was used to extract products from silica gel plates.
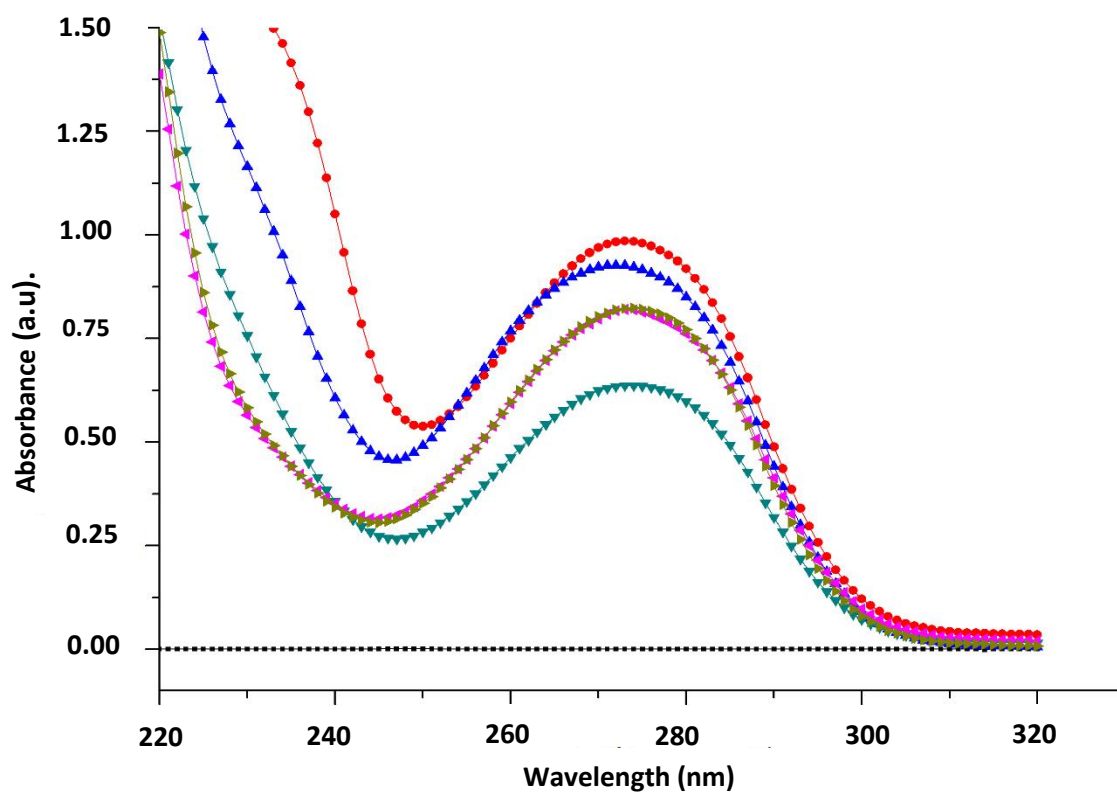
Figure 3.3 UV absorbance spectra of N-trityl-phenylalanyl conjugates (4a-e). Base line(■). (4e) (●). (4d) (▲). (4c) (▼). (4b) (▶). (4a) (◀).
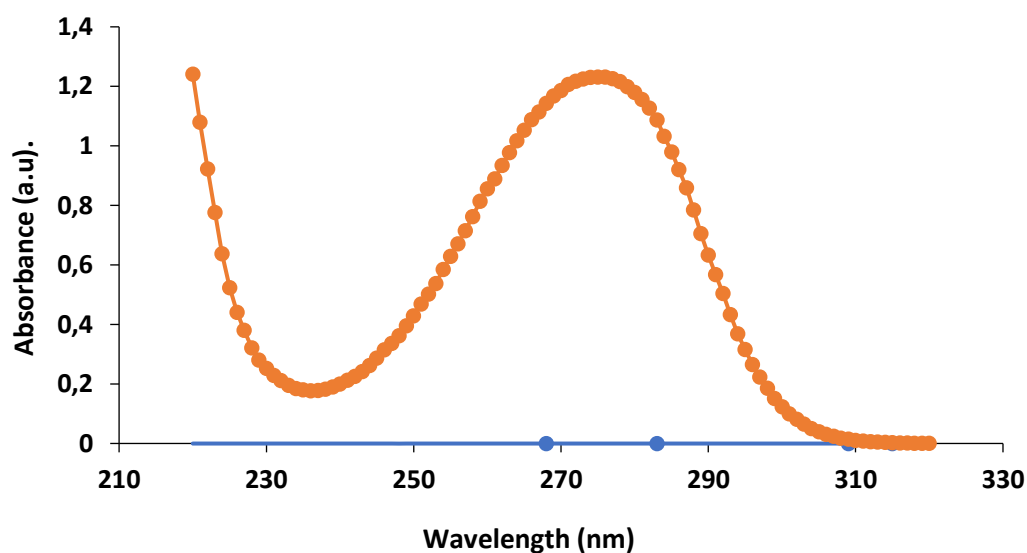
Figure 3.4 UV absorbance spectrum of 8-(6-aminohexyl) aminoadenosine-3′,5′-cyclic-monophosphate.

3.3.2   UV Spectrophotometry

Organic compounds that are highly conjugated absorbs radiation in the ultraviolet region with peak absorbance (A_{max}) at characteristic wavelengths (λ_{max}) as they undergo π-π* transition. Thus, the purine and pyrimidine bases of RNA and DNA display pH-dependent λ_{max} values in the 250-275 nm range. The Beer-Lambert law (equation 3.2) states that absorbance (A) of a solute which is the log of incident over transmitted radiation, is equal to the product of the molar extinction co-efficient (ε) of the solute, its water concentration (c) and the length of the solution (l) through which the light passes (measured in centimetres).

$$A = \varepsilon \times c \times l \qquad\qquad (3.2)$$

At very high solute concentrations the law breaks down, more especially if the solution is light scattering in nature. To avoid these inaccuracies concentrations of test solutions are adjusted to afford A_{max} values in the region 0.8-1.2. A and ε vary as the wavelength of incident light changes and it is customary in UV spectroscopy to report ε at λ_{max}. Therefore 5′-AMP at pH 7.0 exhibits λ_{max} at 259nm with $\varepsilon_{max} = 1.5 \times 10^4$ L M^{-1} cm^{-1} (Cavaluzzi and Borer, 2004). However, substitution of the C-8 proton on the adenine ring with an amino group or diaminoalkane results in a λ_{max} shift to a longer wavelength (279 nm) (Muneyama *et al*, 1971). In our hands, the λ_{max} values for 8-AHA-cAMP and 4a-e occurred in a range (272-275 nm. Table 3.4). A graphical representation of Table 3.4 is illustrated in Figure 3.3 and 3.4. Although the ε_{max} values vary from 1.19×10^4 (4c) to 2.03×10^4 L M^{-1} cm^{-1} (4a), the contributions of the trityl and phenylalanyl moieties to the ε_{max} are modest, as the former reflects a molar extinction coefficient of 1×10^3 at 273 nm, while the phenylalanine ring system absorbs radiation at this wavelength extremely weakly (140 L M^{-1} cm^{-1}). The λ_{min} values of 4a-e are, however, shifted by 9-14 nm to longer wavelengths than that of 8-AHA-cAMP (236 nm at pH 5.5). This is attributed almost entirely to the trityl component with $\varepsilon = 5010$ at 236 nm (Appendix B, Figure 4.1). This is confirmed by considering the $\lambda_{max}/ \lambda_{min}$ ratios (Table 3.4). While for the untritylated compound 8-AHA-cAMP the ratio is 6.9, those for 4a-e lie in the range 1.8-2.6.

Table 3.4 UV spectral data of 8-(6-aminohexyl) adenosine-3′,5′-cyclic-monophoshate and of N-trityl-phenylalanyl conjugates of 8-(6-aminohexyl) adenosine-3′,5′-cyclic-monophoshate (4a-e).

Compounds	λ_{max} (nm)	λ_{min} (nm)	ε_{max} (L M^{-1}cm^{-1})	$Log_{10}\varepsilon_{max}$	$\lambda_{max}/\lambda_{min}$
4a	275	245	2.03×10^4	4.31	2.68
4b	273	245	1.42×10^4	4.10	2.60
4c	273	244	1.19×10^4	4.07	2.25
4d	272	246	1.72×10^4	4.20	2.03
4e	273	250	1.63×10^4	4.20	1.82
8-AHA-cAMP[a]	275	236	1.60×10^4	4.19	6.95

[a] 8-(6-aminohexyl) aminoadenosine-3′,5′-cyclic monophosphate.

Table 3.5 Calculated molecular weights (g/mol) and those obtained by MALDI-TOF MS analysis.

Compound	Molecular formula	Molecular mass (Da)	MALDI-TOF	
			Found	Calculated
4a	$C_{44}H_{49}O_7N_8P_1$	832.35	878.83	878.33 [M-H+2 Na]$^+$
4b	$C_{44}H_{48}O_7N_{10}F_1P_1$	850.33	886.96	886.40 [M+2NH$_4$]$^+$
4c	$C_{44}H_{48}O_7N_8Cl_1P_1$	866.31	914.02	911.28 [M-H+2Na]$^+$
4d [a]	$C_{44}H_{48}O_7N_8Br_1P_1$	910.26;912.26	958.06	956.24;958.23 [M+2Na]$^+$
4e	$C_{44}H_{48}O_7N_8I_1P_1$	958.24	959.38	959.25 [M+H]$^+$

[a] Bromine comprises of two stable isotopes of almost equal abundance separated by approximately 2 mass units (78.9.9, 51% and 80.916,49%). Therefore, in mass spectrometry two molecular ion peaks separated by 2 Da are observed for mono bromo derivates.

3.3.3 MALDI-TOF MS

MALDI-TOF MS normally used to analyse large molecules such as peptides and protons however has been useful in confirming structures of conjugates in this study with molecular masses < 1000 Da.

The sodiated species $[M-H+2Na]^+$ are often encountered in mass spectrometry (Lattova *et al*., 2005). These ions gave prominent peaks with spectra (positive mode) of 4a and 4e while the $[M+2Na]^+$ species (Shackleton *et al*., 2013) was reflected in the spectra of 4a and 4d. Of interest is the occurrence of two $[M+2 Na]^+$ peaks for bromo derivative (4d) at $^m/_z = 956.24$ and 958.23 reflecting the contribution of the two stable isomers of bromo in the structure (Table 3.5). The fluoro derivative 4b displayed the diammonium ion $[M+2 NH^4]^+$ while the $[M+H]^+$ peak was seen in the spectrum of 4e.
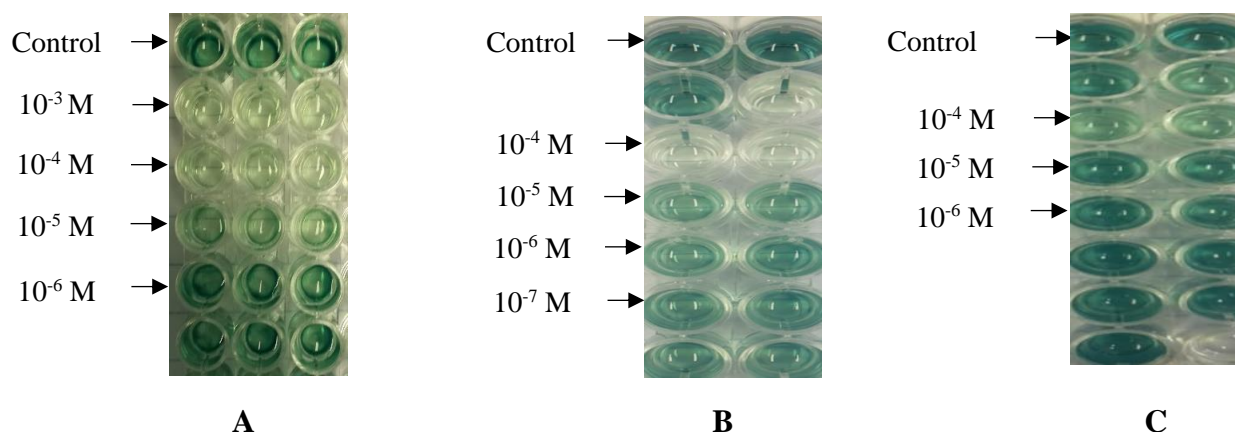
Figure 3.5   Detection of inhibitory effect on HIV-1 reverse transcriptase using the reverse transcriptase colorimetric assay kit. **(A)** Nevirapine **(B)** fluoro derivative 4b **(C)** phenylalanyl derivative 4a.

3.3.4   RT Colorimetric Assay

Reverse transcriptase colorimetric assays were performed to determine the activity of the recombinant HIV-RT in the presence of the front-line NNRTI Nevirapine and the N-trityl-para-

halo-phenylalanyl-8-AHA-cAMP 4a-e. Assays were carried out using a template/primer hybrid poly(A). oligo $(dT)_{15}$, lyophilizate to generate newly synthesized cDNA with the incorporation of addition of biotinylated and digoxygeninylated deoxyuridine monophosphates by RT onto the growing RNA-DNA. (Section 1.9.5).

As seen in Figure 3.5 A, Nevirapine inhibited the RT enzyme at concentrations 10^{-3}, 10^{-4} and 10^{-5} M. The fluoro derivative (Figure 3.5 B) showed excellent inhibition at 10^{-7} M and 10^{-5} M, dropping RT activity down to 69 % and 57 %, while Nevirapine was shown to be active at 10^{-5} M with a reduced RT activity to 43 %. The "parent" derivative, phenylalanine did not inhibit the RT enzyme at the lower concentrations ($< 10^{-5}$ M). Also, the absorbances wavelength at 10^{-5} M and 10^{-6} M (1.108, 1.216, respectively) were higher than that of the control (0.918). On the other hand, there was excellent inhibition activity at the highest concentration 10^{-4} M.

A

8-AHA-cAMP

B

Phenylalanine derivative (4a)

C

Fluoro derivative (4b)

D

Chloro derivative (4c)

E

Bromo derivative (4d)

F

Iodo derivative (4e)
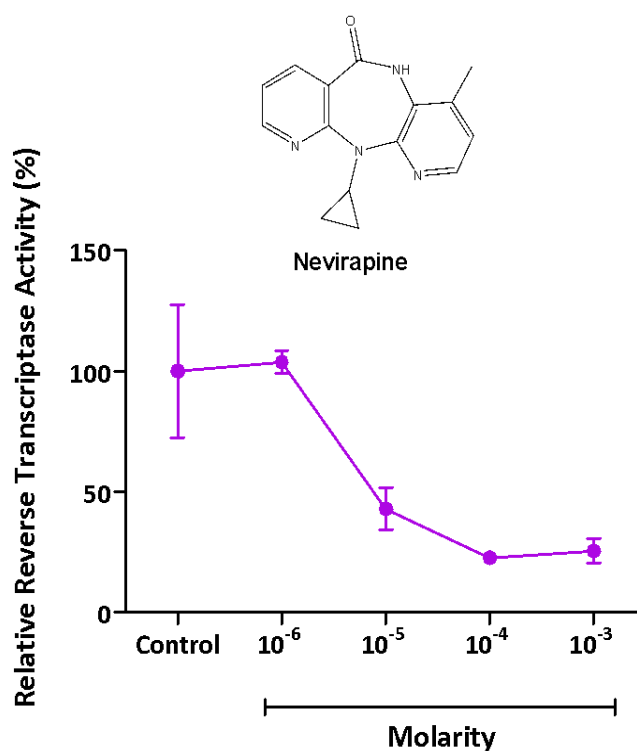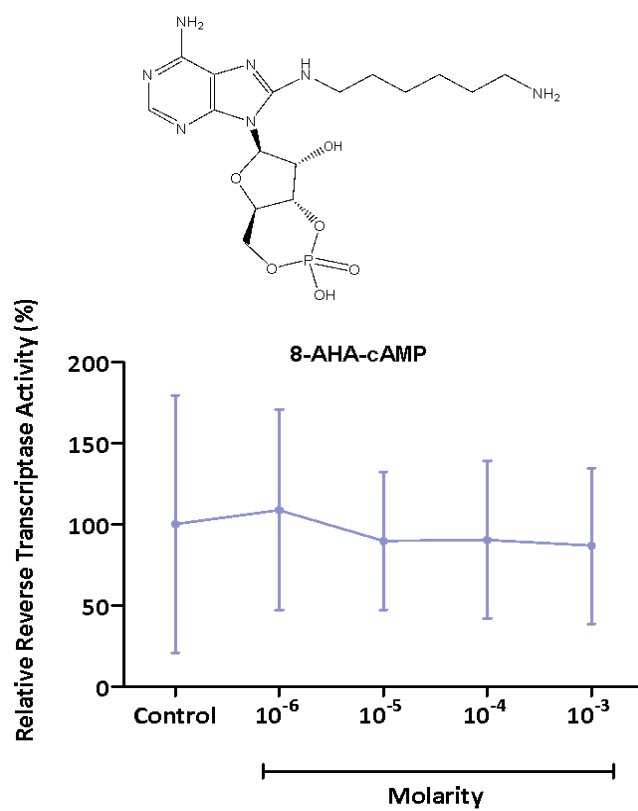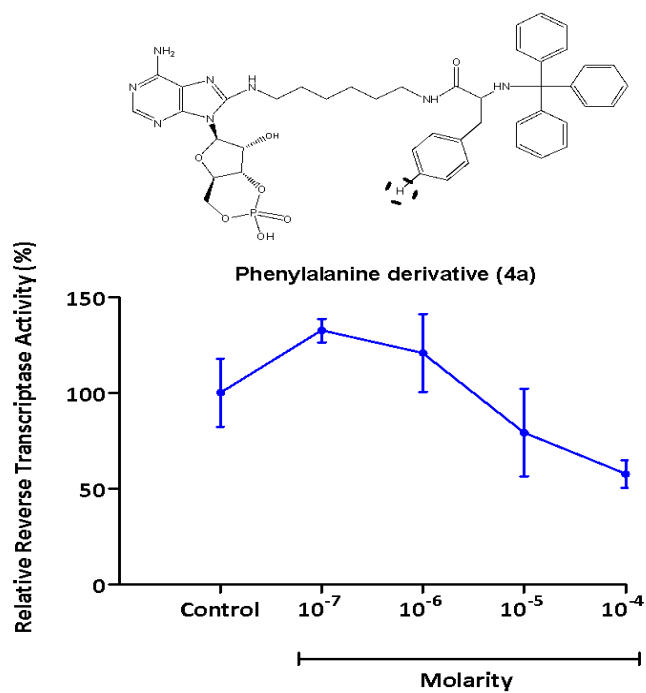
G

Figure 3.6   Relative reverse transcriptase activity (%) plotted against Molarity of inhibitor (**A**) Nevirapine, (**B**) 8-(6-aminohexyl) adenosine,3′,5′-cylic-monophosphate (**C**) 4a (**D**) 4b (**E**) 4c (**F**) 4d (**G**) 4e. RT mixed with lysis buffer and DMSO was used as the control (positive). Results were reported as mean +/- SD (n=3). Structures of Nevirapine, 8-(6-aminohexyl) adenosine,3′,5′-cylic-monophosphate, (4a-e) were drawn with ChemDraw.

Table 3.6   The estimated IC_{50} values for Nevirapine and N-trityl-p-substituted-phenylalanine-8-(6-aminohexyl)amino-adenosine-3′,5′-cyclic monophosphates against HIV-1 RT *in vitro.*
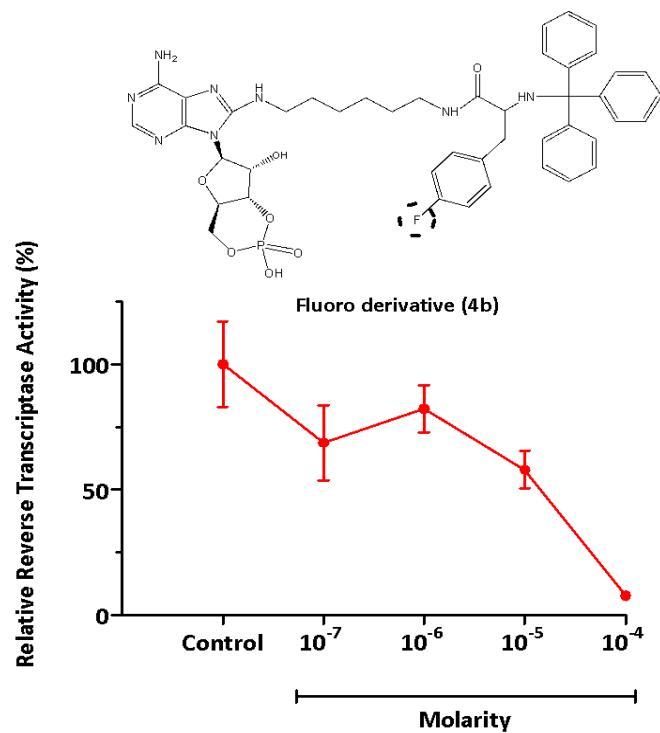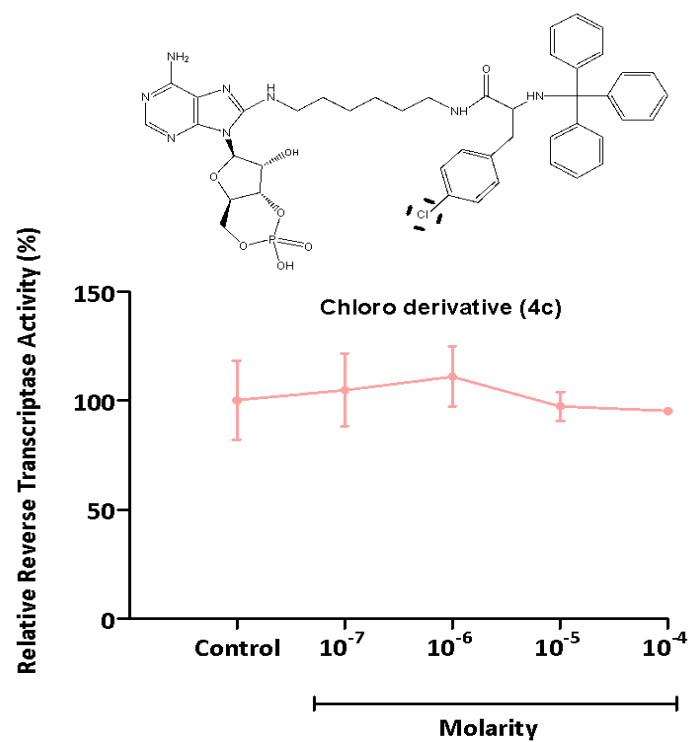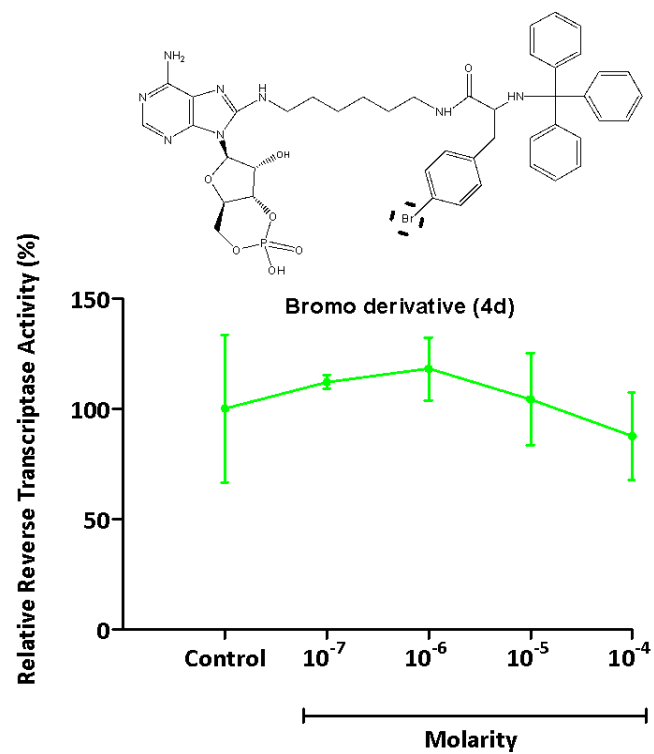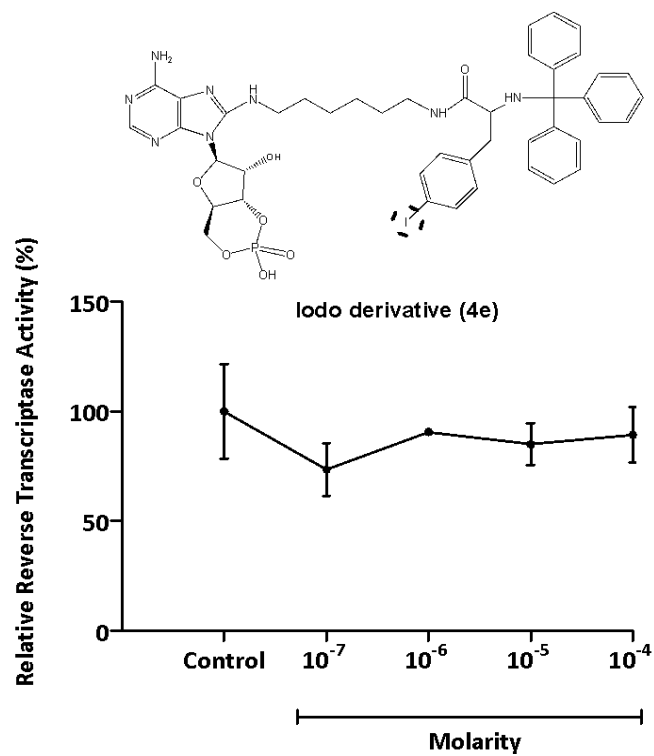
Compounds	IC_{50} (μM)
Nevirapine	3.30
4a	>100
4b	29.2
4c	>100
4d	>100
4e	>100
8-AHA-cAMP	>100

The line graphs as seen in Figure 3.6 were constructed using GraphPad Prism 2010 and show a graphical representation of the mean reverse transcriptase activity values of the five compounds para-H (4a), para-F (4b), para-Cl (4c), para-Br (4d), para-I (4e) and 8-AHA-cAMP. Nevirapine showed good inhibitory activity being effective at 10^{-5} M (Figure 3.6 A). 8-AHA-cAMP was inactive over the concentration range of 10^{-3}-10^{-6} M (Figure 3.6 B). The N-trityl-fluoro derivative showed excellent activity against reverse transcriptase acting at the concentrations 10^{-4}, 10^{-5} and 10^{-7} respectively (Figure 3.6 D). At 10^{-7} M, the phenylalanine derivative showed no sign of inhibitory activity on the RT enzyme, instead showed an increase in RT activity. This could have been due to assay conditions and interference. However, at higher concentrations of 10^{-5} M and 10^{-4} M, a decrease in reverse transcriptase enzyme activity was shown (Figure 3.6 C). Para-halo derivatives 4c, 4d and 4e (Cl, Br, I) were inactive at all concentrations. The IC_{50} values shown in Table 3.6 indicate that Nevirapine and the para-fluoro derivative (4b) were the most active inhibiotors with IC_{50} values of 3.30 μM and 29.2 μM respectively. At low concentration under the described assay conditions, Nevirapine, fluoro (4b) and bromo (4d) HIV-1 RT activity exceeded that of the control in the absence of inhibitors indicating poor inhibition activity under the assay conditions.

Nevirapine, a non-nucleoside reverse transcriptase inhibitor was one of the first successful agents used in the treatment of HIV-1. In this study, it was used as a standard to compare against all synthesised 'chiral' compounds. In the presence of Nevirapine, a decrease in RT activity (43 %) was shown at 10^{-5} M (Figure 3.6 A). Thereafter, at lower concentration (10^{-6} M and 10^{-7} M) RT activity increased markedly. However, in a study conducted done by Grob *et al*., (1992), Nevirapine showed strong inhibitory activity against the RT at a lower concentration with an IC_{50} of 84 nM (approximately 1×10^{-7} M). Frezza *et al*.,(2013) also reported Nevirapine to be active at low concentration of 100 nM (1×10^{-7} M). Possible reason for this outcome could be the sensitivity of the assay kit and assay conditions (i.e colour reactions can take up to one to 15 hours to develop). In past studies, cell-based assays were shown to be sucessful in determining the activity of compounds against HIV-1 RT (Aldeson *et al*., 2003). However, at the department of Biochemistry, Westville Campus, the appropriate equipment and a set of biocontainment (Biosafety level 2/3) precautions required to isolate HIV-1 RT in an enclosed laboratory facility was not available.

In another study Nevirapine was shown to be active against HIV-1 RT with an IC_{50} value ranging from 0.01 μM to 0.1 μM (Hermsen *et al*., 2010). However, according to our results the calculated IC_{50} value was 3.30 μM. In the same report (Hermsen *et al*., 2010), Delavirdine, another NNRTI was showed an IC_{50} value of 0.26 μM.

The inhibitory mechanism of NRTIs is such that they compete with naturally occurring nucleosides usually at the triphosphate level to prevent their incorporation into the viral DNA (Section 1.4). The reverse transcriptase enzyme adds NRTIs onto the growing DNA molecule. Therefore, naturally occurring nucleosides can no longer be added to the growing viral DNA, which is thereby terminated. In this study, the use of biotin and digoxigenin labelled dUTP are used to tag cDNA for colorimetric dectection. Biotin is relatively small and due to the fast rate of reverse transcription; the RT enzyme can easily mistake the compounds for dTTP and add them onto the growing RNA/DNA strand of the heteroduplex along with naturally occurring nucleotides. Thus, to detect the presence of biotin labelled RNA/DNA, streptavadin is pre-coated on microtitre plates. An antibody-peroxidase conjugate, antiDIG-peroxidase, was used to bind immoblised DIG-labelled cDNA and quantify it with an appropriate peroxidase substrate in a colorimetric assay.

The N-trityl-p-F-DL-phenylalanine-8-(6-aminohexyl)aminoadenosine-3′,5′-cyclic-monophosphate was the strongest RT inhibitor (69 %) acting at 10^{-7}M, while the N-trityl-L-phenylalanine-8-(6-aminohexyl) amino adenosine-3′,5′-cyclic monophosphate and N-trityl- p-l-DL-phenylalanine-8-(6-aminohexyl) amino adenosine- 3′,5′-cyclic monophosphate were weak inhibitors or otherwise remained inactive. According to Figure 3.6 D RT enzyme activity in the presence of para-fluoro derivative at 10^{-4} M was extremely low (7.5 %). The L-phenylalanyl derivative (4a), on the other hand, inhibited RT activity down to 57 % at the same concentration. And if we continue to compare results of fluoro and phenylalanine derivatives (Figure 3.6 D and C), we notice that the fluoro derivative at a higher concentration is a more effective inhibitor than the remaining para-halo derivatives (4c-e).

Previous studies have shown that para substitution of the phenylalanine ring in N-trityl-phenylalanyl-8-AHA-cAMP has a strong influence on M-MuLV RT activity (van Zyl *et al*., 2010). The halide substituent at the para position of the phenyl ring in the phenylalanyl component may have influenced the inhibitory effect of each chimeric compound. It is shown that the atomic radius of each halogen increases as atomic number increases. Therefore, the fluorine atom has an atomic radius of 0.71Å, chlorine atom 0.99Å, bromine atom 1.14Å and iodine 1.33Å. It was suggested that the size of the substituent might also influence the entry of the inhibitor in the RT active site or NNRTI-BP (van Zyl *et al*., 2010).

The low activity of the 'parent' derivative L-phenylalaninyl derivative (4a) could have resulted from the absence of an electron withdrawing halo substituent on the para position of the phenylalanine ring.

The uniqueness of our derived compounds is that the 8-(6-aminohexyl) aminoadeosine-3′,5′-cyclic monophosphate component is a nucleotide and not a preferred nucleoside. As mentioned earlier, NtRTIs are polar in nature as they contain a phosphate group, a 5-carbon sugar and a nitrogenous base thus, making it difficult to move across the hydrophobic membrane to enter the cell.

The nature of the NNRTI-BP is hydrophobic, thus it would be only expected to 'favour' hydrophobic interactions/molecules rather than polar molecules/interactions. Therefore, the results obtained in this study may be explained, in part, by the smaller atomic radius of fluorine leading to a more favourable fit in the BP.

The NRTI, TFV was modified to Tenofovir disoproxil (TDF) and has become one of the most commonly used drugs for the treatment of HIV-1 infection. *In vivo*, TFV is not very effective and the reason is that at physiological pH, it is negatively charged making it hydrophilic. This quality possibly makes it difficult to move across a hydrophobic plasma membrane (Van Rompay *et al*., 2012). For this reason, Tenofovir was esterified with chloromethyl isopropyl carbonate to (TDF) thus making the drug hydrophobic and more active than TFV (Wang *et al*., 2016).

Similarly, compounds in this study have a cyclic phosphate group and future work on the most active compound N- trityl-p-F-DL-phenylalanine -8-(6-aminohexyl) amino adenosine-3′,5′-cyclic monophosphate can be aimed at esterifying the hydroxyl group and making the compound even more hydrophobic. This could improve the compound's activity *in vitro*.

3.3.5   Effect of organic solvents on HIV- 1 RT activity

The use of organic solvents in some enzyme assays is based on the hydrophobic nature of certain substrates and inhibitors, which are insoluble in aqueous media. In these cases, the substrate or inhibitor is first dissolved in the appropriate organic solvent and then introduced to reaction mixtures where the solvent is diluted to levels that do not inactivate or cause adverse effect to the enzyme activity and the substrate or inhibitor. In this study, DMSO, a dipolar aprotic solvent is used (Cevallos *et al*., 2017) and its ability to dissolve water insoluble polar and non-polar molecules and its low toxicity levels make it a popular choice. Although the DMSO final concentration in cell-based *in vitro* assays for HIV-1 RT assays is $\leq$ 1% (Wildum *et al*., 2013), enzyme-based assays tolerate higher DMSO concentrations up to 5% (Lingham *et al*., 1996; Tewtrakul *et al*., 2002) and 10% (Lai *et al*., 2009; Lai *et al*., 2014). In this present study, 10× stock solutions of the relatively hydrophobic tritylated compounds 4a-e, Nevirapine and 8(6-aminohexyl)aminoadenosine-3′,5′-cyclic monophoshate were made up in 99 % DMSO. Serial dilutions were carried out with DMSO. Stock solutions aliquots (6 µl) were diluted to 60 µl with aqueous assay components yielding reaction mixtures containing 10% DMSO. It was imperative to maintain the final concentration of DMSO at this level to avoid possible precipitation of test compounds, that incorporate the very hydrophobic and bulky trityl group at lower levels of the solvent. Results presented in Figure 3.7 showed that 10% DMSO

in the reaction mixture had no significant effect on HIV-1 RT activity in the colorimetric assay. In other related studies on M-MuLV RT (van Zyl *et al.*, 2010; Hawtrey *et al.*, 2008) tritylated test compounds were dissolved in ethanol which was present in assay mixtures at 10 %. The inhibition of M-MuLV RT activity by DMSO has been shown to be dose dependent in the range 12-30 % although relative activity in the range 0-10% was $\geq$ 100% (Yasukawa *et al.*, 2002).
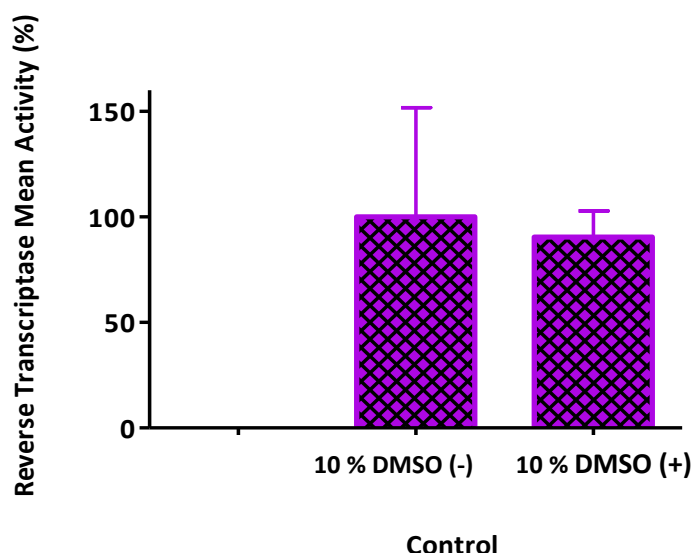
Figure 3.7   10 % DMSO on HIV-1 reverse transcriptase activity.

3.3.6   Computational studies

Molecular docking is a computational technique used to predict orientation of a ligand with its target protein based on their binding affinity. This technique is imperative as it serves to screen for drug-like molecules for improved drug development in various research laboratories and pharmaceutical companies (Trott and Olson, 2010). In this study AutoDock Vina was used to determine the binding energies and probable binding orientation of Nevirapine and the N-tritylated-phenylalanyl compounds with HIV-1 RT allosteric site. AutoDock Vina is the newest docking programme commonly used due to its speed and improved accuracy qualities (Trott and Olson, 2010). Figure 3.8 (B-F) clearly shows that the N-tritylated derivatives (4a-e) are positioned in the same spatial environment of the HIV-1 RT allosteric site occupied by Nevirapine (Figure 3.8 A). However, Nevirapine and the fluoro derivative (4b) have shown to

be satisfactorily accomodated by the enzyme (ribbons), whilst the other compounds don't seem to fit correctly. Table 3.7 provides an indication of the most probable active and least active compounds according to their calculated binding energies. The para-fluoro derivative (4b) was shown to be most active (-8.4 kcal/mol), of the tritylated compounds and second to Nevirapine (-9.9 kcal/mol). The para-chloro derivative (4c) showed lower binding affinity (-7.8 kcal/mol) while, para-bromo (4d) and para-Iodo (4e) showed the lowest binding affinities (-7.1 and -6.5 kcal/mol, respectively). Figure 3.9 shows the specific interactions between Nevirapine and compounds 4a-e with the RT amino acid residues in close proximity to the compounds in and about the allosteric binding pocket. The aromatic amino acid residues Tyr181, Tyr188, Phe227, Trp229 (Section 1.2) are seen lining the NNRTI-BP and showed excellent van de Waals and π-π interactions that contributed to the binding of NNRTIs to the allosteric site (Figure 3.9).

The investigated chimeric compounds as well as Nevirapine were docked into the allosteric site. Honarparvar *et al*., (2013) explained the various parameters that influence docking studies. Thus it was shown that small rigid molecules are easier to dock than larger molecules. Also, a thorough understanding of inhibitor and enzyme interactions is required. It is also essential to confirm the flexibility of the enzyme and whether it has more than one possible conformation. According to results (Table 3.7) the control, Nevirapine performed better than the synthesized compounds (-9.9 kcal/mol). This was expected as Nevirapine and other non-nucleoside RT inhibitors for example Rilpivirine have shown excellent inhibitory properties in previous reports (Nizami *et al*., 2016). In a past study done by Nizami *et al*., (2016), Rilpivirine, a non-nucleoside RT inhibitor was used against the RT enzyme and showed that this drug had the ability to take on multiple conformations upon entry into the allosteric binding pocket. Table 3.7 indicates that the docking results seem to have supported the experimental findings. The para-fluoro derivative (4b) had a docking score of -8.8 kcal/mol which is indicative of good binding interaction with the RT enzyme compared to the para-iodo derivative which showed poor binding affinity (-6.5 kcal/mol). Other compounds included in this study (4a,c,d) showed intermediate affinties (-7.1-7.8 kcal/mol). The lower performance of the synthesised compounds is probably due to the torsional penalty, i.e. there are several rotatable bonds and molecules are quite bulky. Therefore, considerable energetic barriers need to be overcome for these molecules to fit into the RT binding site. That NNRTI-BP is hydrophobic in nature is well established. It is assumed therefore that the three benzene rings of the trityl components in test compounds would contribute to the hydrophobicity and thus have a better chance of interacting with the hydrophobic residues lining the binding pocket. It is believed that the

benzene rings of the para-fluoro derivative probably formed hydrophobic interactions with non-aromatic amino acid residues Pro176 and Val179. The close proximately of the aromatic residues: Tyr188, Tyr318, His235, Phe227 and Trp229 suggests that these amino acid side chains may contibute to the interactions between ligand and RT allosteric site.

Apart from hydrophobic residues, hydrophilic residues such as Ser105, Lys101, Lys103, Asp192, Glu224 and Glu138 form part of the binding pocket. Figure 3.9 reveals that both hydrophilic and hydrophobic amino acid residues contributed to the binding interactions. In a study by Miceli *et al*., (2013), (6R)-6-hydroxydichotoma-3,14-diene-1,17-dial (HDD) docked into the wild type and mutant HIV-1 RT formed hydrogen bond interactions with the side chains of aromatic residue Tyr188 and with Glu138 (Section 1.9.4, Figure 1.12). In this similar case para-fluoro derivative may have formed hydrogen bond interaction with Glu28 and Glu138. The fluoro substituent on the phenyl ring may have also contributed to the binding interactions. Hydrogen bond interactions between charged amino acid residue Lys101, Lys103 and Pro236 mainly with the 3′,5′-cyclic phosphate moiety of chiral compounds are believed to have contributed significantly to the binding affinities (Figure 3.9 B-F). The para-fluoro derivative (4b) is predicted to have formed three hydrogen bonds with Lys101, Lys103 and Pro236, while the para-iodo derivative (4e) is calculated to have formed only one hydrogen bond with Pro236 in the allosteric site. Hydrogen bonds are represented as green dashed lines as seen in Figure 3.9.

Table 3.7   Dock binding energy (kcal/mol) of Nevirapine and test compounds with HIV-1 RT allosteric pocket as predicted by AutoDock Vina.

Compound	Affinity (kcal/mol)
Nevirapine	-9.9
4a	-7.3
4b	-8.4
4c	-7.8
4d	-7.1
4e	-6.5
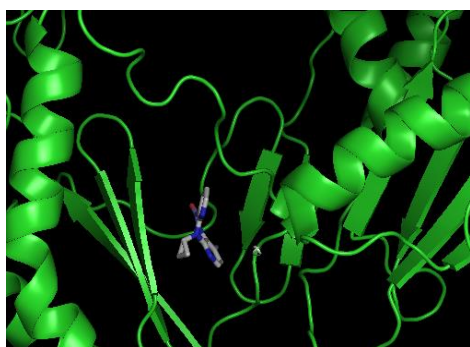
A
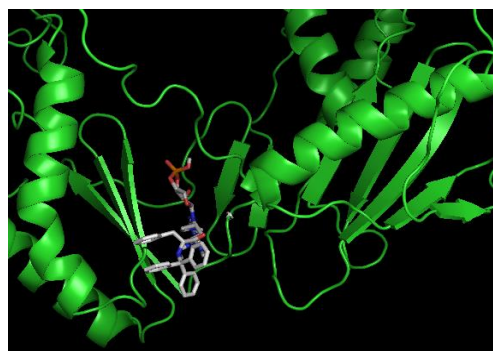
B

C
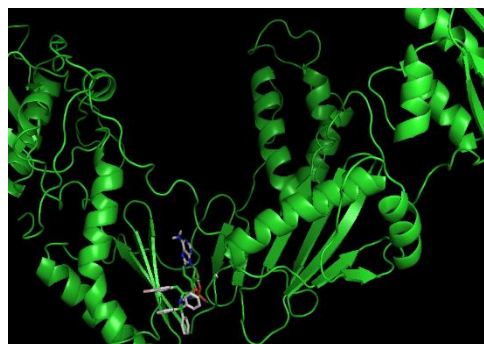
D

E

Figure 3.8   3D docking interaction of : **(A)** Nevirapine **(B)** 4a **(C)** 4b **(D)** 4c **(E)** 4d **(F)** 4e and HIV-1 reverse transcriptase allosteric site located between the palm (left) and thumb (right) subdomains. Compounds are in stick representation while the RT allosteric site is in ribbon representation.

A
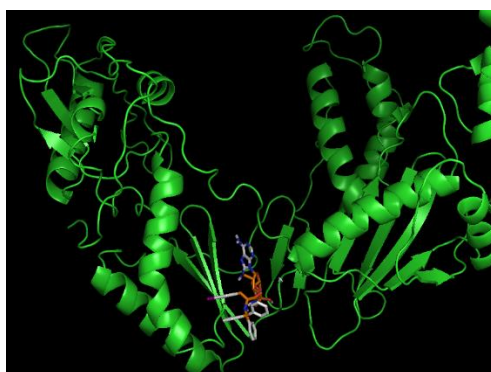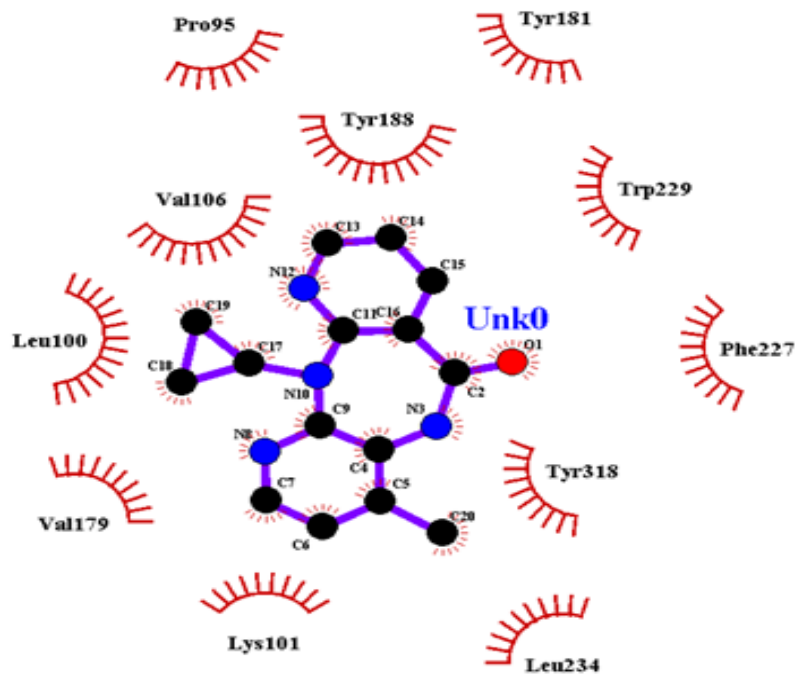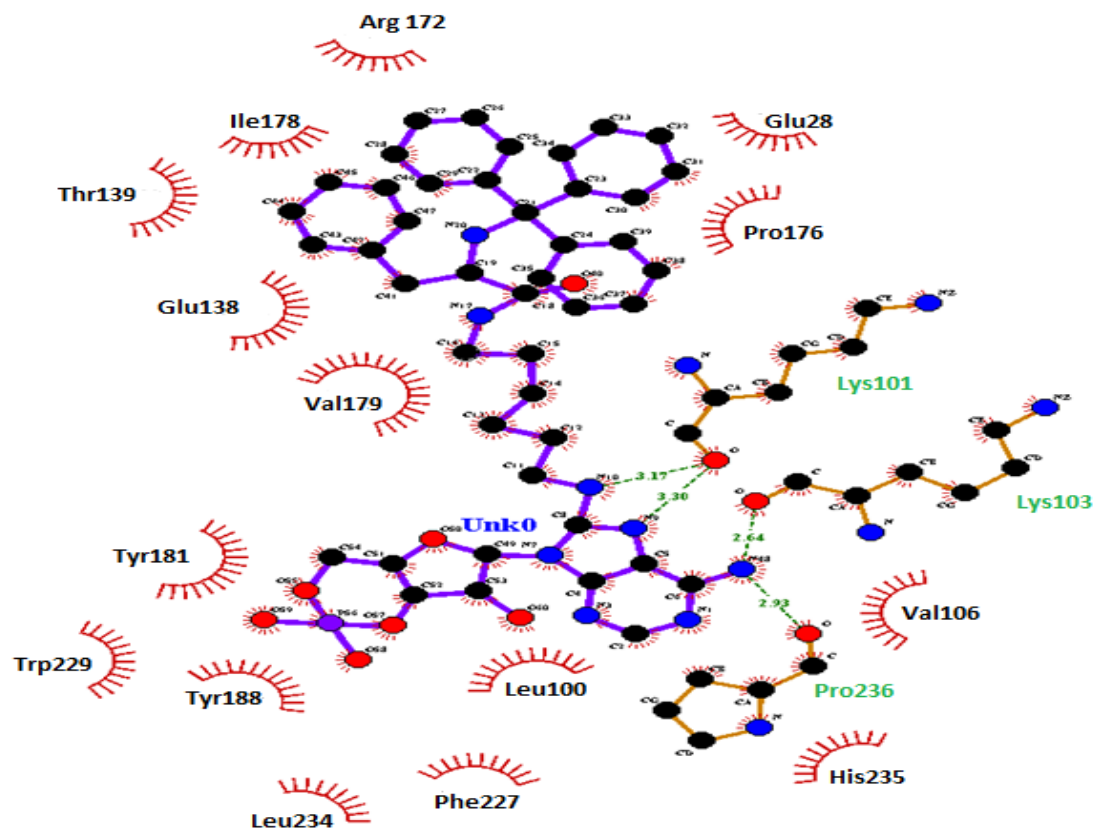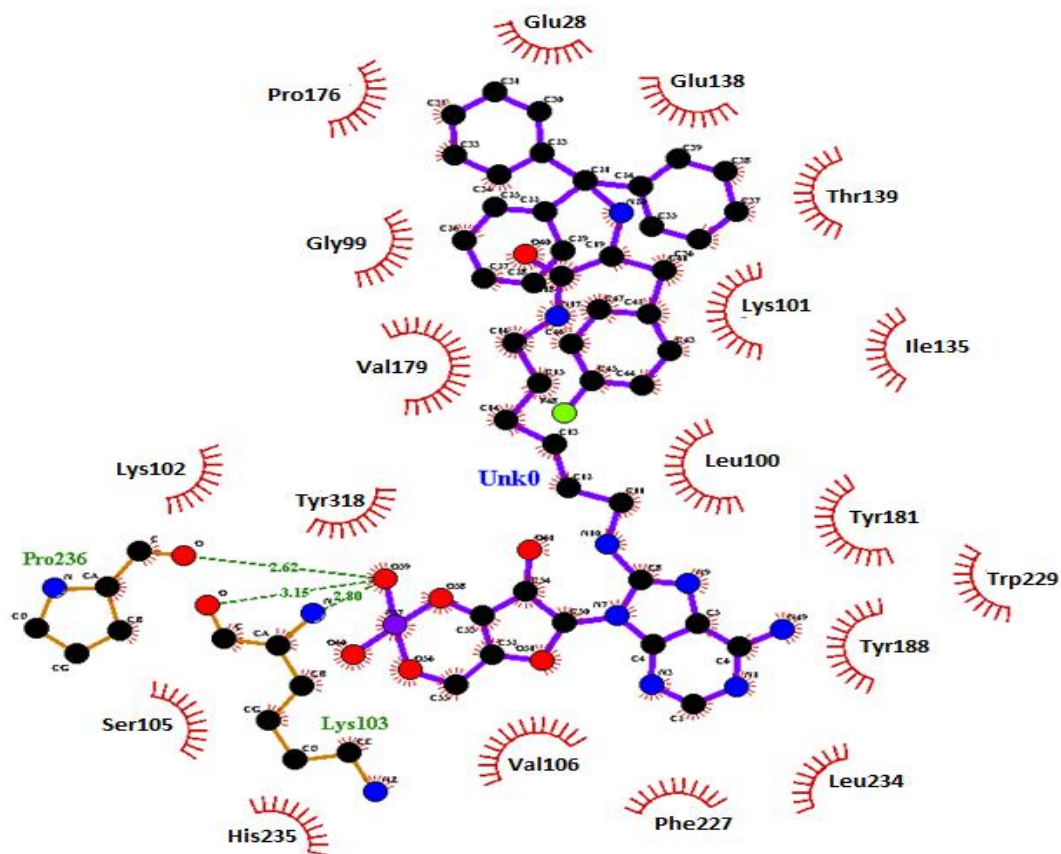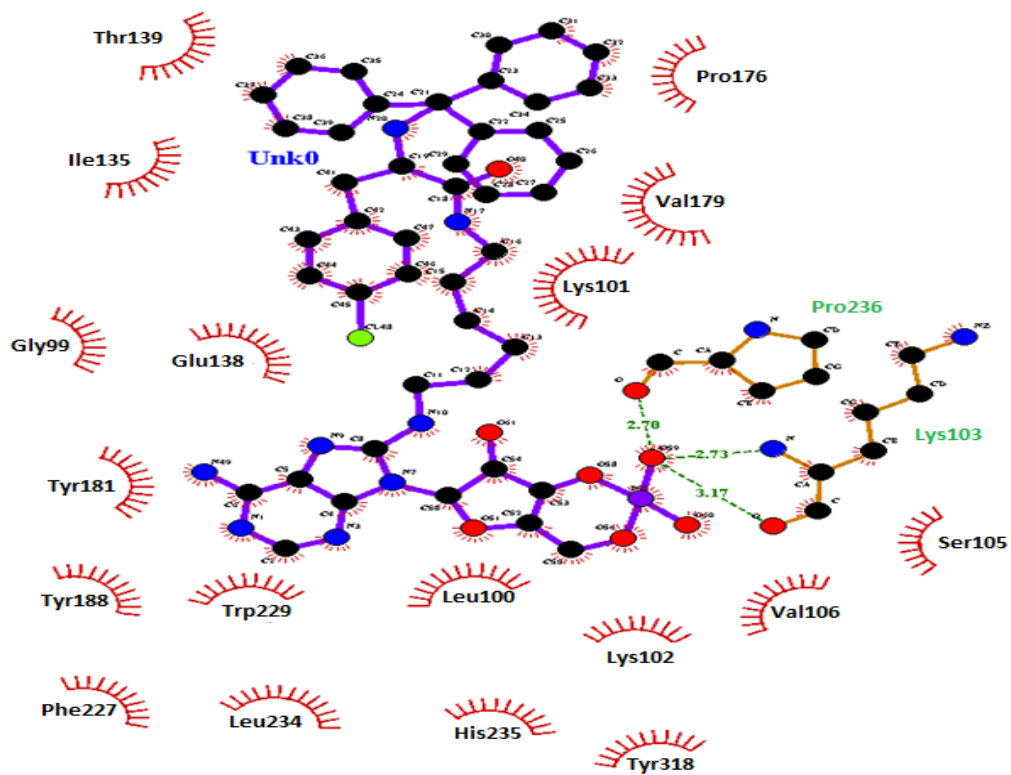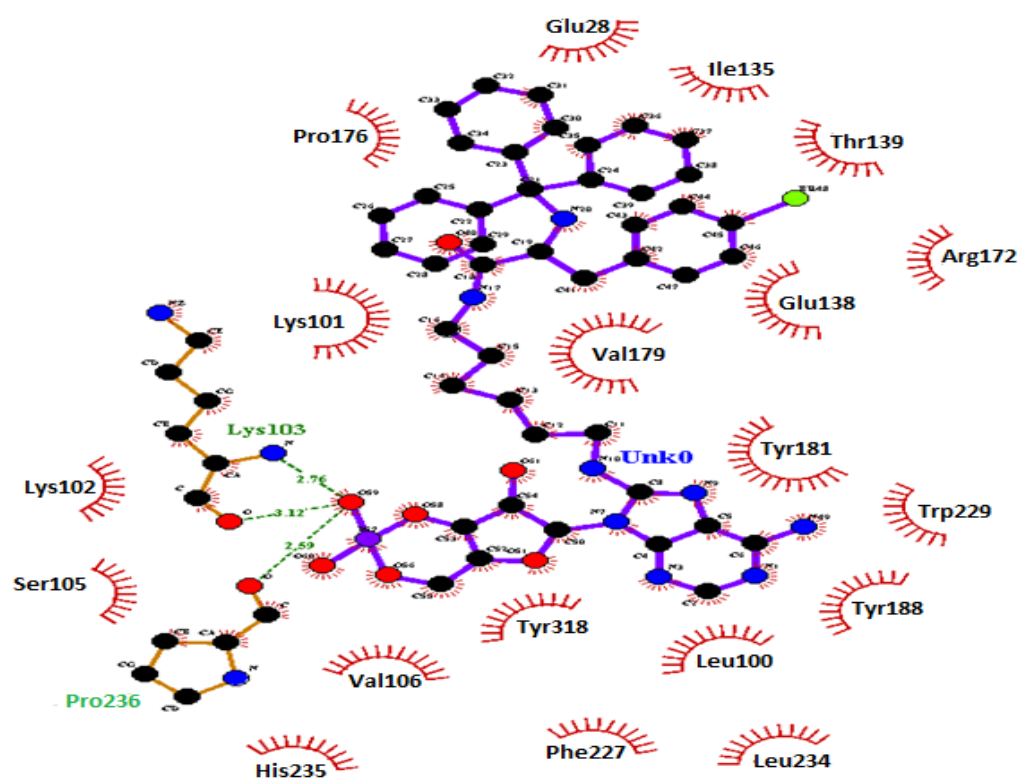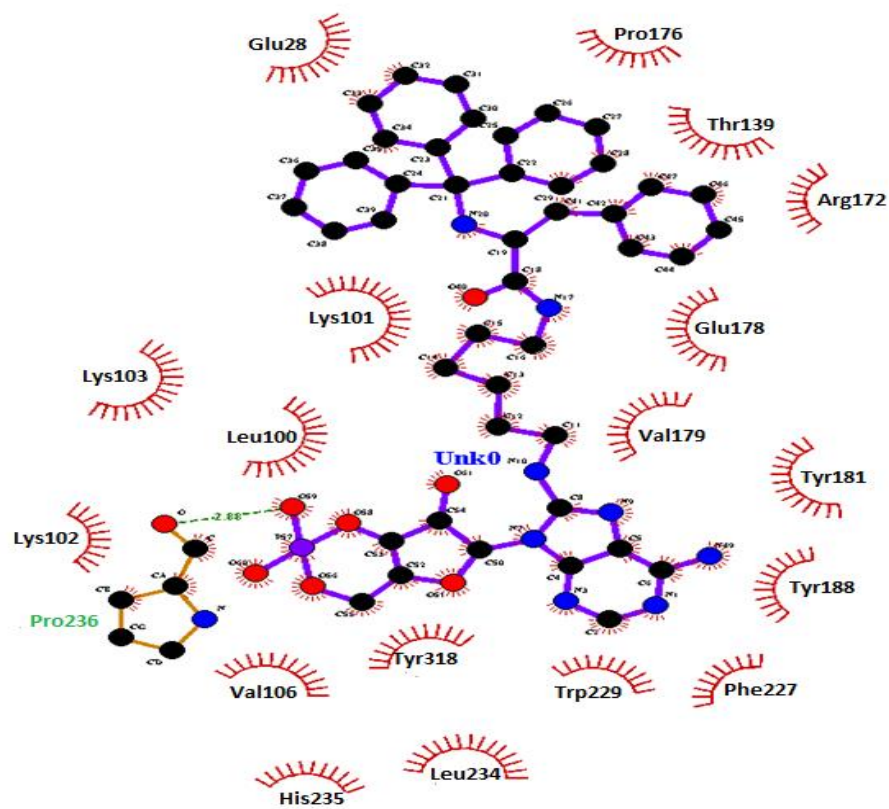

B

C

D

E

F

Figure 3.9 Ligplot predicted docking binding interactions between: (**A**) Nevirapine (**B**) 4a (**C**) 4b (**D**) 4c (**E**) 4d (**F**) 4e and HIV-1 RT allosteric site. Hydrogen bonds are indicated by green dashed lines between atoms involved, while hydrophobic contacts are shown as an arc with red spikes pointing towards the atoms they contact (Wallace *et al*., 1995) ⬤━⬤━⬤ Ligand atoms.

In a study by Sluis-Crèmer *et al*., (2004) Delavidine, a NNRTI was compared against other NNRTIs. From the structure of Delavidine (Figure 1.7) it can be noted that it is much bulkier than most NNRTIs. It has a volume of ~ 380Å^3 while other NNRTIs are in the range 230–290 Å^3 (Sluis-Crèmer *et al*., 2005). This bulkiness is said to support another binding mode when compared to the smaller NNRTIs. The size and shape of this inhibitor causes it to project/extend further than the binding pocket into the solvent. Another quality of this NNRTI is that it can interact with regions that most NNRTIs are restricted from. The piperazine ring component on delavirdine causes the inhibitor to position itself close to the hydrophobic residue Val106. Similarly, the benzene rings in the para fluoro derivative showed binding interactions with the hydrophobic side chain of Val179.

Nevirapine, on the other hand showed strong van der Waals interactions with Val106 ,Val179 and Tyr188 due to the aromatic properties of the pyridine ring (Figure 3.9 A). Possible π-π stacking between phenyl rings of Nevirapine and Tyr 181/Tyr188 aromatic side chains may also be present. Hydrogen bond interactions between Tyr318 and Nitrogen atom (N3) from the diazepine ring of Nevirapine could have also formed. Additionally, Tyr318 amino acid residue in the NNRTI-BP probably formed π-π interaction with Nevirapine. This result is supported by a study carried out by Kroeger Smith *et al*., (1996). In another study by Raju *et al*., (2010) the interaction energies (IE) of amino acid residues surrounding Nevirapine were calculated and discussed. Trp229 was calculated to be 4.58 kcal/mol. The aromatic residues Tyr318 and Phe227 interact with Nevirapine through weak hydrogen bonds and thus had a smaller IE value than Trp229. Lys101, Leu100, Lys103, Val106, Leu234, Gly190, His235 and Pro236 were also shown to be imperative in the binding of Nevirapine to HIV-1 RT. Figure 3.9A shows that all the above-mentioned amino acid residues are in close contact with Nevirapine confirming binding interactions with it.

Nevirapine is a non nucleoside inhibitor. Therefore, it seems resonable to assume that it will bind to the NNRTI-BP only. Most of the residues surrounding the NNRTI-BP could comfortably help bind Nevirapine to RT via hydrophobic interactions. (Leu100, Trp229,

Tyr188, Tyr318, Pro95). The charged amino acid residue Lys101 could have formed hydrogen bond interaction between the carbonyl oxygen of Lys101 and H5 of Nevirapine. Similar results were presented and discussed by Raju *et al.,* (2010). It was also evident that the four hydrophobic residues (Trp229, Phe227, Tyr318, Leu234) played a role in binding. This was supported by results from an earlier study (Smerdon *et al.*, 1994) wherein an x-ray crystal structure of HIV-1 RT with Nevirapine itself was reported. With this information the overall binding site and interactions have been described. The x-ray structure revealed that residues (Trp229, Phe227, Tyr318, Leu234) played an important role in binding interactions. Results of docking studies presented here (Figure 3.9) correlated with co-crystallization data of HIV-1 RT with Nevirapine indicating that molecular docking findings generated by the LigPlot platform are validated.

The chloro derivative (4c) showed a lower binding affinity (-7.8 kcal/mol) than that of the fluoro derivative (-8.4 kcal/mol). This is in agreement with data from the *in vitro* assay, which displayed poor activity of the chloro compound (4c) against the HIV-1 RT. Nevertheless, docking studies were performed to establish a possible correlation with *in vitro* results. Chlorine perhaps contributed to the bulkiness of the hydrophobic component making it less likely to fit in the NNRTI-BP. It is of much interest that the nature of the para halo substituent on the phenylalanine benzene ring in structures 4a-e determines their docking aspect in the NNRTI-BP.

Murine leukemia virus reverse transcriptase virus (M-MuLV RT) and Human immunodeficnecy virus reverse transcriptase (HIV-1 RT) display similar structural features that enable researchers to carry out initial screening to test for new anti-viral dugs. Coté and Roth, (2008) demonstrated the similarties by x-ray crystallography of the M-MuLV RT and HIV-1 RT. More specifically M-MuLV RT was found to be a monomer consisting of 671 amino acids, whilst HIV-1 RT is a heterodimer consisting of a 560 amino acid subunit designated p66 and a (small 440 amino acid) p51 subunit. Interestingly, both the HIV-1 RT P66 subunit and the M-MuLV RT contain the palm, fingers, connection, thumb subdomains and the RNase H domain. In a study by van Zyl *et al.*, 2010 a related investigation was conducted. However, N-tritylated phenylalanine derivatives of amino-adenosine -3′,5′-cyclic monophospahtes were evaluated against M-MuLV RT and not HIV-1 RT. It was concluded that the iodo derivative with a higher halogen covalent radius (1.33 Å) showed better inhibitory activity when compared to its fluoro and chloro counterparts. This was rather suprising since the para-iodo derivative in this current study proved to be inactive. Indeed p-iodo derivative

was predicted to have the lowest binding affinity (Table 3.7) (-6.5 kcal/mol). However, one H-bond interaction is predicted for the iodo derivative. Here Pro236 and an unesterfied oxygen in the ribosyl 3′,5′-cyclic phosphate are involved.

A comparison of sequences found in M-MuLV RT and the HIV-1 RT p66 subunit was discussed by Coté and Roth, (2008) and it was shown that the respective subdomains have a specific sequence similarity. For example, the palm and fingers subdomain have approximately 25 % similarity in the amino acid sequences. There is approximately 12% similarity in the thumb subdomain whilst the connection subdomain conisits of merely 6% similarity. It was also noted that there is a further 111 amino acid sequence in the M-MuLV RT that is not present in the HIV-1 RT p66 subunit (671 versus 560 amino acids). The reason that the inhibition data of 4e in the HIV-1 system did not correlate with data obtained by van Zyl *et al*., (2010) could be that the derivative had more space to bind with more amino acid residues in the M-MuLV RT. In this regard it is important to note that the NNRTI-BP of HIV-1 is defined by both large and small subunit amino acid residues and is spatially well-defined. The M-MuLV RT NNRTI-BP has a more 'open' structure involving the monomeric RT and is theoretically able to accommodate molecules that extend beyond the allosteric site.

This study was conducted to establish if the nature of the para halo substituent on the phenylalanine benzene ring of the of N-trityl-phenylalanyl 8(6-aminohexyl)aminoadenosine-3′,5′-cyclic monophoshate (4a-e) has influence on the potency of chiral compounds as inhibitors of HIV-1 RT. Results suggest that the size of the para halo atom bears an inverse correlation with inhibitory potency. Therefore the para-fluoro derivative (4b) is most active and the para-iodo compound (4e) is the least active.

CHAPTER FOUR

CONCLUSION

HIV-1 reverse transcriptase inhibitors continue to play an imperative role in the treatment of HIV/AIDS, changing this fatal illness into a more controllable chronic infection. However, drug resistance is still a common cause of treatment failure. Over the years, extensive study has led to approved drugs for the treatment of the HIV infection. Anti-viral compounds comprising a nucleotide component separated from a hydrophobic amino acid derivative by a hydrophobic spacer element have shown promising activity against murine leukaemia reverse transcriptase. The synthesis of various N-tritylated para substituted phenylalanine derivatives (fluoro, nitro and iodo) coupled to the 8-(6-aminohexyl)aminoadenosine $3',5'$-cyclic monophosphate had previously been carried out to form chiral compounds, where the 8-(6-aminohexyl) amino-adenosine $3',5'$-cyclic monophosphate was directed toward the polymerization active site, while the tritylated para substituted phenylalanine components were designed to serve as the non-nucleoside and bind to non-nucleoside hydrophobic binding pocket, simultaneously. However, it was reported by van Zyl *et al*., (2010) that the chimeric compound N-tritylated meta fluoro-DL -phenylalanine-8-(6-aminohexyl) amino-adenosine $3',5'$-cyclic monophosphate acted as a non -competitive inhibitor.

The polymerase site of the monomeric M-MuLV RT has remarkable similarities to the polymerase site (p66) of the heterodimer HIV-1 RT. In this study, the L-phenylalanine derivative (4a) and the para-fluoro derivative (4b) showed RT inhibitory activity, while the para-chloro, para-bromo and para-iodo derivatives (4c-e) remained inactive. The atomic radius of the halide substituent has affected RT inhibition by the tritylated compounds. More especially, this parameter may therefore have a determining effect on the accommodation of derivatives in the proposed binding sites. The fluoro derivative (4b) showed comparable activity to the frontline drug Nevirapine in both *in vitro* and computational experiments. Apparent binding and possible interaction with aromatic residues (Tyr181, Tyr188, Phe227, Trp229), along with hydrophilic residues (Lys101, Lys103, Glu28 and Glu138) and

hydrophobic amino acid residue (Val106, Val179) in the allosteric site suggests that compounds may be acting as NNRTIs. Nevirapine showed inhibitory effect agaisnt RT activity, however at very high concentrations with an IC_{50} of 3.30 µM as compared to past liertaure where IC_{50} was as low as 84 nM. Cell-based assays could have been performed to compare with the RT colorimetric assay kit however, at the department of Biochemistry, Westville Campus, the appropriate equipment and a set of biocontainment (Biosafety level 2/3) precautions required to isolate HIV-1 RT in an enclosed laboratory facility was not available.

As previously mentioned the NRTI, Tenofovir (TVF) was modified to Tenofovir disoproxil (TDF) by esterification with chloromethyl isopropyl carbonate. This has made the drug more successful than the esterfied TFV. Similarly, future studies directed towards potentiation of N-trityl-p-F-DL-phenylalanyl-8-(6-aminohexyl)aminoadenosine-3′,5′-cyclic-monophosphate, penetration of cellular plasma membrane must be considered if this system is to be assessed in cell culture and in *in vivo* studies.

Therefore esterfication of the polar ribosyl 2′-OH group and the unesterfied OH group in the 3′,5′-cyclic phosphodiester to achieve higher levels of hydrophobicity may prove to be fruitful. Other future work could include the investigation of the synthesized compounds in cell-based assays in an appropriate laboratory facility.

REFERENCES

Aldeson, M.E., Pacchia, A.L., Kaul, M., Rando, R.F., Ron, Y., Pelts, S.W. and Dougherty, J.P. Toward the Development of a Virus-Cell-Based Assay for the Discovery of Novel Compounds against Human Immunodeficiency Virus Type 1. *Antimicrobial agents and chemotherapy*.47(2): 501–508.

Adetokunboh, O.O., Schoonees, A. and Wiysonge, C.S. (2014). Antiviral efficacy and safety of abacavir-containing combination antiretroviral therapy as first-line treatment of HIV-infected children and adolescents*:* a systematic review protocol. *Systematic Reviews*.12;3:87.

Anderson, G.W., Zimmerman, J.E. and Callahan, F.M. (1967). Reinvestigation of the mixed carbonic anhydride method of peptide synthesis. *Journal of the American Chemical Society*. 89(19), 5012–5017.

Arts, E.J. and Hazuda, D.J. (2012). HIV-1 Antiretroviral drug therapy. *Cold Spring Harbor Perspectives In Medicine*. 2(4): a007161.

Asahchop, E.L., Wainberg, M.A., Sloan, R.D. and Tremnlay, C.L. (2012). Antiviral drug resistance and the need for development of new HIV-1 reverse transcriptase inhibitors. *Antimicrobial Agents and Chemotherapy*. 56(10): 5000–5008.

Behera, S., Ghanty, S., Ahmad, F., Santra, S. and Banerjee, S. (2012). UV-visible spectrophotometric method development and validation of assay of paracetamol tablet formulation. *Journal of Analytical and Bioanalytical Techniques*. 3(6):151.

Betancor, G., Álvarez, M., Marcelli, B., Andrés, C., Martínez, M.A. and Menéndez-Arias, L. (2015). Effects of HIV-1 reverse transcriptase connection subdomain mutations on polypurine tract removal and initiation of (+)-strand DNA synthesis. *Nucleic Acids Research*. 43(4): 2259–2270.

Biswas, N., Rodriguez-Garcia, M., Shen, Z., Crist, S.G., Bodwell, J.E., Fahey, J.V. and Wira, C.R. (2014). Effects of tenofovir on cytokines and nucleotidases in HIV-1 target cells and the mucosal tissue environment in the female reproductive tract. *Antimicrobial Agents and Chemotherapy*. 58(11): 6444-53.

Bock, C. and Lengauer, T. (2012). Managing drug resistance in cancer: Lessons from HIV therapy. *Nature Review. Cancer*. 12(7): 494-501.

Borges, A.H., Lundh, A., Tendal, B., Bartlett, J.A., Clumeck, N., Costagliola, D., Daar, E.S., Echeverrial, P., Gisslen, M., Huedo-Medina, T.B., Hughes, M.D., Hullsiek, K.H., Khanbol, P., Komati, S., Kumar, P., Lockman, S., MacArthur, R.D., Maggiolo, F., Matteelli, A., Miro, J.M., Oka, S., Petoumenos, K., Puls, R.L., Riddler, S.A., Sax, P.E., Sierra-Madero, J., Sierra, J., Torti, C. and Lundgren, J.D. (2016). Nonnucleoside reverse-transcriptase inhibitor vs ritonavir-boosted protease inhibitor-based regimens for initial treatment of HIV infection: a systematic review and meta analysis of randomized trials. *Clinical infectious diseases*. 63(2): 268-280.

Brittain, H.G. (1993). Analytical profiles of drug substances and excipients. Didanosine. Nassar, M.N., Chen, T., Reff, M.J. and Agharkar, S.N (editors). *Science Direct*. 22: 185-227.

Bukrinsky, M. and Adzhubei, A. (1999). Viral protein R of HIV-1. *Reviews in Medical Virology*. 9(1): 39-49.

Casiday, R. and Frey, R. (2001). Drug strategies to target HIV: enzyme kinetics and enzyme inhibitors. Chemical kinetics experiment.

Cavaluzzi, M.J. and Borer, P.N. (2004). Revised UV extinction coefficients for nucleoside-5′-monophosphates and unpaired DNA and RNA. *Nucleic Acids Research*. 32(1): e13.

Cevallos, A.M., Herrera, J., López-Villaseñor, I. and Hernández, R. (2017). Differential effects of two widely used solvents, DMSO and ethanol, on the growth and recovery of trypanosoma cruzi epimastigotes in culture. *Korean Journal of Parasitology*. 55(1): 81-84.

Chevalier, J., Yi, J., Michel, O. and Tang, X.M. (1997). Biotin and digoxigenin as labels for light and electron microscopy *in situ* hybridization probes: Where do we stand? *The Journal of Histochemistry and Cytochemistry*. 45(4): 481–491.

Chong, Y. and Chu, C.L. (2004). Understanding the molecular mechanism of drug resistance of anti-HIV nucleosides by molecular modeling. *Frontiers in Bioscience*. 9: 164-186.

Coffin, J.M. and Fan, H. (2015). The discovery of reverse transcriptase. *Annual Review of Virology*. 3(1):29-51.

Corey, E.J., Czako, B. and Kurti, L. (2007). Molecule and medicine. Jeffries, D.J (editor). *Science.*

Coté, M.L. and Roth, M.J. (2008). Murine leukemia virus reverse transcriptase: structural comparison with HIV-1 reverse transcriptase. *Virus Research.* 134(1-2): 186–202.

Craigie, R. and Bushman, F.D. (2012). HIV DNA integration. *Cold Spring Harbor Perspective in Medicine.* 2(7): a006890.

Das, K. and Arnold, E. (2014). HIV-1 reverse transcriptase and antiviral drug resistance (Part 1 of 2). *Current Opinion in Virology*. 3(2):111-118.

Das, K., Bauman, J.D., Clark, A.D.Jr, Frenkel, Y.V., Lewi, P.J., Shatkin, A.J., Hughes, S.H. and Arnold, E. (2007). High-resolution structures of HIV-1 reverse transcriptase/TMC278 complexes: Strategic flexibility explains potency against resistance mutations. *Proceedings of the National Academy of Sciences of USA.* 105(5): 1466–1471.

Das, K., Clark, A.D Jr., Lewi, P.J., Heeres, J., de Jonge, M.R., Koymans, L.M.H., Vinkers, H.M., Daeyaert, F., Ludovici, D.W., Kukla, M.J., Corte, B.D., Kavash, R.W., Ho, C.Y., Ye, H., Lichtenstein, M.A., Andries, K., Pauwels, R., Bethune, M.P.D., Boyer, P.L., Clark, P., Hughes, S.H., Janssen, P.A.J. and Arnold, E. (2004). Roles of conformational and positional adaptability in structure-based design of TMC125-R165335 (etravirine) and related non-nucleoside reverse transcriptase inhibitors that are highly potent and effective against wild-type and drug-resistant HIV-1 variants. *Journal of Medicinal Chemistry.* 47(10): 2550-60.

Das, K., Martinez, S.E., Bauman, J.D. and Arnold, E. (2012). HIV-1 reverse transcriptase complex with DNA and nevirapine reveals nonnucleoside inhibition mechanism. *Nature Structural and Molecular Biology.* 19(2): 253-259.

Das, S.R. and Jameel, S. (2005). Biology of the HIV nef protein. *Indian Journal of Medical Research.* 121(4): 315-332.

De Clercq, E. (2009). Anti-HIV drugs: 25 compounds approved within 25years after the discovery of HIV. *International Journal of Antimicrobial Agents*. 33(4): 307-320.

Dias, D.M. and Ciulli, A. (2014). NMR approaches in structure-based lead discovery: recent developments and new frontiers for targeting multi-protein complexes. *Progress in Biophysics and Molecular Biology*. 116(2-3): 101-112.

Engelman, A. and Cherepanov, P. (2013). The structural biology of HIV-1: mechanistic and therapeutic insights. *Nature Reviews Microbiology*. 10(4): 279–290.

Ensoli, B., Cafaro, A., Monini, P., Marcotullio, S. and Ensoli, F. (2014). Challenges in HIV vaccine research for treatment and prevention. *Frontiers in Immunology*. 5: 417.

Esnouf, R.M., Ren, J., Hopkins, A.L., Ross, C.K., Jones, E.Y., Stammers, D.K. and Stuart, D.I. (1997). Unique features in the structure of the complex between HIV-1 reverse transcriptase and the bis(heteroaryl)piperazine (BHAP) U-90152 explain resistance mutations for this nonnucleoside inhibitor. *Proceedings of the National Academy of Sciences of USA.* 94(8): 3984-3989.

Esposito, F., Kharlamova, T., Distinto, S., Zinzula, L., Cheng, Y.C., Dutschman, G., Floris, G., Markt, P., Corona, A. and Tramontano, E. (2011). Alizarine derivatives as new dual inhibitors of the HIV-1 reverse transcriptase-associated DNA polymerase and RNase H activities effective also on the RNase H activity of non-nucleoside resistant reverse transcriptase. *The FEBS Journal.* 278(9): 1444-1457.

Evans, F.E., Lee, C.H., Kapmeyer, H. and Kaplan, N.O. (1978). Proton magnetic resonance study of 8-(Aminohexyl)-aminoadenosine 5′-monophoshate. *Bioorganic Chemistry.* 7(1): 57-67.

Eswara Rao, K.V.S., Chitturi, R.T., Kattappagari, K.K., Kantheti, L.P.C., Poosarla, C. and Baddam, V.R.R. (2015). Impact of highly active antiretroviral therapy on oral manifestations of patients with human immunodeficiency virus/acquired immuno deficiency syndrome in South India. *Indian Journal of Sexually Transmitted Diseases and AIDS.* 36(1): 35–39.

Famiglini, V. and Silvestri, R. (2016). Review focus on chirality of HIV-1 non-nucleoside reverse transcriptase inhibitors. *Molecules.* 21(2). pii: E221.

Fasman, G.D. (1975). Handbook of biochemistry and molecular biology, 3rd Edition, *Nucleic Acids,* Vol I, pp. 65-215, CRC Press, Cleveland, Ohio.

Feigl, F. (1943). Laboratory manual of spot tests. Oesper, R.E. (translator). 186-188. *Academic press Inc.*

Frezza, C., Balestrieri, E., Marino-Merlo, F., Mastino, A. and Macchi, B. (2014). A novel, cell-free PCR-based assay for evaluating the inhibitory activity of antiretroviral compounds against HIV reverse transcriptase. *Journal of Medical Virology.* 86(1): 1-7.

Furman, P.A., Fyfe, J.A., St Clair, M.H., Weinhold, K., Rideout, J.L., Freeman,G.A., Lehrman,S.N., Bolognesi, D.P. and Mitsuya, H. (1986). Phosphorylation of 3'-azido 3'-deoxythymidine and selective interaction of the triphosphate with human immunodeficiency virus reverse transcriptase. *Proceeding of the National Academy of Sciences of USA.* 83 (21): 8333-8337.

Gaida, R., Truter, I. and Grobler, C. (2015). Efavirenz: A review of the epidemiology, severity and management of neuropsychiatric side-effects. *South African Journal of Psychiatry.* 21(3): 94-97.

Gaskin, S., Brazil, C. and Pickering, D. (2000). The sharing of injecting paraphernalia by intravenous drug users (IDUs) within a worcestershire cohort, with specific reference to water and filters. *International Journal of Drug Policy.* 11(6): 423-435.

Goldschmidt, V., Didierjean, J., Ehresmann, B., Ehresmann, C., Isel, C. and Marquet, R. (2006). Mg^{2+} dependency of HIV-1 reverse transcription, inhibition by nucleoside analogues and resistance. *Nucleic Acids Research.* 34(1): 42–52.

Goody, R.S., Müller, B. and Restle, T. (1991). Factors contributing to the inhibition of HIV reverse transcriptase by chain-terminating nucleotides *in vitro* and *in vivo*. *FEBS Letters*. 291(1):1-5.

Gostin, L. (1991). The needle-borne HIV epidemic: causes and public health responses. *Behavioural Sciences and the Law*. Summer; 9(3): 287-304.

Gottlieb, H.E., Kotlyar, V. and Nudelman, H. (1997). NMR chemical shifts of common laboratory solvents as trace impurities. *Organic. Chemistry.* 62 (21): 7512–7515.

Gottlieb, M.S., Schanker, M.D., Fan, P.T., Saxon, M.D. and Weisman, J.D. (1981). Centers for Disease Control (CDC). *Mobility and Mortality Weekly Reports*. 30: 250–252.

Griffiths, J. (2008). Brief history of mass spectrometry. *Analytical Chemistry*. 80(15): 5678–5683.

Grob, P.M., Wu, J.C., Cohen,K.A., Ingraham, R.H., Shih, C.K., Hargrave, K.D., McTague, T.L. and Merluzzi, V.J. (1992). Nonnucleoside inhibitors of HIV-1 reverse transcriptase: nevirapine as a prototype drug. *AIDS Research and Human Retroviruses*. 8(2):145-52.

Gunthard, H.F., Aberg, J.A., Eron, J.J., Hoy, J.F., Telenti, A., Benson, C.A., Burger, D.M., Cahn,P., Gallant, J.E., Glesby,M.J., Reiss, P., Saag,M.S.,Thomas,D.L., Jacobsen, D.M., Volberding, P.A. and International Antiviral Society-USA Panel. (2014). Antiretroviral treatment of adult HIV infection: 2014 recommendations of the international antiviral society-USA panel. *JAMA*. 312(4): 410-25.

Gupta, S.K. (2011). Intention-to-treat concept: A review. Perspective in clinical research. 2(3): 109–112.

Hawtrey A., Piesterse, A. and Van Zyl, Van der Bijl, P., Van der Merwe, M., Nel, W. and Ariatti, M. (2008). Studies on the inhibition of moloney murine leukemia virus reverse transcriptase by N-trityl amino acids and N-trityl amino acid nucleotide compounds. *Nucleoside nucleotides and Nucleic acids*. 27(9): 1011-1023.

Hermsen, E.D., Fletcher, C.V., Para, M. and Swindells, S. (2010). Nonnucleoside Analogues (Delavirdine, Efavirenz, Etravirine, Nevirapine). *Antimicrobe.*

Hogg, R.S. Yip. B., Kully. C., O'Shaughnessy,M.V., Schechter, M.T. and Montaner, J.S. (1999). Improved survival among HIV-infected patients after initiation of triple-drug antiretroviral regimens. *CMAJ.*160(5): 659–665.

Honarparvar, B., Govender, T., Maguire, G.E.M., Soliman, M.E.S. and Kruger, H.G. (2010). Integrated approach to structure- based enzymatic drug design: Molecular modeling, spectroscopy, and experimental bioactivity. *Chemical Reviews*. 114 (1): 493–537.

Hsiou, Y., Ding, J., Das, K., Clark, J.A.D., Boyer, P.L., Lewi, P., Janessen, P.A., Kleim, J.P., Rösner, M., Hughes, S.H. and Arnold, E. (2001). The Lys103Asn mutation of HIV-1 RT: a novel mechanism of drug resistance. *Journal of Molecular Biology*. 309(2): 437-445.

Hu, W.S. and Hughes, S.H. (2012). HIV-1 reverse transcription. *Cold Spring Harbor Perspectives in Medicine.* 2(10).

Isogai, H. and Hirayama, N. (2016). *In silico* analysis of interactions between nevirapine-related compounds, HLA-B*14:02 and T-cell receptor. *Chem-Bio Informatics.* 16:9-12.

Iyidogan, P. and Anderson, K.S. (2014). Current Perspectives on HIV-1 antiretroviral Drug resistance. *Viruses.* 6(10): 4095-4139.

Iyidogan, P., Sullivan, T.J., Chordia, M.D., Fred, K.M. and Anderson, K.S. (2013). Design, synthesis and antiretroviral evaluation of chimeric inhibitors of HIV reverse transcriptase. *ACS Medicinal Chemistry Letters.* 4(12): 1183–1188.

Izumiya, N. and Muraoka, M. (1969). Racemization test in peptide synthesis. *Journal of the Americal Chemical Society.* 91(9): 2391–2392.

Killian, M.S. and Levy, J.A. (2011). HIV/AIDS: 30 Years of progress and future challenges. *European journal of Immunology*. 41(12): 3401–3411.

Klickstein, L.B., Neve, R.L. and Gyuris, J. (2001). Conversion of mRNA into double-stranded cDNA. *Current Protocols in Molecular Biology*. Chapter 5: Unit5.5.

Kline, M.W., Fletcher, C.V., Federici, M.E., Harris, A.T., Evans, K.D., Rutkiewics, V.L., Shearer, W.T. and Dunkle, L.M. (1996). Combination therapy with stavudine and didanosine in children with advanced human immunodeficiency virus infection: pharmacokinetic properties, safety, and immunologic and virologic effects. *Pediatrics.* 97(6 Pt 1): 886-890.

Kohlstaedt, L.A., Wang, J., Friedman, J.M., Rice, P.A. and Steitz, T.A. (1992). Crystal structure at 3.5 Å resolution of HIV-1 reverse transcriptase complexed with an inhibitor. *Science.* 256(5065):1783-1990.

Kroeger smith, M.B., Rouzer, C.A., Taneyhill, L.A., Smith, N.A., Hughes, S.H., Boyer, P.L., A.J Janssen, P., Moereels, H., Koymans, L., Arnold, E., Ding, J., Das, K., Zhang, W., J. Michejda, C. and Smith, R.H Jr. (1995). Molecular modelling studies of HIV-1 reverse transcriptase non-nucleoside inhibitors: Total energy of complexation as a predictor of drug placement and activity. *Protein Science*. 4(10): 2203-2222.

Kryst, J., Kawalec, P. and Pilc, A. (2015). Efavirenz-based regimens in antiretroviral-naive HIV-infected patients: A systematic review and meta-analysis of randomized controlled trials. *Plos one.* 10(5): e0124279.

Lai, M-T., Munshi, V., Touch, S., Tynebor, R.M., Tucker, T.J., McKenna, P.M., Williams, T.M., DiStefano, D.J., Hazuda, D. J. and Miller, M.D. (2009). Antiviral activity of MK-4965, a novel nonnucleoside reverse transcriptase inhibitor. *Antimicrobial Agents and Chemotherapy*. 53(6): 2424-2431.

Lai, M-T., Feng, M., Falgueyret, J.P., Tawa, P., Witmer, M., DiStefano, D., Li, Y., Burch, J., Sachs, N., Lu, M., Cauchon, E., Campeau, L.C., Grobler, J., Yan, Y., Ducharme, Y., Côte, B., Asante-Appiah, E., Hazuda, D.J. and Miller, M.D. (2014). *In vitro* characterization of MK-1439, a novel HIV-1 nonnucleoside reverse transcriptase inhibitor. *Antimicrobial. Agents and Chemotherapy*. 58(3): 1652-1663.

Lattová, E., Snovida, S., Perreault, H. and Krokhin O. (2005). Influence of the labelling group on ionization and fragmentation of carbohydrates in mass spectrometry. *Journal of The American Society of Mass Spectrometry.* 16(5): 683-696.
.

Lingham, R.B., Hsu, A.H., O'Brien, J.A., Sigmund, J.M., Sanchez, M., Gagliardi, M.M., Heimbuch, B.K., Genilloud, O., Martin, I., Diez, M.T., Hirsch, C.F., Zink, D.L., Liesch, J.M., Koch, G.E., Gartner, S.E., Garrity, G.M., Tsou, N.N. and Salituro, G.M. (1996). Quinoxapeptins: novel chromodepsipeptide inhibitors of HIV-1 and HIV-2 reverse transcriptase. The producing organism and biological activity. *Journal of Antibiotics*. 49(3): 253-9.

Lobritz, M.A., Ratcliff, A.N. and Arts, E.J. (2010). Review HIV-1 entry, inhibitors, and resistance. *Viruses*.2(5): 1069-1105.

Lu, X., Liu, L., Zhang, X., Lau, T.C.K., Tsui, S.K.W., Kang, Y., Zheng, P., Zheng, P., Zheng, B., Liu, G. and Chen, Z. (2011). F18, a novel small-molecule nonnucleoside reverse transcriptase inhibitor, inhibits HIV-1 replication using distinct binding motifs as demonstrated by resistance selection and docking analysis. *Antimicrobial Agents and Chemotherapy.* 56 (1): 341-351.

Lyama, T. and Wilson, D.M.3rd. (2013). DNA repair mechanisms in dividing and non-dividing cells. *DNA Repair*. 12(8): 620-636.
.

Mansfield, E.S., Worley, J.M., Mckenzie, S.E., Rappaport, E. and Fortina, P. (1995). Nucleic acid detection using non-radioactive labelling methods. *Molecular and Cellular Probes*. 9(3): 145-56.

Mehellou, Y. and De Clereq, E.D. (2010). Twenty six years of antiviral drug discovery: Where do we stand and where do we go? *Journal of Medicinal Chemistry*. 53(2): 521–538.

Miceli, L.A., Teixeira, V.L., Castro, H.C., Rodridges, C.R., Mello, J.F.R., Albuquerque, M.G., Cabral, L.M., De Brito, M.A. and De Souza, A.M.T. (2013). Molecular docking studies of marine diterpenes as inhibitors of wild-type and mutants HIV-1 reverse transcriptase. *Marine Drugs*. 11(11): 4127-4143.

Michailidis, E., Marchand, B., Kodama, E.N., Singh, K., Kirby, K.A., Ryan, E.M., Sawani, A.M., Nagy, E., Ashida, N., Mitsuya, H., Parnjak, M.A. and Sarafianos, S.G. (2009). Mechanism of inhibition of HIV-1 reverse transcriptase by 4'-Ethynyl-2-fluoro-2'-deoxyadenosine triphosphate, a translocation-defective reverse transcriptase inhibitor. *Journal of Biological Chemistry*. 284(51): 35681-35691.

Montaner, J.S., Reiss, P., Cooper, D., Vella, S., Harris, M., Conway, B., Wainberg, M.A., Smith, D., Robinson, P., Hall, D., Myers, M. and Lange, J.M. (1998). A randomized, double-blind trial comparing combinations of nevirapine, didanosine, and zidovudine for HIV-infected patients: the INCAS trial. Italy, The Netherlands, Canada and Australia Study. JAMA. 279(12): 930-7.

Muhanji, C.L. and Hunter, R. (2007). Current developments in the synthesis and biological activity of HIV-1 double- drug inhibitors. *Current Medicinal Chemistry*. 14: 1207-1220.

Muneyama, K.M., Bauer, R.J., Shuman, D.A., Robins, R.K. and Simon, L.N. (1971). Chemical synthesis and biological activity of 8-substituted adenosine 3',5'-cyclic-monophsophate derivatives. *Biochemistry*. 10(12): 2390–2395.

Nizami, B., Sydow, D., Wolberb, G. and Honarparvar, B. (2016). Molecular insight on the binding of NNRTI to K103N mutated HIV-1 RT: molecular dynamics simulations and dynamic pharmacophore analysis. *Molecular Biosystems*. 12(11): 3385-3395.

Nizami, B., Tetko, I.V., Koobanally, N.A. and Honarparvar, B. (2015). QSAR models and scaffold-based analysis of non-nucleoside HIV RT inhibitors. *Chemometrics and Intelligent Laboratory Systems*. 148: 134–144.

O'Brien, W.A. (2016). Resistance against reverse transcriptase inhibitors. *Clinical Infectious Diseases*. 30(Suppl 2): S185–92.

Padariya, M., Kalathiyaa, U. and Baginskia, M. (2016). Molecular basis and potential activity of HIV-1 reverse transcriptase towards triethylamine based compounds. *Biotechnology and Applied Biochemistry*. 64(6): 810–826.

Pata, J.D., Stirtan, W.G., Goldstein, S.W.M. and Steitz, T.A. (2004). Structure of HIV-1 reverse transcriptase bound to an inhibitor active against mutant reverse transcriptase resistant to other nonnucleoside inhibitors. *Proceedings of the National Academy of Sciences of USA*. 101(29): 10548–10553.

Pellecchia, M., Bertini, I., Cowburn, D., Dalvit, C., Giralt, E., Jahnke, W., James, T.L., Homans, S.W., Kessler, H., Lachinat, C., Meyer, B., Oschikinat, H., Peng, F., Schwalbe, H. and Siegal, G. (2008). Perspectives on NMR in drug discovery: a technique comes of age. *Nature Reviews Drug Discovery*. 7(9): 738–745.

Perilla, J.R., Hadden, J.A., Goh, B.C., Mayne, C.G. and Schulten, K. (2016). All-atom Molecular dynamics of virus capsids as drug targets. *The Journal of Physical Chemical Letters.* 7(10): 1836–1844.

Pozniak, A. (2000). Why switch from protease inhibitors (PI) to non-nucleoside reverse transcriptase inhibitors (NNRTI)? *British HIV Association.* (s1): 7–10.

Pyka, A. (2014). Detection progress of selected drugs in TLC. *BioMedical Research International.* 19; 2014, Article ID 732078, 19 pages.

.

Raju, R.K., Burton, N.A. and Hillier, I.H. (2010). Modelling the binding of HIV-reverse transcriptase and nevirapine: an assessment of quantum mechanical and force field approaches and predictions of the effect of mutations on binding. *Physical Chemistry Chemical Physics*. 12(26): 7117-7125

Ramírez, D. (2016). Computational Methods Applied to Rational Drug Design. *The Open Medicinal Chemistry Journal*. 10: 7–20.

Regina, G.L., Coluccia, C. and Silvestri, R. (2010). Looking for an active conformation of the future HIV type-1 non-nucleoside reverse transcriptase inhibitors. *Antiviral Chemistry & Chemotherapy.* 20:213–237.

Ridder, S.A., Haubrich, R., Gregory DiRienzo, A., Peeples, L., Powderly, W.G., Klingman, K.L., Garren, K.W., George, T., Murphy, R.L., Swindells, S., Havlir, D. and Mellors, J.W. (2008). Class-sparing regimens for initial treatment of HIV-1 infection. *The New England Journal of Medicine.* 358(20): 2095-2106.

Santos, L.H., Ferreira, R.S. and Caffarena, E.R. (2015). Computational drug design strategies applied to the modeling of human immunodeficiency virus-1 reverse transcriptase inhibitors. *Memorias do Instituto Oswaldo Cruz, Rio de Janeiro*. 110(7): 847-864.

Sarafianos, S.G., Marchand, B., Das, K., Himmel, D., Parniak, M.A., Hughes, S.H. and Arnold, E. (2010). Structure and function of HIV-1 reverse transcriptase: molecular mechanisms of polymerization and inhibition. *Journal of Molecular Biology*. 385(3): 693–713.

Seckler, J.M., Barkley, M.D. and Wintrode, P.L. (2011). Allosteric suppression of HIV-1 reverse transcriptase structural dynamic upon inhibitor binding. *Biophysical Journal*. 100(1): 144-153.

Seniya, S., Yadav, A., Khan, G.J. and Sah, N.K. (2015). *In-silico* studies show potent inhibition of HIV-1 reverse transcriptase activity by a herbal drug. *IEEE/ACM transactions of computational biology and bioinformatics*. 12(6): 1355-1364.

Shackleton, C.H., Mattox, V.R. and Honour, J.W. (2013). Analysis of intact steroid conjugates by secondary ion mass spectrometry (including FABMS) and by gas chromatography. In James, V.H.T. and Paraqualine J.R.(edition). *Proceedings of the Sixth International Congress On Hormonal Steroids*. Elsevier. 209-218.

Shan, L. and Siliciano, R.F. (2013). From reactivation of latent HIV-1 to elimination of the latent reservoir: The presence of multiple barriers to viral eradication. *Prospects and Overviews*. 35(6): 544–552.

Sharma, K.K., Przybilla, F., Restle, T., Godet, J. and Mély, Y. (2016). FRET- based assay to screen inhibitors of HIV-1 reverse transcriptase and nucleocapsid protein. *Nucleic Acids Research*. 44(8) e74.

Sharma, K.K., Przybilla, F., Restle, T., Godet, J. and Mély, Y. (2015). Reverse transcriptase in action: FRET-based assay for monitoring flipping and polymerase activity in real time. *Analytical Chemistry*. 87(15): 7690-7697.

Shuker, S.B., Hajduk, P.J., Meadows, R.P. and Fesik, S.W. (1996). Discovering high-affinity ligands for proteins: SAR by NMR. *Science*. 274(5292): 1531-4.

Sluis-Crèmer, N., Alpay Temiz, N. and Bahar, I. (2004). Conformational changes in HIV-1 reverse transcriptase induced by nonnucleoside reverse transcriptase inhibitor binding. *Current HIV Research*. 2(4): 323–332.

Sluis-Crèmer, N. and Tachedjian, G. Mechanisms of inhibition of HIV replication by nonnucleoside reverse transcriptase inhibitors. (2008). *Virus research*. 134(1-2): 147–156.

Smerdon, S.J., Jäger, J., Wang, J., Kohlstaedt, L.A., Chirino, A.J., Friedman, J.M., Rice, P.A. and Steitz, T.A. (1994). Structure of the binding site for nonnucleoside inhibitors of the reverse

transcriptase of human immunodeficiency virus type 1. *Proceedings of the National Academy of Science of USA*. 91(9):3911-5.

Smolira, A. and Szponder, J.W. (2015). Importance of the matrix and the matrix/sample ratio in MALDI-TOF-MS analysis of cathelicidins obtained from porcine neutrophils. *Applied Biochemistry and Biotechnology*. 175: 2050–2065.

Sundquist, W.I. and Kräusslich, H.G. (2012). HIV-1 assembly, budding, and maturation. *Cold Spring Harbor Perspectives in Medicine*. 2(7): a006924.

Swanstrom, R., Varmus, H.E. and Bishop, J.M. (1982). The terminal redundancy of the retrovirus genome facilitates chain elongation by reverse transcriptase. *Journal of Biological Chemistry*. 256(3): 1115-1121.

Tewtrakul, S., Nakamura, N., Hattori, M., Fujiwara, T. and Supavita, T. (2002). Flavanone and flavonol glycosi Swanstrom, R., Varmus, H.E. and Bishop, J.M. The terminal redundancy of the retrovirus genome facilitates chain elongation by reverse transcriptase. *Journal of Biological Chemistry*. 50(5): 630-650.

Thammaporn, R., Yagi-Utsumi,M., Yamaguchi, T., Boonsri, P., Saparpakorn,P., Choowongkomon, K., Techasakul, S., Kato, K. and Hannongbua, S. (2015). NMR characterization of HIV-1 reverse transcriptase binding to various non-nucleoside reverse transcriptase inhibitors with different activities. *Scientific Reports*. 5: 15806.

Trott, O. and Olson, A.J. (2010). AutoDock Vina: improving the speed and accuracy of docking with a new scoring function, efficient optimization and multithreading. *Journal of Computational Chemistry*. 31(2): 455–461.

UNIAIDS.www.unaids.org/sites/default/.../JC2702_GARPR2013guidelines_en.pdf, (Accessed on 03 Jun 2016).

UNIAIDS.www.unaids.org/sites/default/files/media_asset/global-AIDS-update-2016_en.pdf, (Accessed on 09 May 2017).

 Usach, I., Melis, V. and Peris, J.E. (2013). Non-nucleoside reverse transcriptase inhibitors: a review on pharmacokinetics, pharmacodynamics, safety and tolerability. *Journal of International AIDS Society*.16:1-14.

Van Rompay, K.A., Babusis, S., Abbott, Z, Geng, Y., Jayashankar, K., Johnson, J.A., Lipscomb, J., Heneiene, W., Abel, K. and Ray, A.S. (2012). Compared to subcutaneous tenofovir, oral tenofovir disoproxyl fumarate administration preferentially concentrates the drug into gut- associated lymphoid cells in simian immunodeficiency virus-infected macaques. *Antimicrobial Agents and Chemotherapy* 56(9): 4980–4984.

Van Zyl, J.M., Ariatti, M. and Hawtrey, A.O. (2010). The effect of certain *N*-tritylated phenylalanine conjugates of amino-adenosine-3',5'-cyclic monophosphate on moloney murine leukaemia virus reverse transcriptase activity. *South African Journal of Science.* 106(7-8) :1-5.

Volberding, P.A., Sande, M.A., M.A Lange, J., Greene, W.C., Gallant, J.E. (2008). Global HIV/AIDS medicine. Volberding, P.A (editor). *Science Direct.* 978-1-4160-2882-6. 1st Edition, pg. 140, (2008).

Wainberg, M.A. (2012). The need for development of new HIV-1 reverse transcriptase and integrase Inhibitors in the aftermath of antiviral drug resistance. *Scientifica.* Article ID 238278, 28 pages.

Wallace, A.C., Laskowski, R.A., Thornton, J.M. (1995). LIGPLOT: a program to generate schematic diagrams of protein-ligand interactions. Protein engineering. 8(2): 127-134.

Wang, H., Lu, X., Yang, X. and Xu, N. (2016). The efficacy and safety of tenofovir alafenamide versus tenofovir disoproxil fumarate in antiretroviral regimens for HIV-1 therapy: meta analysis. *Medicine.* 95(41): e5146.

Wang, J., Zhan, P., Li, Z., De Clercq, E., Pannecouque, C. and Liu, X. (2014). Discovery of nitropyridine derivatives as potent HIV-1 non-nucleoside reverse transcriptase inhibitors via a structure-based core refining approach. *European journal of medicinal chemistry*. 9;76:531-8.

Wang, R.R., Yang, Q.H., Luo, R.H., Peng, Y.M., Dai, S.X., Zhang, X.J., Chen, H., Cui, X.Q., Liu, Y.J., Huang, J.F., Chang, J.B. and Zheng, Y.T. (2014). Azvudine. A novel nucleoside reverse transcriptase inhibitor showed good drug combination features and better inhibition on drug-resistant strains than lamivudine *in vitro*. *Plos one*. 9(8): e105617.

Wang, Y., Xing, H., Liao, L., Wang, Z., Su, B., Zhao, Q., Feng, Y., Ma, P., Liu, J., Wu, J., Ruan, Y. and Shao, Y. (2014). The development of drug resistance mutations K103N Y181C and G190A in long term Nevirapine-containing antiviral therapy. *AIDS Research and Therapy.* 11(1): 36.

Weast, R.C. (1956). Handbook of chemistry and physics. *CRC Press (Boca Ratton).* 56th edition, p. E56.

Wildum, S., Paulsen, D., Thede, K., Ruebsamen-Schaeff, H. and Zimmermann, H. (2013). *In vitro* and *In vivo* activities of AIC292, a novel HIV-1 nonnucleoside reverse transcriptase inhibitor. *Antimicrobial Agents and Chemotherapy*. 57(11): 5320-5329.

Wilen, C.B., Tilton, J.C. and Doms, R.W. (2012). HIV: cell binding and entry. *Cold Spring Harbor Perspectives in Medicine*. 2(8): a006866.

World Health Organization. HIV/AIDS, Fact Sheet n. 360, Updated November 2015. Available online: http://www.who.int/mediacentre/factsheets/fs360/en/, (accessed on 7 Dec 2015).

World Health Organization. More developing countries show universal access to HIV/AIDS services possible. http://www.who.int/mediacentre/news/releases/2010/hiv_universal_access_20100928/en/(accessed on 1 Nov 2016).

Xia, Q., Radzio, J., Anderson, K.S. and Sluis-Cremer, N. (2007). Probing nonnucleoside inhibitor-induced active-site distortion in HIV-1 reverse transcriptase by transient kinetic analyses. *Protein Science.* 16(8): 1728–1737.

Yang, G., Wang, J., Cheng, Y., Dutschman, G.E., Tanaka, H., Baba, M. and Cheng, Y.C. (2008). Mechanism of inhibition of human immunodeficiency virus type 1 reverse transcriptase by a stavudine analogue, 4-ethynyl stavudine triphosphate. *Antimicrobial Agents and Chemotherapy.* 52(6): 2035–2042.

Yasukawa, K., Konishi, A. and Inouye, K. (2010). Effects of organic solvents on the reverse transcriptase reaction by reverse transcriptase from avian myeloblastosis virus and moloney murine leukemia virus. *Bioscience. Biotechnology and Biochemistry*. 74(9): 1925-1930.

Yokoyama, M., Mori, H. and Sato, H. (2010). Allosteric regulation of HIV-1 reverse transcriptase by ATP for nucleotide selection. *Plos one*. 5(1): e8867.

Zervas, L. and Theodoropoulos, D.M. (1956). Tritylamino acids and peptides. A new method of peptide synthesis. *Journal of the American Chemical Society.* 78(7): 1359–1363.

Zhang, X.M.1., Zhang, Q., Wu, H1., Lau, T.C., Liu, X., Chu, H., Zhang, K., Zhou, J., Chen Z.W., Jin, D.Y. and Zheng, B.J. (2016). Novel mutations L228I and Y232H cause nonnucleoside reverse transcriptase inhibitor resistance in combinational pattern. *AIDS Research and Human Retroviruses.* 32(9): 909-17.

Internet references

https://www.aidsmap.com/New-NNRTI-doravirine-suppresses-HIV-as-well-as-efavirenz-but-with-fewer-central-nervous-system-side-effects/page/2987389/ (accessed on 17/11/2017). Gatell, J. (2015). New NNRTI doravirine suppresses HIV as well as efavirenz but with fewer central nervous system side-effects.

http://www.hivandhepatitis.com/hiv-treatment/approved-hiv-drugs/4985-hiv-drug-therapy-lower-dose-efavirenz-may-be-equally-effective-with-fewer-side-effects (accessed on 12/11/2017). Highleyman, L. (2014). HIV Drug Therapy: Lower-dose Efavirenz Equally Effective with Fewer Side Effects.

https://www.google.co.za/search?q=Diagram+of+Human+Immunodeficiency+virus(HIV)+adapted+from+U.S.+National+Institute+of+Health+(U.S.+Department+of+Health+and+Human+Services).&safe=active&source=lnms&tbm=isch&sa=X&ved=0ahUKEwj6ucjv44rUAhXKAcAKHeHECNYQ_AUIBygC&biw=1600&bih=778&dpr=1.2#imgrc=L0AB9qqYklIXfM:&spf=1495706391291

http://webbook.nist.gov/chemistry/(acessed 06/12/2017).

https://www.unicef.org/publications/files/, (Accessed on 20/06/2016). UNICEF_Annual_Report_2013_web_26_June_2014.pdf.

APPENDIX A

CALCULATIONS

---

1. % YIELD of N-trityl-phenylalanyl conjugates (4a-e)

% Yield   **= [Weight of product (mg) / 0.01 mmole product (mg)] × 100**

(4a):

Molecular weight of product	= 878.33 g/mol
Weight of final product	= 3.18 mg
% yield	= 3.18 mg /8.7833 g/L ×100
	= 36.18 %

(4b):

Mw of product	= 886.41 g/mol
Weight of final product	= 4.61 mg
% yield	= 4.61mg/8.8641 g/L × 100
	= 52.00 %

(4c):

Mw of product	= 913.30 g/mol
Weight of final product	= 4.35 mg
% yield	= 4.35 mg /9.1330 g/L× 100
	= 48 %

(4d):

Mw of product	= 956.24 g/mol

Weight of final product   = 4.63 mg

% yield   = 4.63 mg/ 9.5624 g/L $\times$ 100

                                           = 48.41 %

(4e):

Mw of product   = 959.38 g/mol

Weight of final product   = 5.24 mg

% yield   = 5.24 mg/9.5938 g/L $\times$ 100

                                          = 54.62%

2. UV analysis (concentration and ε_{max})

(4a):

Concentration: 20 µl taken from a deutero methanolic solution containing :

3.18 mg / 600 µl CD_3OD

Therefore, $3.18 \times 20 / 600$ = 106 µg / 20 µl CD_3OD

 But 106 µg (20 µl) is added to 3ml EtOH

Therefore, concentration is 106 / 878.33 µmoles in 3ml

                                          = 0.121 µmoles in 3ml

Therefore in 1 litre 0.121 / 3 $\times$ 1000 µmoles

                                          $= 4.03 \times 10^{-5}$ M

$OD_{max} = \varepsilon_{max} \times c \times l$

Therefore, $\varepsilon_{max} = OD_{max}/c \times 1$

                    $= 8.21 \times 10^{-1} / 4.03 \times 10^{-5}$ M

$$= 2.03 \times 10^4 \, \text{L M}^{-1} \, \text{cm}^{-1}$$

Log ε_{max} = 4.30

(4b):

Concentration: 20 µl taken from a deutero methanolic solution containing :

4.61 mg / 600 µl CD$_3$OD

Therefore, $4.61 \times 20/\, 600$ = 154 µg / 20 µl CD$_3$OD

But 154 µg (20 µl) is added to 3ml EtOH

Therefore, concentration is 154/ 886.41 µmoles in 3ml

$$= 0.173 \text{ µmoles in 3ml}$$

Therefore, in 1 litre $0.173\, /\, 3 \times 1000$ µmoles

$$= 5.76 \times 10^{-5} \, \text{M}$$

OD$_{max}$ = $\varepsilon_{max} \times c \times l$ $= 8.2 \times 10^{-1} /\, 5.76 \times 10^{-5} \, \text{M}$

$$= 1.42 \times 10^4 \, \text{L M}^{-1} \, \text{cm}^{-1}$$

Log ε_{max} = 4.1

(4c):

Concentration: 20 µl taken from a deutero methanolic solution containing:

4.35 mg / 600 µl CD$_3$OD

Therefore, $4.35 \times 20\, /\, 600$ = 145 µg / 20 µl CD$_3$OD

But 145 µg (20 µl) is added to 3ml EtOH

Therefore, concentration is 145/ 913.30 µmoles in 3ml

$$= 0.160 \text{ µmoles in 3ml}$$

Therefore, in 1 litre $0.160/\, 3 \times 1000$ µmoles

$$= 5.33 \times 10^{-5} \, \text{M}$$

$OD_{max} = \varepsilon_{max} \times c \times l$ $\qquad = 6.37 \times 10^{-1} / 5.33 \times 10^{-5}$ M

$\qquad\qquad\qquad\qquad\qquad\qquad = 1.19 \times 10^4$ L M^{-1} cm^{-1}

Log ε_{max} $\qquad\qquad\qquad = 4.07$

(4d):

Product weight 4.63

Concentration: 20 µl taken from a deutero methanolic solution containing:

4.63 mg / 600 µl CD_3OD

Therefore, $4.63 \times 20 / 600$ $\qquad = 154$ µg / 20 µl CD_3OD

But 154 µg (20 µl) is added to 3ml EtOH

Therefore, concentration is 154/ 956.24 µmoles in 3ml

$\qquad\qquad\qquad\qquad\qquad = 0.161$ µmoles in 3ml

Therefore in 1 litre $0.161 / 3 \times 1000$ µmoles

$\qquad\qquad\qquad\qquad\qquad = 5.36 \times 10^{-5}$ M

$OD_{max} = \varepsilon_{max} \times c \times l$ $\qquad = 9.27 \times 10^{-1} / 5.36 \times 10^{-5}$ M

$\qquad\qquad\qquad\qquad\qquad\qquad = 1.72 \times 10^4$ L M^{-1} cm^{-1}

Log ε_{max} $\qquad\qquad\qquad = 4.2$

(4e):

Concentration: 20 µl taken from a deutero methanolic solution containing:

5.24 mg / 600 µl CD_3OD

Therefore, $5.24 \times 20 / 600$ $\qquad = 175$ µg / 20 µl CD_3OD

But 175 µg (20 µl) is added to 3ml EtOH

Therefore, concentration is 175/ 959.38 μmoles in 3ml

$$= 0.182 \text{ μmoles in 3ml}$$

Therefore in 1 litre 0.182 / 3 × 1000 μmoles

$$= 6.06 \times 10^{-5} \text{ M}$$

$OD_{max} = \varepsilon_{max} \times c \times l$ $= 9.85 \times 10^{-1}/ 6.06 \times 10^{-5} \text{ M}$

                                         $= 1.63 \times 10^{4} \text{ L M}^{-1} \text{ cm}^{-1}$

Log ε_{max} $= 4.2$

8AMP. cAMP:

Concentration: 200 μl of stock (1.76 mg in 1 ml H_2O) contains 0.352 mg of nucleotide. This is diluted in H_2O to 10 ml.

Therefore, 0.352 mg in 10 ml (H_2O) $= 35.2 \text{ mg/L}$

                                         $= 35.2 / 443.39 \text{ mmol L}^{-1}$

                                         $= 0.079 \text{ mmol L}^{-1}$

                                         $= 0.79 \times 10^{-4} \text{ mole L}^{-1}$

$\varepsilon_{max} = OD_{max} = \times c \times l$ $= 1.23 \times 10^{-1}/ 0.79 \times 10^{-5} \text{ M}$

                                         $= 1.6 \times 10^{4} \text{ L M}^{-1} \text{ cm}^{-1}$

Log ε_{max} $= 4.2$

3. **Reverse Transcriptase Assay**

(4a):

A 10^{-4} M solution of N-Trityl-phenylalanine (in final 60 μl), requires the addition of 6 μl of a 10^{-3} M stock solution in DMSO solution.

Therefore, 878.33 g/mol × 10^{-3} M   = 0.878g/L

= 878.95 mg/ L

= 878.95 µg/ml

= 878.95 µg/ 1000 µl

For 6 µl, we require   = 878.95 /1000 × 6 µl

= 5.26 µg

A stock solution of 87.833 µg / 100 µl in DMSO is made. But we have our stock in deuteromethanol (CD_3OD) of 3.18 mg/ 600 µl.

Therefore, 87.833 µg / 3180 µg × 600 µl

        = 16.57 µl of the deutero methanolic solution is evaporated and the residue is dissolved in 100 µl DMSO (Stock solution)

(4b):

A 10^{-4} M solution of N- Trityl-Fl-phenylalanine (in final 60 µl), requires the addition of 6 µl of a 10^{-3} M stock solution in DMSO.

Therefore, 886.41

886.90 g/mol × 10-3 M   = 0.88641 g/L

= 886.90 mg/ L

= 886.90 µg/ml

= 886.90 µg/ 1000 µl

For 6 µl, we require   = 886.41 /1000 × 6 µl

= 5.31 µg

A stock solution of 88.64 µg / 100 µl in DMSO is made. But we have our stock in deuteromethanol (CD$_3$OD) of 4.61 mg/ 600 µl.

Therefore, 88.69 µg / 4610 µg × 600 µl

> = 11.53 µl of the deutero methanolic solution is evaporated and the residue is dissolved in 100 µl DMSO (Stock solution)

(4c):

A 10^{-4} M solution of N- Trityl-F-phenylalanine (in final 60 µl), requires the addition of 6 µl of a 10^{-3} M stock solution in DMSO.

Therefore, 913.30 g/mol × 10^{-3} M   = 0.9133g/L

> = 913.3 mg/ L
>
> = 913.3 µg/ml
>
> = 913.3 µg/ 1000 µl

For 6 µl, we require   = 913.3 /1000 × 6 µl

> = 5.47 µg

A stock solution of 91.33 µg / 100 µl in DMSO is made. But we have our stock in deuteromethanol (CD$_3$OD) of 4.35 mg/ 600 µl.

Therefore, 91.33 µg / 4350 µg × 600 µl

> = 12.59 µl of the deutero methanolic solution is evaporated and the residue is dissolved in 100 µl DMSO (Stock solution)

(4d):

A 10^{-4} M solution of N- Trityl-Br-phenylalanine (in final 60 μl), requires the addition of 6 μl of a 10^{-3} M stock solution in DMSO.

Therefore, 956. 24 g/mol × 10^{-3} M   = 0.95624 g/L

                                    = 956.86 mg/ L

                                    = 956.86 μg/ml

                                    = 956.86 μg/ 1000 μl

For 6 μl, we require   = 956.24 /1000 × 6 μl

                                    = 5.73 μg

A stock solution of 95.624 μg / 100 μl in DMSO is made. But we have our stock in deuteromethanol (CD_3OD) of 4.63 mg/ 600 μl.

Therefore, 95.624 μg / 4630 μg × 600 μl

                            = 12.39 μl of the deutero methanolic solution is evaporated and the residue is dissolved in 100 μl DMSO (Stock solution)

(4e):

A 10^{-4} M solution of N-Trityl-I-phenylalanine (in final 60 μl), requires the addition of 6 μl of a 10^{-3} M stock solution in DMSO.

Therefore, 959.38 g/mol × 10^{-3} M   = 0.95938 g/L

                                    = 958.7 mg/ L

                                    = 958.7 μg/ml

                                    = 958.7 μg/ 1000 μl

For 6 µl, we require $\qquad$ =959.38 /1000 × 6 µl

$\qquad\qquad\qquad\qquad\qquad$ = 5.75 µg

A stock solution of 95.38 µg / 100 µl in DMSO is made. But we have our stock in deuteromethanol (CD_3OH) of product 5.24 mg/ 600 µl.

Therefore, 95.38 µg / 5240 µg × 600 µl

$\qquad\qquad\qquad\qquad$ = 10.92 µl of the deutero methanolic solution is evaporated and the residue is dissolved in 100 µl DMSO (Stock solution)

APPENDIX B

UV SPECTRUM OF TRITANOL
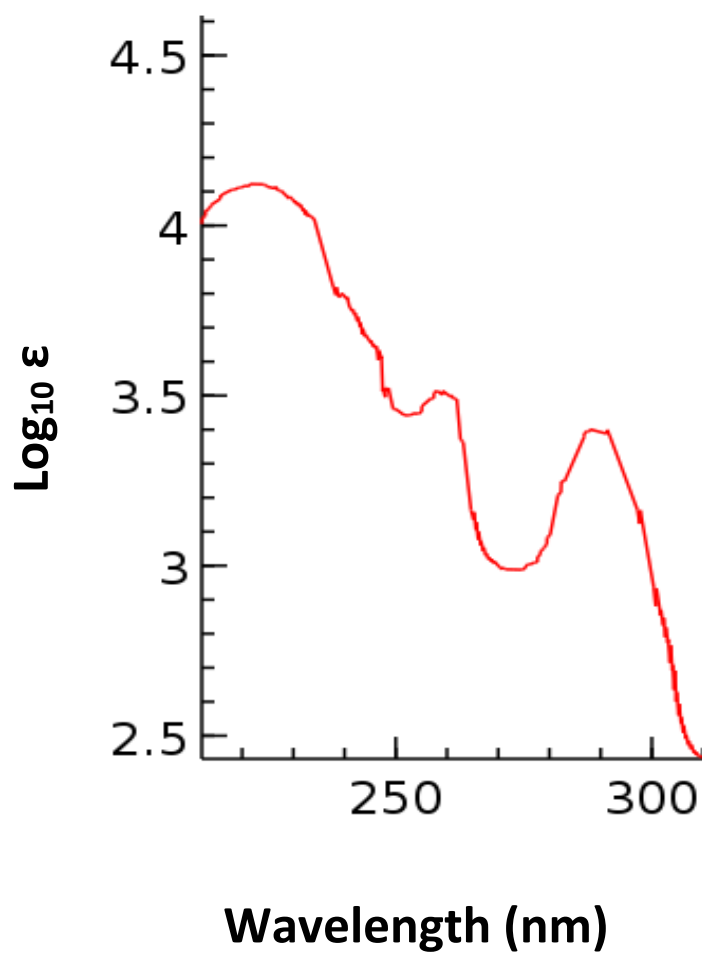
Figure 4.1 UV spectrum of tritanol showing the $\log_{10}\varepsilon$ at specific wavelengths (http://webbook.nist.gov/cgi/cbook.cgi?ID=C76846&Mask=400. Accessed 06/12/2017).

APPENDIX C

PROTON NMR SPECTRA OF N-TRITYL-PHENYLALANYL CONJUGATES (4a-e) AND 8-AHA-cAMP
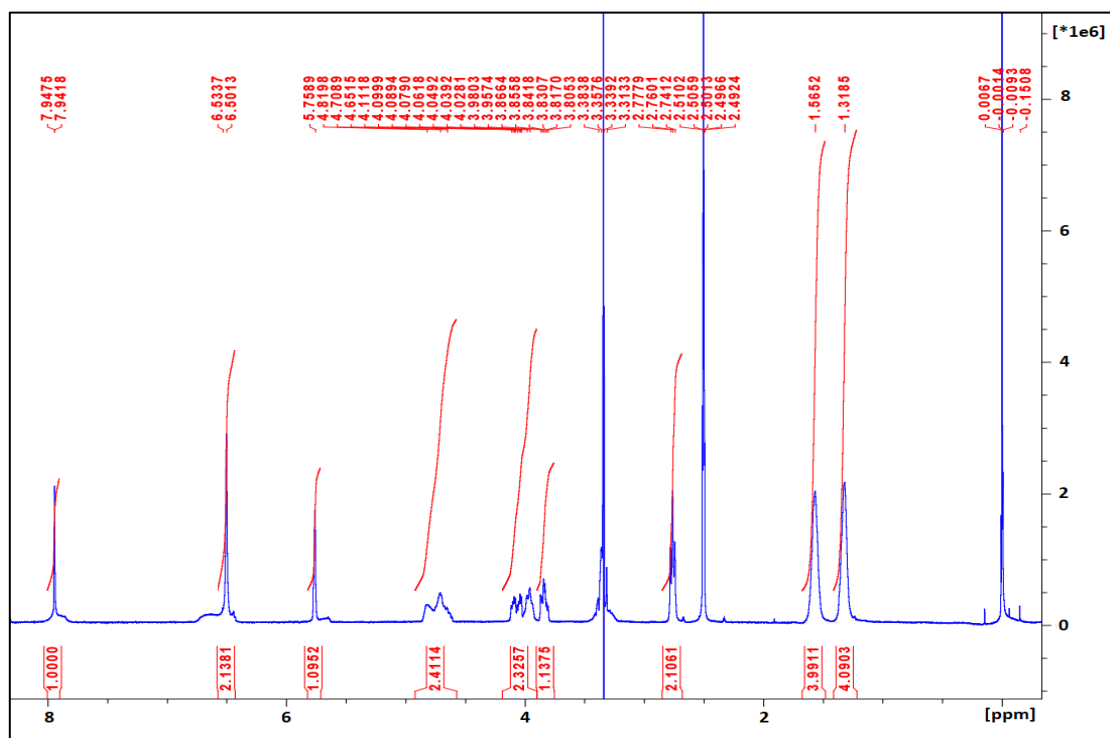
A
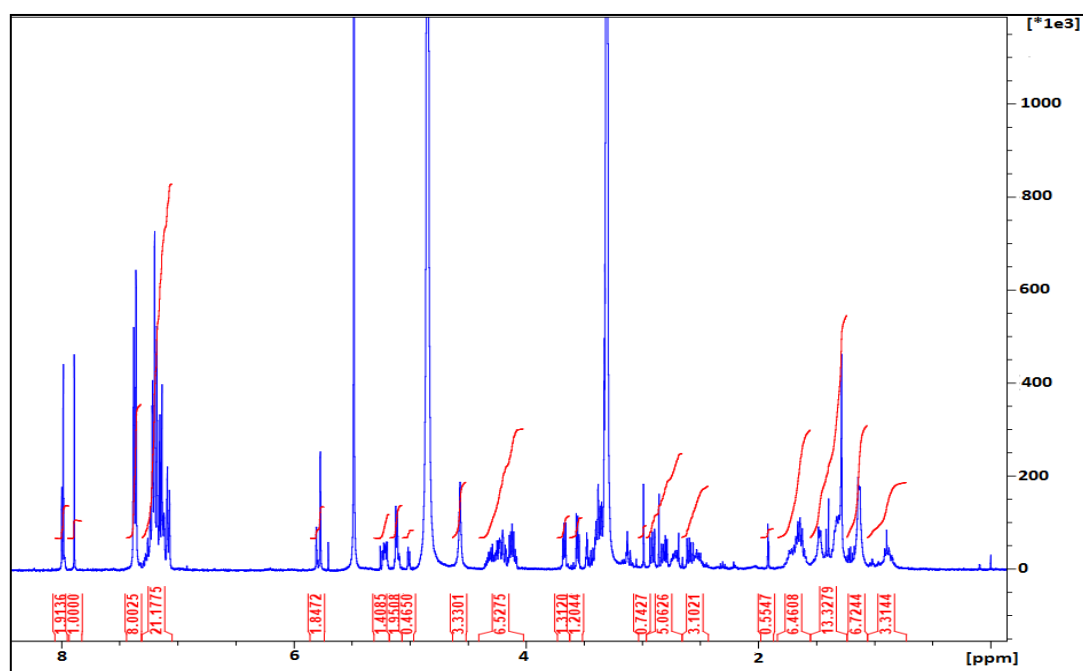
B
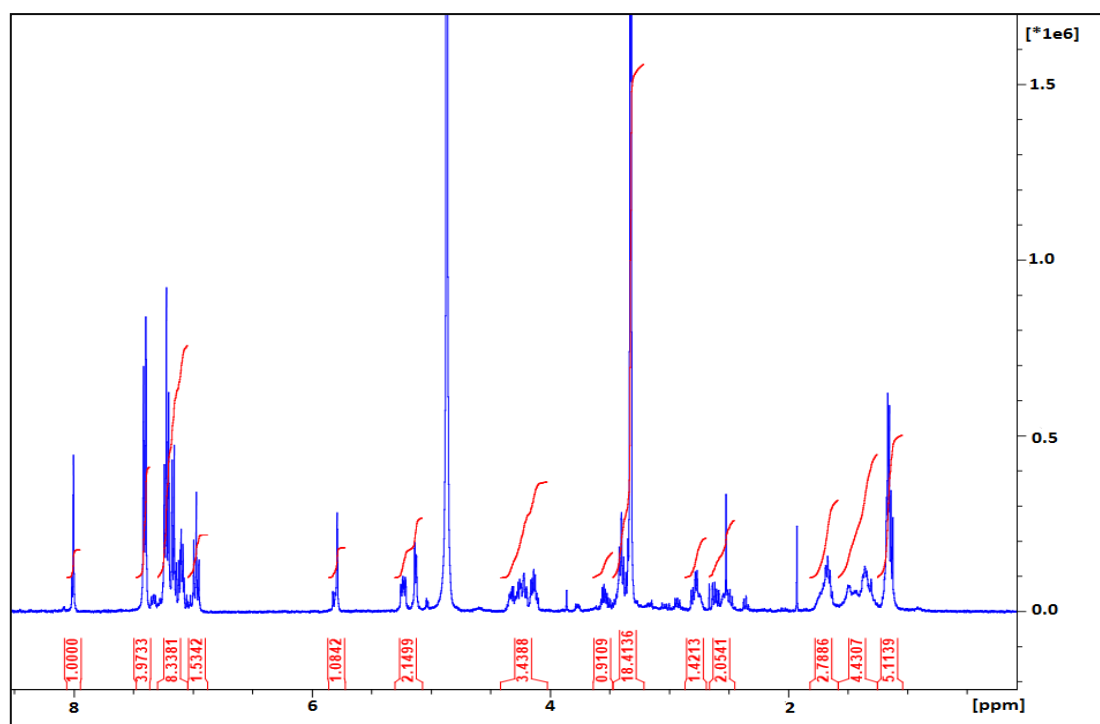
C
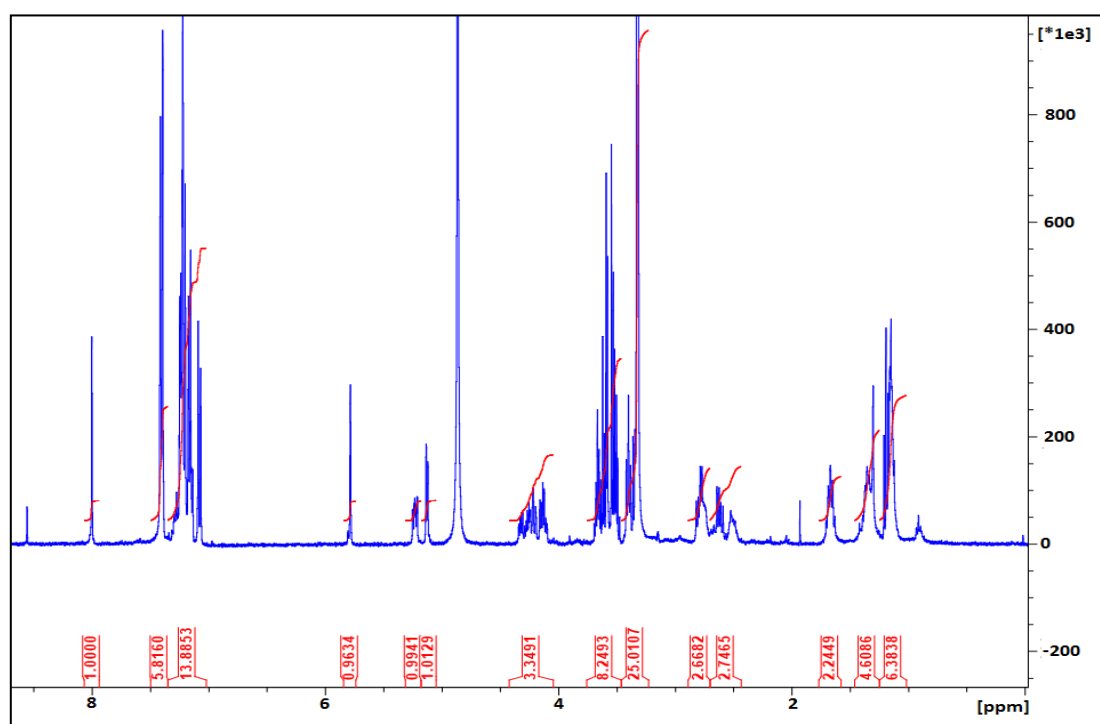
D
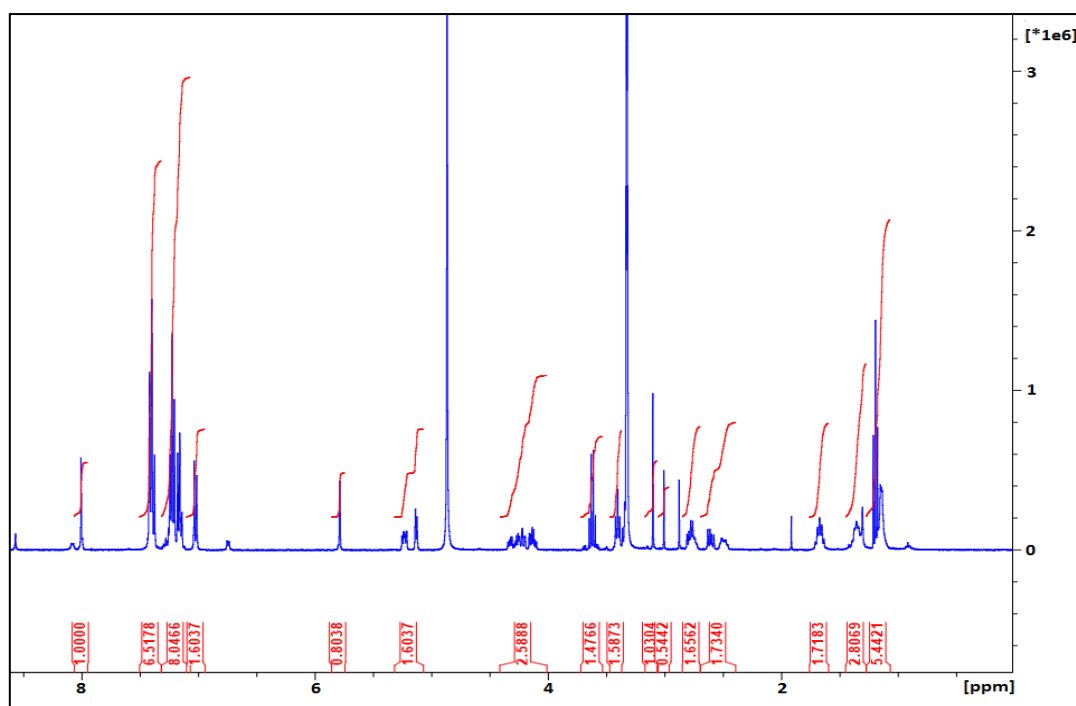
E
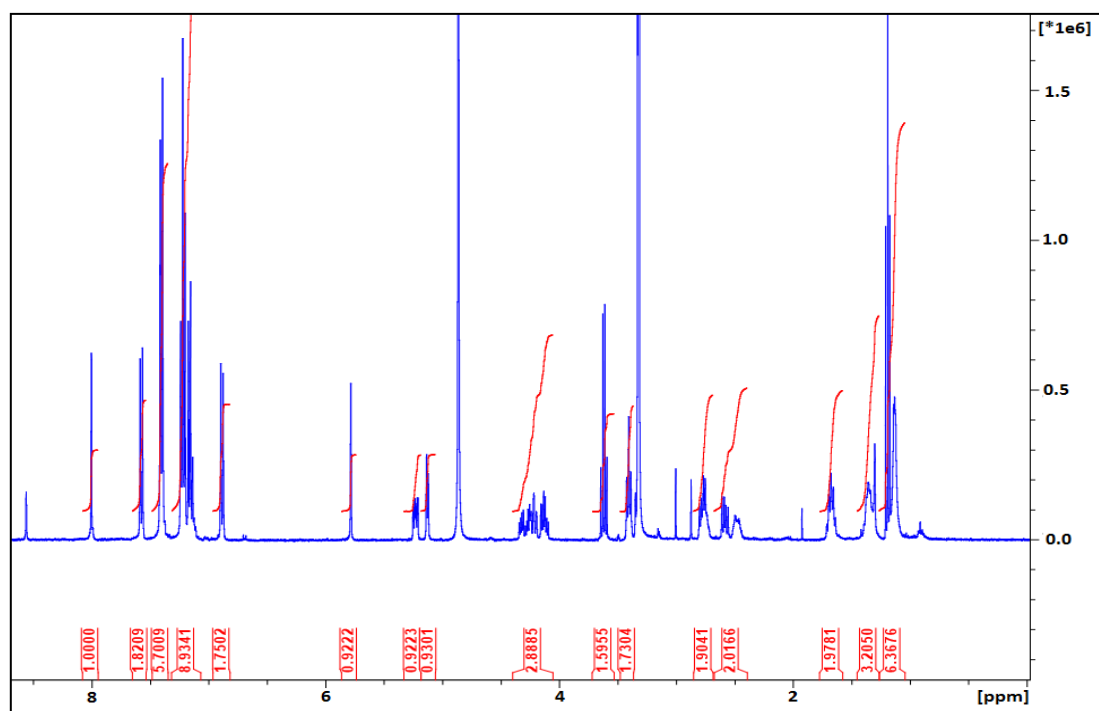
F

Figure 4.2 ¹HNMR spectral analysis of 8(6-aminohexyl) aminoadenosine-3′,5′-cyclic-monophosphate and N-trityl-phenylalanyl derivatives **(A)** 8-AHA-cAMP **(B)** 4a **(C)** 4b **(D)** 4c **(E)** 4d **(F)** 4e.
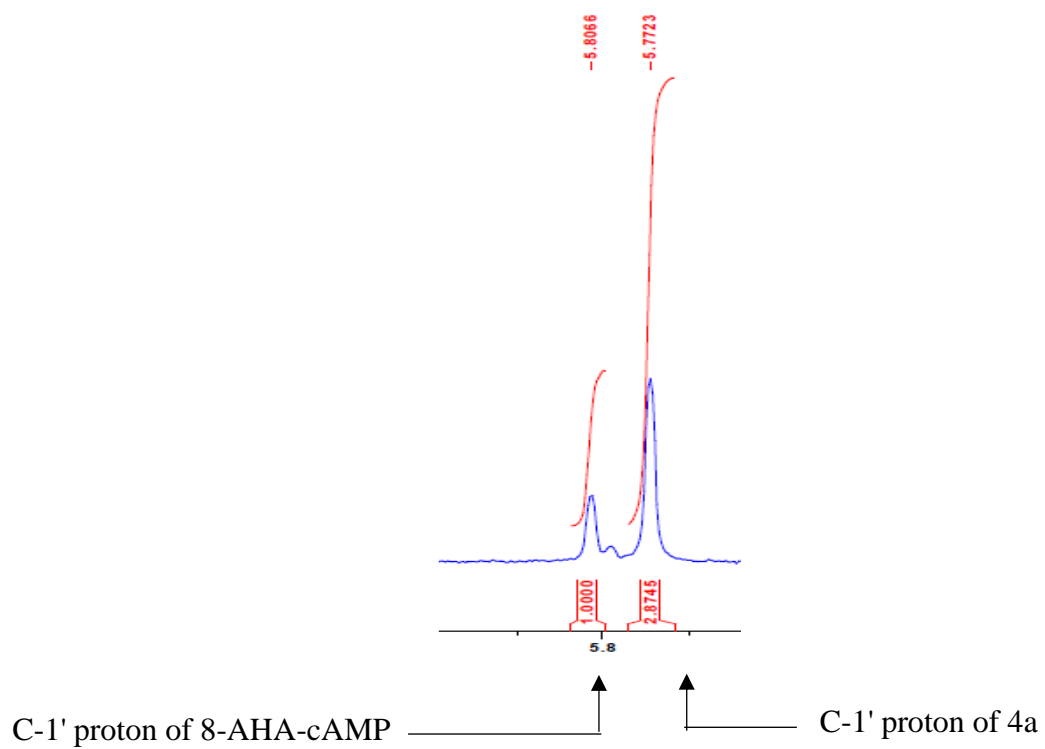
Figure 4.3 Anomeric region of ribosyl moiety (C-1') in preparative sample of N-trityl-L-phenylalanyl-8-(6-aminohexyl) aminoadenosine-cAMP (4a).
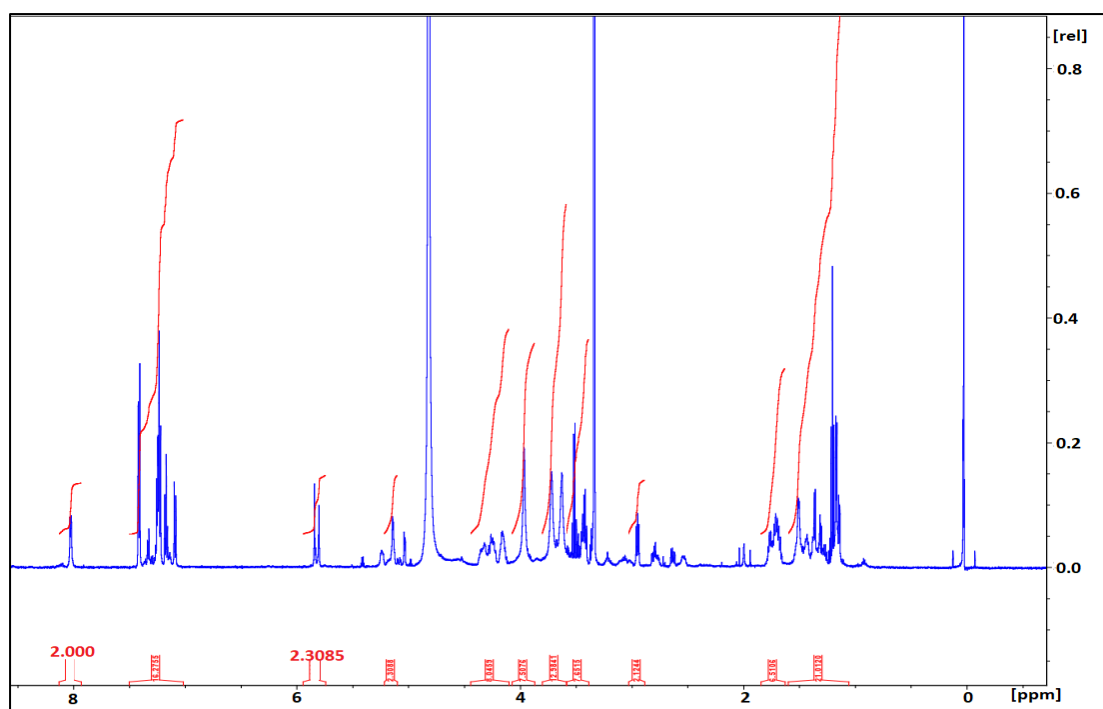
Figure 4.4 ¹HNMR spectral analysis of the first preparative N-trityl-Cl-DL-phenylalanyl conjugate (4c1).

APPENDIX D

THE MATRIX ASSISTED LASER DESORPTION IONISATION-TIME OF FLIGHT MASS SPECTROMETRY (MALDI-TOF) OF N-TRITYL PHENYLALANYL CONJUGATES
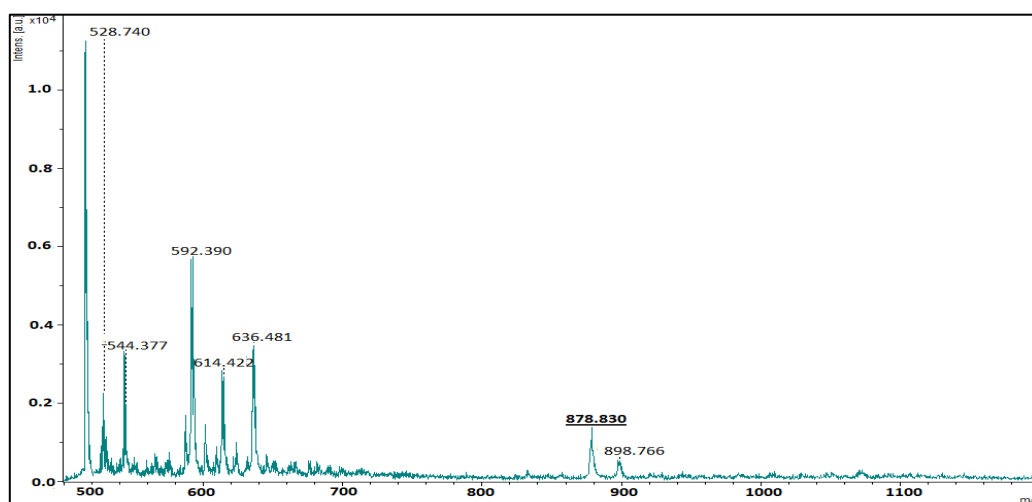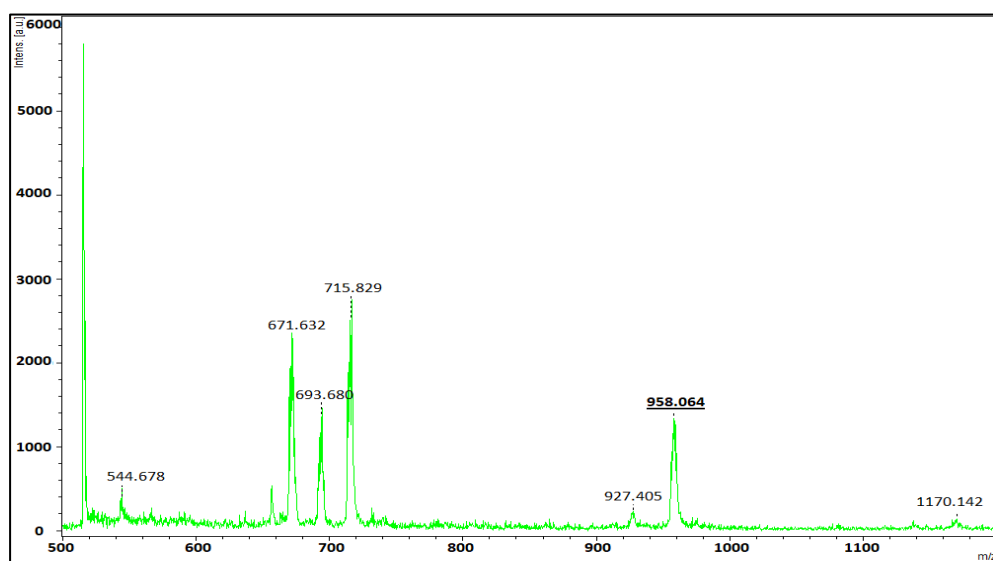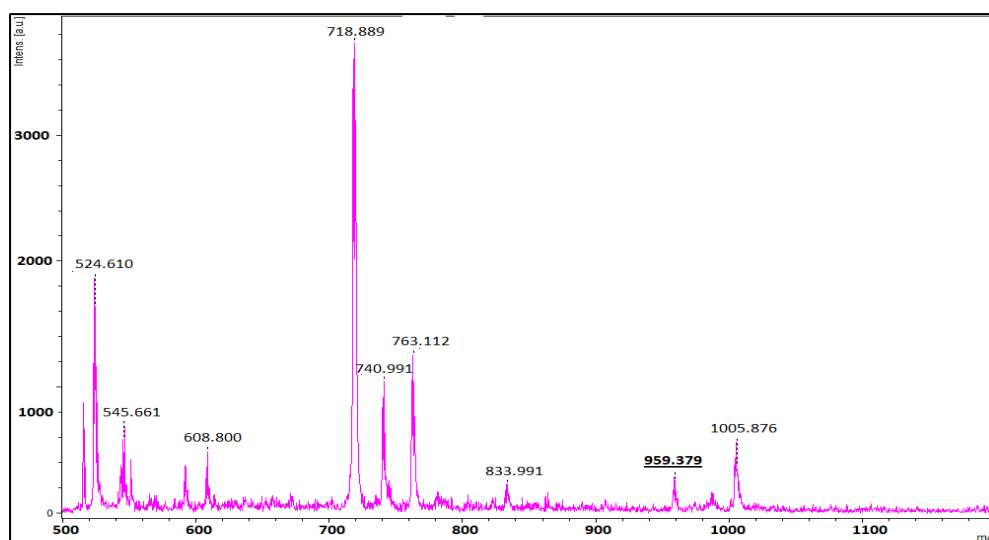

A
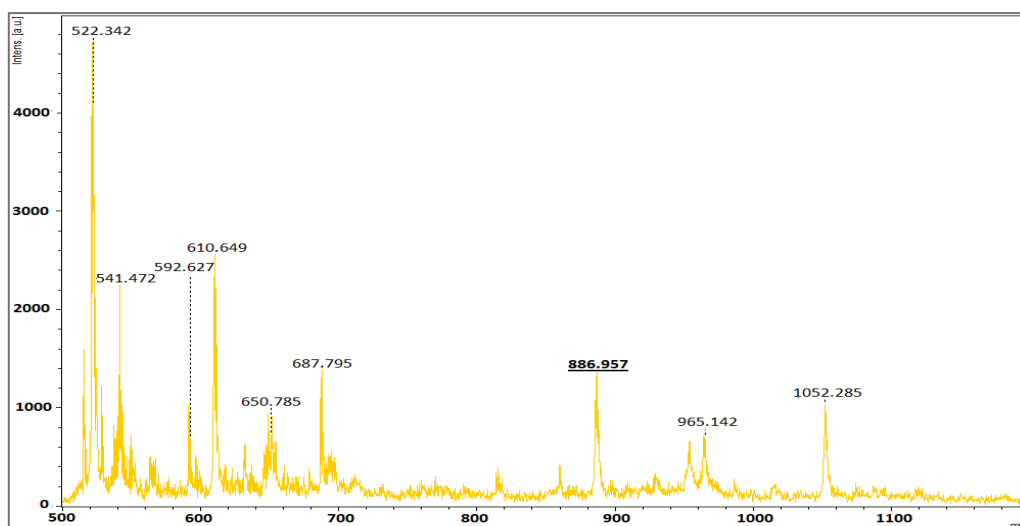
B
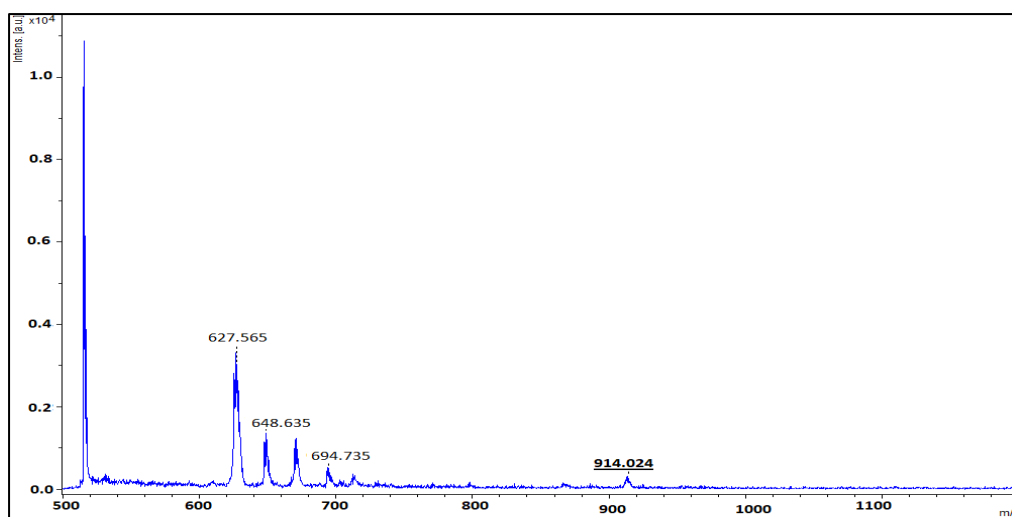
C

D

E

Figure 4.5 MALDI-TOF mass spectra of N-trityl-phenylalanyl conjugates (4a-e)
(**A**) 4a (**B**) 4b (**C**) 4c (**D**) 4d (**E**) 4e.

APPENDIX E

PLAGASRISM REPORT